2019

Development of a friction sliding system for enhanced seismic resilience of selective pallet racking systems

Zhenghao Tang
University of Wollongong

UNIVERSITY
OF WOLLONGONG
AUSTRALIA

Development of a friction sliding system for enhanced seismic resilience of selective pallet racking systems

Zhenghao Tang

This thesis is presented as part of the requirement for the conferral of the degree:
Doctor of Philosophy

University of Wollongong

School of Civil, Mining & Environmental Engineering

June 2019

Abstract

Industrial steel storage pallet racking systems are used extensively worldwide to store goods. Forty percent of all goods are stored on storage racks at some time during their manufacture-to-consumption life. In 2017, goods worth USD 16.5 billion were carried on cold-formed steel racking systems in seismically active regions worldwide. Historically, these racks are particularly vulnerable to collapse in severe earthquakes. In the 2010/2011 Christchurch earthquakes, around NZD 100 million of pallet racking stored goods were lost, with much greater associated economic losses due to disruptions to the national supply chain.

A novel component, the friction slipper baseplate, has been designed and developed to very significantly improve the seismic performance of a selective pallet racking system in both the cross-aisle and the down-aisle directions. This thesis documents the whole progress of the development of the friction slipper baseplate from the design concept development to experimental verification and incorporation into the seismic design procedure for selective pallet racking systems.

The test results on the component joint tests, full-scale pull-over and snap-back tests and full-scale shaking table tests of a steel storage racking system are presented. The extensive experimental observations show that the friction slipper baseplate exhibits the best seismic performance in both the cross-aisle and the down-aisle directions compared with all the other base-connections tested. It protects the rack frame and concrete floor from damage, reduces the risk of overturning in the cross-aisle direction, and minimises the damage at beam-end connectors in the down-aisle direction, without sustaining damage to the connection itself. Moreover, this high level of seismic performance can be delivered by a simple and cost-effective baseplate with almost no additional cost. The significantly reduced internal force and frame acceleration response enable the more cost-effective and safer design of the pallet racking system with minimal extra cost for the baseplate.

The friction slipper baseplate also provides enhanced protection to the column base from operational impact damage compared with other seismic resisting and standard baseplates.

Acknowledgments

There are so many who have contributed to the accomplishment of this research. Without these people, this study would never be possible.

First of all, I would like to express my sincere gratitude to my supervisors, A/Prof. G. Charles Clifton, A/Prof. James B. P. Lim, Dr. Tam Lakin, A/Prof. Lip H. Teh for providing me with consistent support, technical guidance and critical reviews along my research journey. Without their supervision and encouragement, I would have not been able to come this far.

Secondly, I would like to thank Dexion New Zealand, my boss Craig Landon and Jeff Darby for supporting this research without the slightest hesitation.

I would also like to express my sincere appreciation to all the faculty staff and lab technicians: Magdalene Woo (Mags), Pervin Suntoke, Mark Byrami, Dan Ripley, Ross Reichardt etc. for their helpful assistance and technical suggestions.

Craig and Ross, I am deeply saddened at your passing.

My sincere gratitude is also extended to my friends and colleagues: Dr. Majid Ali, Dr. Bo Li, Dr. Libo Yan, Dr. Yuanzi Chen, Dr. Shahab Ramhormozian, Dr. Gary Djojo, Dr. Xiaozhou Xiong, Dr. Sushil Khatiwada, Dr. Xiaoyang Qin, Dr. Miguel Ormeno, Fei Dong, Dr. Wentao Li, Dr. Wenjie Wang, Chao Xu, Ruxandra Macfarlane, James Maguire, Dr. Kang Jin, also, the third party editor Keith Gregory for his valuable time in improving the manuscript.

A special acknowledgement is reserved for my parents and sister for their unflagging love and endless support. Without them, this wonderful journey would not have begun. Especially my most loved and supportive mother, she is a little woman but extremely determined. She works as hard as I could ever imagine for me and my sister, enable us to go as far as we can. I am so proud to be your son.

Certification

I, Zhenghao Tang, declare that this thesis submitted in fulfilment of the requirements for the conferral of the degree of Doctor of Philosophy, from the University of Wollongong, is wholly my own work unless otherwise referenced or acknowledged. This document has not been submitted for qualifications at any other academic institution.

_____

Zhenghao Tang
1st June 2019

Table of Contents

List of Figures

List of Tables

Chapter 1 Introduction

1.1 Background

Industrial steel storage pallet racking systems are used extensively worldwide to store goods. Forty percent of all goods are stored on storage racks at some time during the manufacture-to-consumption system [1]. A few different types of racks are commonly used for industrial storage including selective pallet racks, drive-in or drive-through racks, cantilever racks and stacker racks as shown in Figure 1.1. This thesis focuses on improving the seismic performance of selective pallet racks. However, the design concept described in this study has high potential to be applied to all types of racks and even other forms of light steel framed structures such as scaffoldings or cold-formed steel framed houses.

Figure 1.1: (a) Selective pallet racks; (b) Drive-in racks; (c) Cantilever racks; (d) Stacker racks

Selective pallet racks are the most common type of rack used in industrial storage. Figure 1.1 (a) shows a photo and Figure 1.2 a common configuration of a typical selective pallet rack assembly. The standard pallet rack modular assembly consists of prefabricated uprights (columns) and bracings in the rack transverse direction and horizontal beams spanning between uprights in the longitudinal direction. An upright frame typically has two transverse uprights about 900 mm apart.

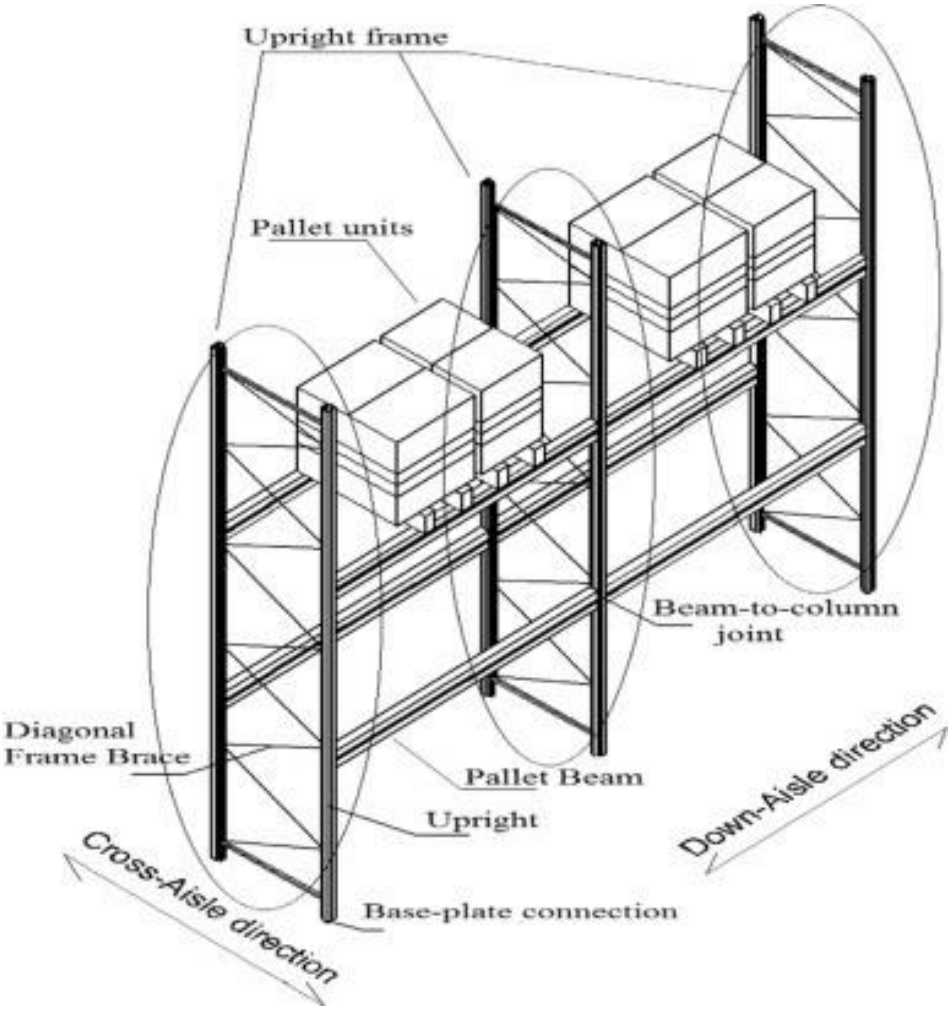

Figure 1.2: A standard selective pallet rack frame (from [2])

The two principal axes for seismic design of pallet racking systems are the cross-aisle direction, which is parallel to the braced system and the down-aisle direction, which is parallel to the beam span, see Figure 1.2 for details.

The uprights are braced in their plane with various patterns of bracing. Uprights have baseplates at the bottom. These are required in the standards [3] to be fixed to the building floor with anchorages, while other pallet racking systems are unanchored.

The horizontal beams supporting the pallets have spans that are usually either one to two pallets widths (from 1.3 to 2.8 meters). The beam-to-upright connections are typically clip-in or bolt-in, and the uprights are slotted along their full height to allow variations in beam height up the rack. The beam-to-upright connections are semi-rigid moment resisting connections and form a semi-rigid frame in the down-aisle direction. The degree of rotational stiffness and degree of rotation allowance varies with the manufacturer's material and the section design.

In structural analysis, the horizontal load-carrying system of standard selective racks is typically considered as a braced frame in its cross-aisle direction (transverse direction) and a moment frame in its down-aisle direction (longitudinal direction); with or without bracing at the back vertically (spine bracing) and/or at the beam level horizontally (plan bracing).

1.2 Seismic performance of selective pallet racking system

Traditionally, criteria for design and construction of industrial racks have been developed by their manufacturers and have been directed primarily at gravity loading, with little attention given to earthquake loading. Being heavily loaded with slender thin-wall cold-formed steel section members, the selective pallet racking system is complex with complicated load transfer through the structure. There are several factors make it vulnerable to seismic events: a lack of understanding of its dynamic behaviour, poor energy dissipation capacity, heavy loading and low residual capacity due to the behaviour of the complex cold-formed steel section.

As a result, there is a lower level of design and performance for steel racking systems compared with steel buildings, as evidenced by severely damaged racks being found in steel buildings, of similar age, which have no damage [4]. Extensive failure of cold-formed steel storage racking systems has been observed to occur due to the peak ground accelerations being substantially higher than the design values. In addition, a collision with the structure is disastrous for a pallet racking warehouse, a minor collision can result in total collapse of the racking due to the dynamics of falling pallets; falling just like a stack of dominos, as shown in Figure 1.3. The collapse of pallet racks and loss of contents in many past earthquakes have led to heavy economic loss: for example: the 1987 Edgecumbe Earthquake; the 2001 Nisqually Earthquake; the 2010 Darfield Earthquake and the 2011 Lyttleton Earthquake [5][6][7][8][9]. As a result, the seismic resilience of racking systems is getting increased consideration in design.

The world-wide market for pallet racking system is very competitive. To survive in this highly competitive market, the members of a pallet racking system are designed to be as thin as possible and carry loads as heavy as possible to give a more economical design solution. The conventional method of increasing the seismic resilience is to increase the section size and weight of the member to obtain a larger residual capacity and carry a larger seismic load. However, this is not cost effective for a business and hence is not readily adopted by the industry. A better seismic solution is required.

Figure 1.3: A minor collision can result in total collapse due to the dynamics of falling pallets

1.3 The friction slipper baseplate concept

The rocking behaviour of buildings was observed in the 1960 Chile Earthquake and extensively investigated over the next few decades. It was found to be beneficial to the seismic resilience of some buildings to reduces the seismic demand of the system by allowing column base uplift from its foundation. However, uncontrolled rocking behaviour could be fatal. The controlled rocking system was then introduced.

The concept of the sliding friction joint developed by Clifton [10] fitted the needs of a controlled rocking system with large energy dissipation capacity, when applied to the column base. The baseplate is connected to the column through a friction sliding joint. Through controlling the tightness of a bolt group, a upright was clamped to the rigid stub connected to a thick steel plate. The design concept was adopted by a few researchers as the major energy dissipation component of their seismic-resistance rocking systems [11]–[13]. The experimental results obtained by these researchers demonstrated satisfactory seismic performance with low damage and indicated that the sliding friction connector concept has high potential to be applied to the design of baseplate-column connections for a racking system.

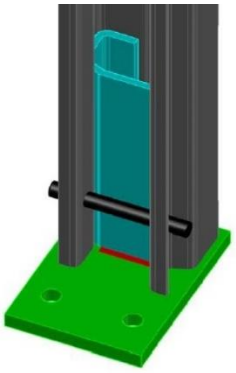

Figure 1.4: Concept drawing of a friction slipper baseplate

By allowing column uplift with a friction damper for energy dissipation, the seismic resilience of the pallet racking system is increased through a combination of higher damping, limited actions in the superstructure, and increased deformation capacity. This concept can lead to economical and low-damage seismic solutions for pallet racking systems.

1.4 Objectives

The aim of this PhD project is to develop a seismic resistant pallet racking system with a controlled rocking, friction sliding baseplate. The research objectives are:

1. To develop a cost-effective friction sliding baseplate for selective pallet racks that allows uplift and dissipates seismic energy during strong ground shaking;
2. To evaluate the behaviour of the baseplate in both the cross-aisle and the down-aisle directions through component joint tests;
3. To evaluate the dynamic response of a full-scale rack frame using the developed baseplate;
4. To compare the dynamic response of the developed baseplate with that of other types of

baseplates;

5. To assess the seismic performance of a rack frame using the developed baseplate through a shaking table test;
6. To provide design and detailing guidance for practising engineers in the design of racks with the developed baseplates.

1.5 Methodology

The objectives of this research are achieved through the following means:

a) In order to gain a sufficient understanding of the selective pallet racking system and its performance in seismic events, a comprehensive literature review is undertaken. The literature review also includes the development of rocking structures and energy dissipation devices.

b) Based the knowledge obtained from the literature review, a preliminary design is developed, namely the friction slipper baseplate. The prototype friction slipper baseplate is fabricated for an experimental investigation.

c) The prototype friction slipper baseplate is experimentally tested in the cross-aisle direction, in a joint component test, for its friction sliding behaviour under cyclic static loading; and in the down-aisle direction in a floor connection test for its moment-rotation behaviour. A few typical conventional baseplates are investigated for comparison.

d) In order to capture the dynamic characteristics of the rack frames with different types of baseplates, a series of full-scale pull-over and snap-back tests are conducted in the cross-aisle direction. The pull-over force-displacement curves and the free-vibration behaviour are obtained. The energy dissipation capacity of different types of baseplates is evaluated. The ductility factors of the racking systems using different baseplates are determined.

e) To verify the benefits of the developed friction slipper baseplates, a series of full-scale shaking table tests are conducted. Rack frames using different types of baseplates are tested under simulated earthquake ground motion to reveal their seismic resilience in cross-aisle and down-aisle directions.

1.6 Thesis outline

This thesis consists of 8 chapters as follows:

Chapter 1 presents an introduction to the thesis.

Chapter 2 reviews the literature relevant to this thesis: the general knowledge and seismic performance of racking systems; the development of rocking structures and energy dissipation devices.

Chapter 3 describes the concept development of the friction slipper baseplate based on the knowledge obtained in the previous chapter.

Chapter 4 presents the component test of the friction slipper baseplate in both directions. In the cross-aisle direction, the friction slipper baseplate shows its stable friction sliding behaviour; in the down-aisle direction, it shows robust moment resistance and stable rotational stiffness.

Chapter 5 presents full-scale pull-over and snap-back tests of the rack frames with the friction slipper

baseplate, and its performance is compared with that of other types of baseplate. The quasi-static and free-vibration behaviour of the rack frames are observed and analysed in this chapter.

Chapter 6 presents a series of full-scale shaking table tests of rack frames with different types of baseplate.

Chapter 7 provides a guide for practising engineers to design a racking system with the developed friction slipper baseplates.

Chapter 8 draws conclusions from this research and makes recommendations for future investigations.

Chapter 2 Literature review

This chapter examines the main characteristics of pallet racks, briefly describes the studies reported on the seismic performance of racking systems, reviews the previous studies on storage racks for improving seismic resilience and introduces the concepts of rocking behaviour and dampers used in structures as seismic measures.

2.1 Basic information about storage racks

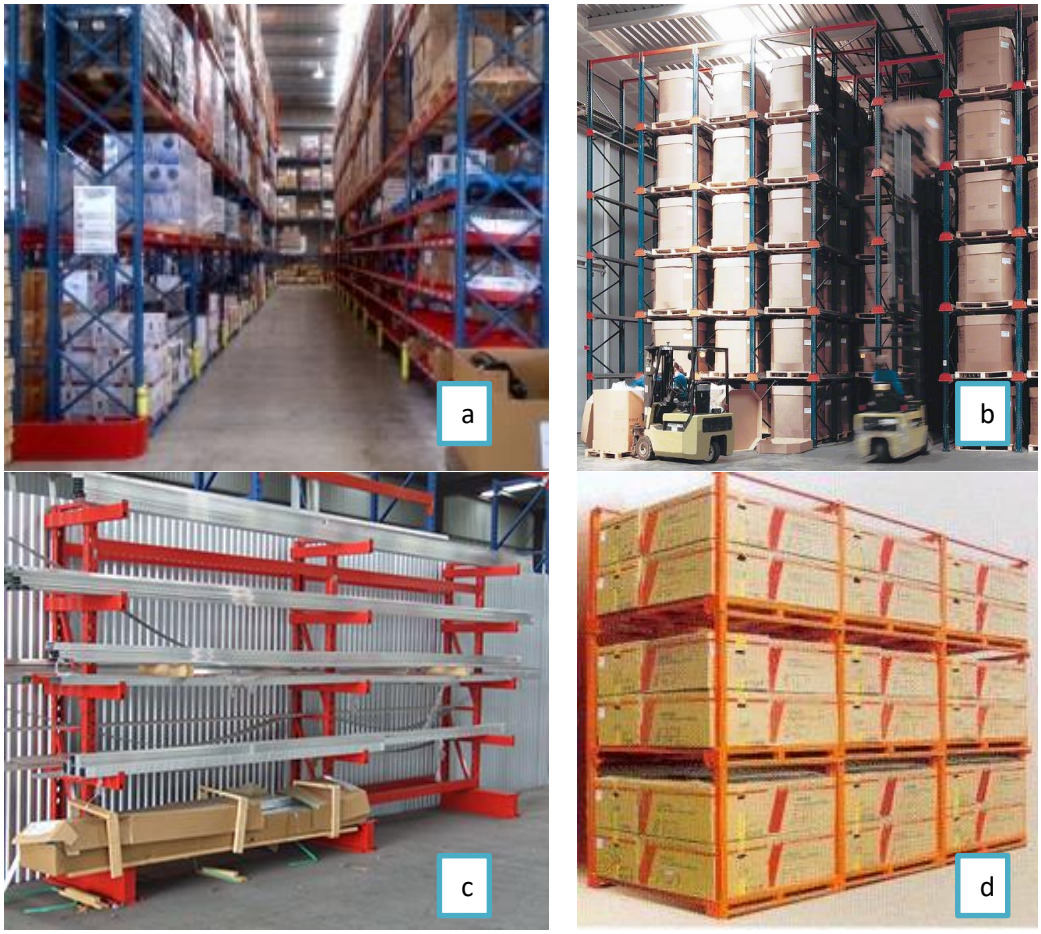

Figure 2.1 : (a) Selective pallet racks; (b) Drive-in racks; (c) Cantilever racks; (d) Stacker racks

Industrial steel storage pallet racking systems are used world-wide to store goods. Worldwide, 40% of all goods are stored on storage racks at some time during the manufacture-to-consumption process [1]. A few different types of rack are commonly used for industrial storage. These include standard selective pallet racks, drive-in, drive-through or shuttle racks, cantilever racks and stacker racks, etc. In this research, we are mainly focused on improving the seismic performance of standard selective pallet racks, as these are the most commonly used by to a significant extent. However, the design concept described in this study has high potential to be applied to all types of rack and even to other types of light steel framed structures, i.e., scaffolding or cold-formed steel framed houses.

Standard selective pallet racks are the most common type of rack used in industrial storage. Figure 2.1(a) and Figure 2.2 show a photo and common configuration of a typical selective pallet rack

assembly. The standard pallet rack modular assembly consists of prefabricated uprights (columns) and beams spanning between successive uprights in the longitudinal direction. An upright frame typically has two uprights spaced about 900 mm apart. The uprights are braced in their plane with various patterns of bracing. Uprights have baseplates, typically connected at the bottom into the floor slab with cast in or screw in bolts [3]. The horizontal beams supporting the pallets have spans that are usually from one to two pallet widths (from 1.3 to 2.8 meters). The beam-to-upright connections are typically clip-in or bolt-in, and the uprights are slotted along their full height to allow the beam position to be varied. Properly designed beam-to-upright connections are capable of transmitting moments. The degree of rotational stiffness and degree of rotation allowance varies with the manufacturers' material and section design details. In structural analysis, the horizontal load-carrying structural system of standard selective racks is typically considered as a braced frame in its cross-aisle direction (transverse direction) and a moment frame in its down-aisle direction (longitudinal direction), as shown in Figure 2.2.

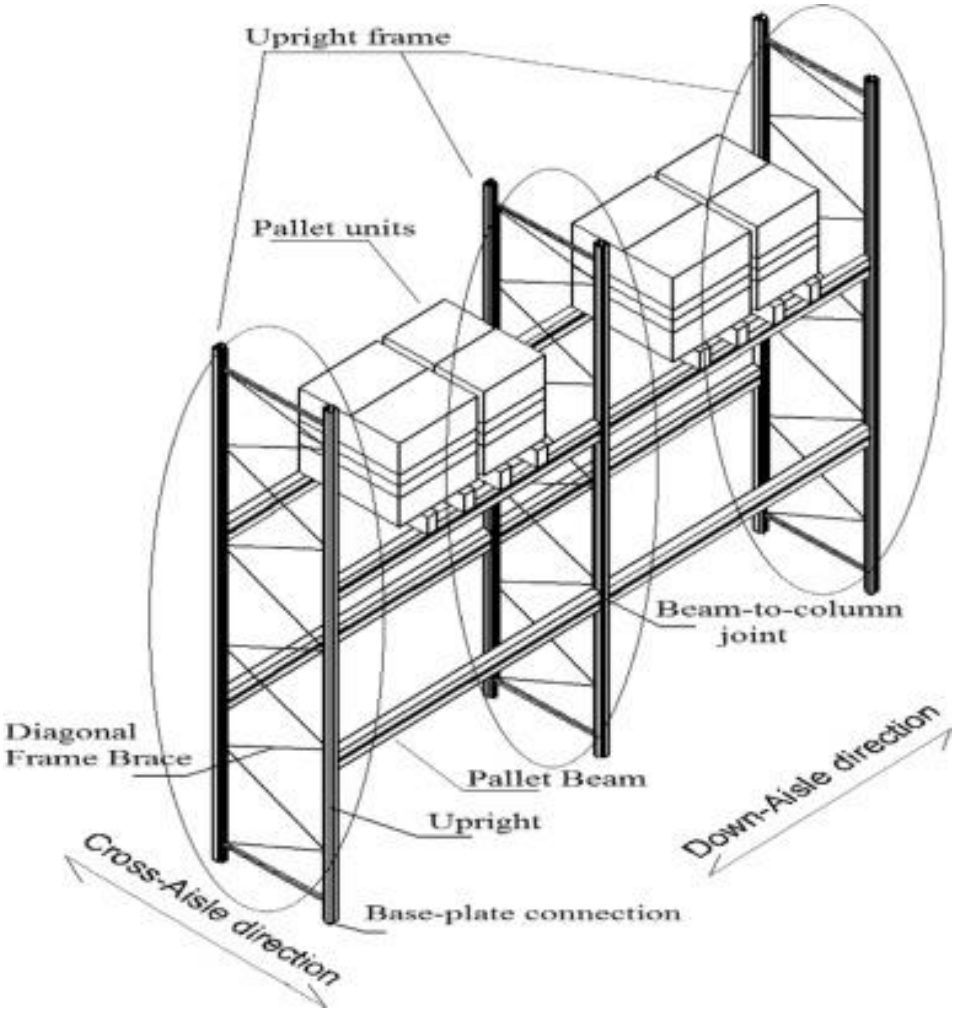

Figure 2.2 : A standard selective pallet rack frame (from [2])

Figure 2.3: A minor collision can result in total collapse due to the dynamics of falling pallets

2.2 Racking systems and their seismic performance: cross-aisle & down-aisle

Traditionally, criteria for design and construction of industrial racks have been developed by their manufacturers and have been directed primarily at gravity loading, with little attention given to earthquake loading. As a result, there is a lower level of design and performance for steel racking systems compared with steel buildings; as evidenced by severely damaged racks observed in steel buildings of similar age with no damage after an event [4]. Also, a minor collision with a rack can result in total collapse due to the dynamics of falling pallets , as shown in Figure 2.3.

The collapse of pallet racks and loss of contents in many past earthquakes have led to heavy economic loss: for example in the 1987 Edgecumbe Earthquake; the 2001 Nisqually Earthquake; the 2010 Darfield Earthquake and the 2011 Lyttleton Earthquake [5][6][7][8][9]. As a result, the seismic resilience of racking systems is getting increased consideration in design, especially as a result of disruption to the "just in time" method of global manufacturing in which major rack collapses can cause international scale disruption to the manufacturing supply chain.

Extensive failure of cold-formed steel storage racking systems has been observed due to the peak ground accelerations being substantially higher than the design values. Research by Hoogeveen 2011 [14] on conventional selective pallet racking systems in the down-aisle direction, has shown that the threshold for the collapse is a peak ground acceleration (PGA) greater than 1.3 times the design PGA. In a severe earthquake, this is often the case; for example as shown in Figure 2.4.

This is in contrast to modern steel frame buildings which deliver excellent response with PGA of over 2.5 times the design value [6][15]. Also, it is worth noting that most of the steel selective storage racks are made of cold-formed steel members. The ultimate capacity of a cold-formed member tends to be unpredictable when demand gets moderately over the design level.

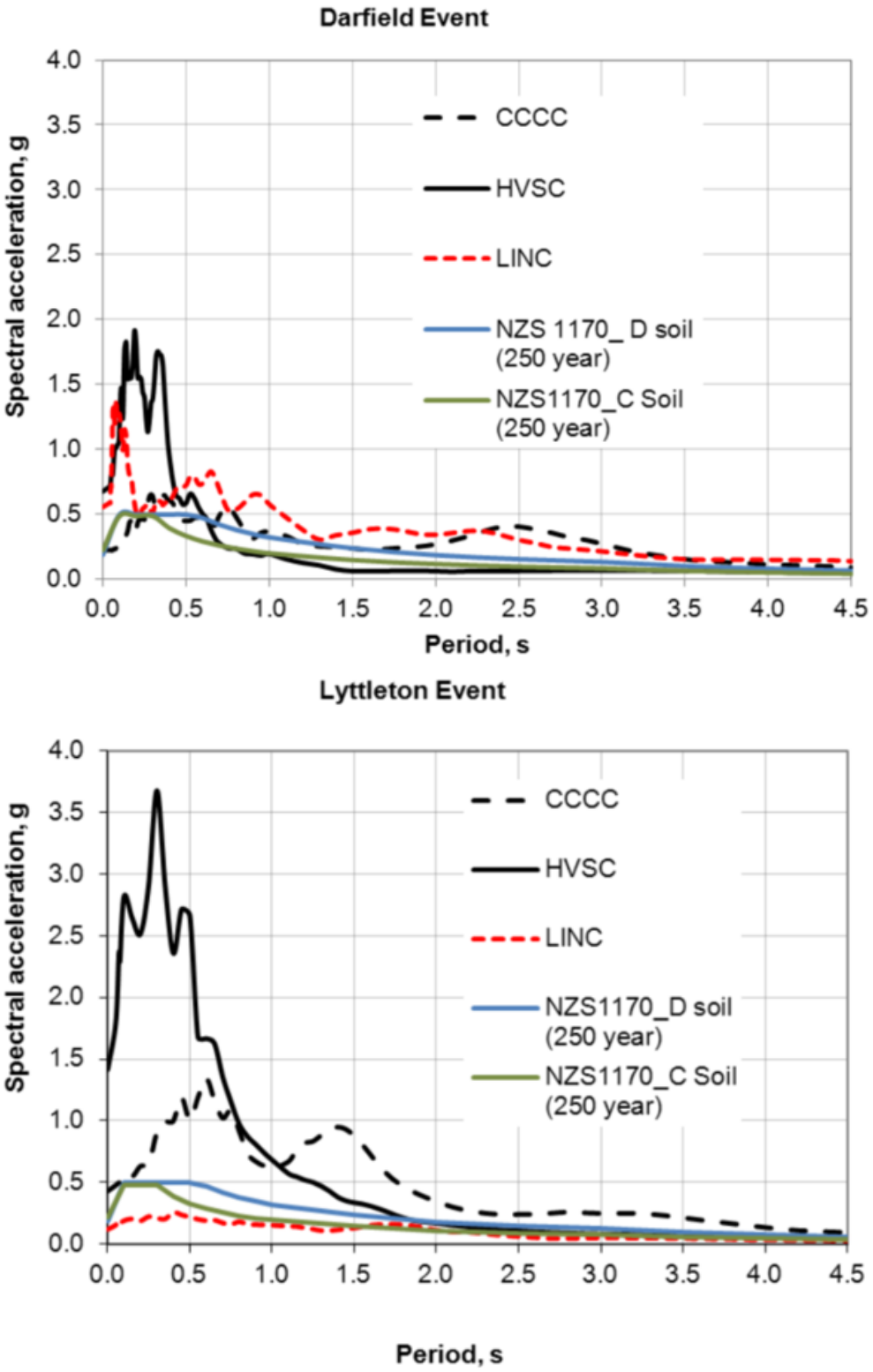

Figure 2.4: Response spectra plots for ground motion at Cathedral College (CCCC), Port Hills (HVSC) and Lincoln (LINC) from the Darfield and Lyttelton earthquake events.

The collapse modes of the racking systems can be one or more of:

(**a**) Cross-aisle direction collapses due to column buckling under higher-than-design earthquake intensity and heavy loading, as shown in Figure 2.5 and Figure 2.6. For some racks most, of the structural components remain in the elastic range, except the diagonal members of the bracing system of the vertical frames that, beyond a certain level, cannot withstand the applied compressive forces and buckle. The resulting unbalanced forces in the column from one brace at a connection point in compression buckling and the other brace in tension not buckling can lead to local column crippling or section failure.

(**b**) A whole rack frame assembly overturns due to insufficient base plate stiffness, inadequate ground anchors fixing the base plates to the floor or poor weld quality between the base plates and rack uprights, as shown in Figure 2.7;

(**c**) Down-aisle direction collapse due to the combination of higher than design moment and P-Δ effect causing beam to column or base plate to upright connector fracture, as shown in Figure 2.8 and Figure 2.9.

Figure 2.5 : Column local buckling [16]

Figure 2.6 : Cross-aisle direction collapse of pallet racking system [5]

Figure 2.7 : Failure of the baseplate to upright connection [17]

Figure 2.8 : Fractured beam-to-column connectors [14]

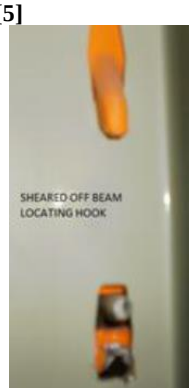

Figure 2.9 : sheared off beam steel hook[17]

2.3 Previous studies on improving the seismic performance of the racking system

Based on observations of the seismic performance of racking systems in past earthquake events, engineers and researchers working in this field have focused their attention on three study directions:

(**1**) Identify the local and global seismic behaviour of pallet racking systems and determine proper seismic design criteria for a racking system by numerical modelling and experimental verification, for example, the pushover test conducted by [18] as shown in Figure 2.10. In structural analysis, the horizontal load-carrying structural system of selective racks are typically considered as a braced frame in its cross-aisle direction (transverse direction) and a moment frame in its down-aisle direction (longitudinal direction). In some studies, researchers are concentrating on the down-aisle direction more than the cross-aisle direction; in some other studies, the situation is reversed; for example, in a series of studies conducted by Chen *et al*. from 1975-1984 [1], [18]–[21]. From full-scale shaking table tests in the down-aisle direction, it was concluded that the seismic forces developed in the structures by a strong earthquake could be greatly reduced by the high damping capacity of the inelastic action of a rack frame and the early nonlinear behaviour at its beam-column connections. However, in the structure's cross-aisle direction, the energy dissipation opportunities from the structural system is much weaker. The damping values obtained experimentally ranged from 3% - 9% in the rack's down-aisle direction and 1% - 1.6% in its cross-aisle direction [19]. The weakest spots were detected in the column-base connection. It began to fracture at a very low level of excitation (1/4 of Parkfield 1966 Earthquake recording) with noticeable buckling of all columns near their base plates.

Figure 2.10 : Test setup in cross-aisle direction pushover test (from [22])

However, Hoogeveen 2012 [14] observed that in the 2011 Christchurch Earthquake pallet racking systems performed well in the cross-aisle direction and major failures were identified in the down-aisle direction with fractures at the beam-to-column connections, as shown in Figure 2.8. Several

experiments have been conducted by Bernuzzi and Castiglioni 2001 [23] and other researchers [24], [25]. Most of them focused on the behaviour of rack frames, more specifically, the behaviour of beam-to-upright connections under monotonic and cyclic loading. The fractures at beam-to-upright connections have also observed and reported.

It could be concluded that different racking systems produced by different manufacturers, perform differently in specific situations. The design of the racking system needs to be considered in a case-by-case manner. Nevertheless, it is a common view that the beam-to-upright connections and base-to-upright connections of pallet racking systems are weak spots in earthquake events.

(**2**) Develop design procedures for racking systems, for example, Bernuzzi *et al*. [2][26][23] studied the joint behaviour of racking systems and developed a "reasonably efficient" seismic design procedure using the non-linear time-history method combined with the low-cycle fatigue damage approach. Filiatrault *et al*. [27] developed a performance-based seismic design procedure for racking systems accessible by the public. The last procedure has been included in FEMA 460 (2005).

(**3**) Other studies developed some innovative concepts to increase the seismic resilience of racking systems. For example:

Sideris *et al*. [28] investigated the frictional behaviour at the interface between loaded pallets and rack shelves and proposed the concept of incorporating slightly inclined shelving as a measure for mitigating merchandise shedding, as shown in Figure 2.11. Traditionally, engineers only considered the structural capacity of the rack frame itself. FEMA 460 suggests both the seismic performance of the rack itself and the response of stored contents should be considered in the seismic design of the racking system. Shaking table test results show that Sideris' concept of slightly inclined shelving appears to be very effective. An inclination of only 3.5 degrees reduced the observed seismic merchandise shedding fragility to zero for the ground excitations considered.

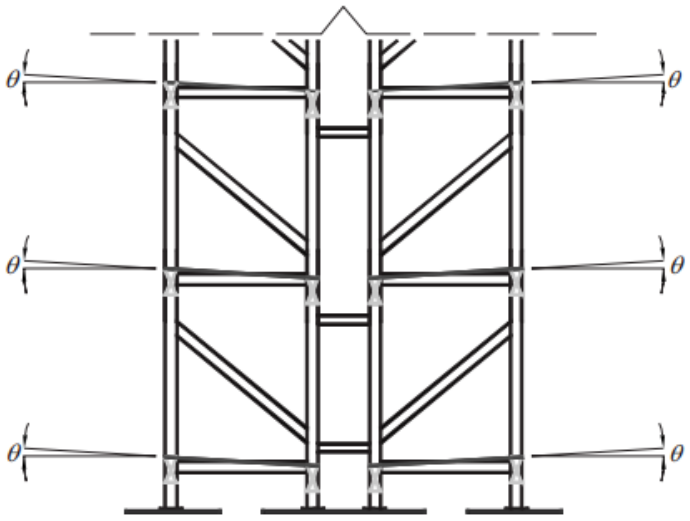

Figure 2.11 : Concept of inclined shelving for back-to-back pallet-type rack configuration

The designs of beam-to-column connections and base-to-upright connections were improved for better moment resistance, for example, the L-shape connection was replaced by a T-shape connection [29], Figure 2.12 and Figure 2.13, a bolted connection Figure 2.14, was also introduced [30].

Figure 2.12 : L-shape connection

Figure 2.13 : T-shape connection

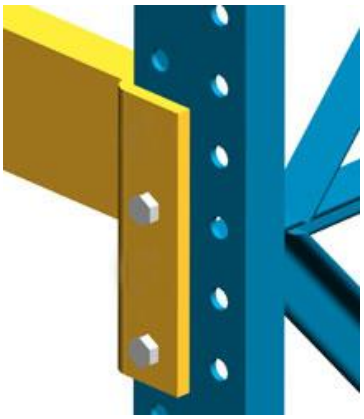

Figure 2.14 : Bolted moment connection

Various baseplates designs were investigated [31][32][33]. For the down-aisle direction, the key features for baseplate assembly are the rotational stiffness and the moment-rotation curvature relationship. For the cross-aisle direction, the uplift stiffness, energy dissipation capacity by yielding of steel plates, and pull-out resistance were investigated.

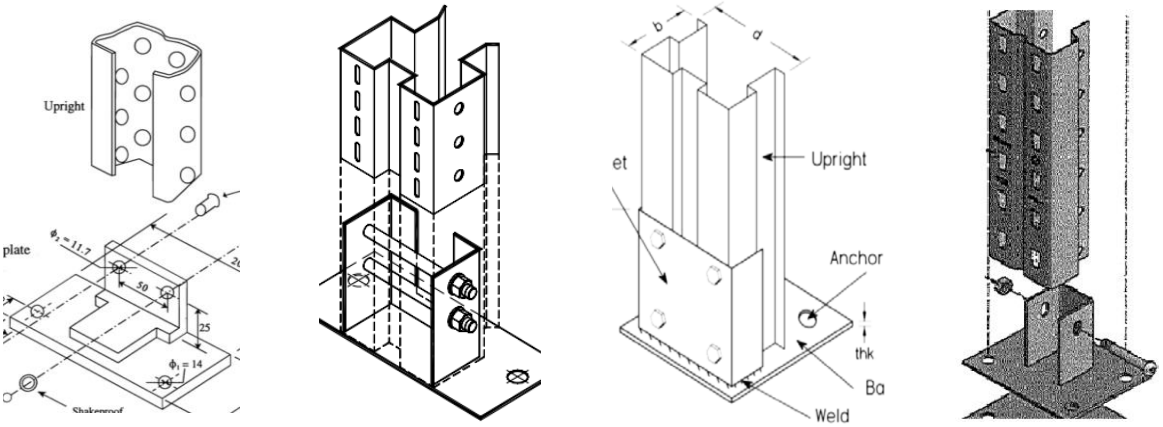

(a) **(b)** **(c)** **(d)**

Figure 2.15 : Various types of baseplate connection assembly

Base isolation techniques, used as a seismic measure for important buildings like hospitals and museums, have been introduced for pallet racking systems. Various types of rack base isolators have been invented. Filiatrault *et al.* [34]; Kilar *et al.* [35] and Michael [36] investigated the seismic behaviour of pallet racking systems with various types of base isolator, as shown in Figure 2.16 (a). An Italian company Lokibase has developed a bi-directional base isolator for storage racking systems, as shown in Figure 2.16 (b) [37]. The concept has been verified by a large number of experiments, including full-scale shaking table tests and worked very well.

Figure 2.16 : Pallet rack base isolators (a): single direction (from [34]**); (b) bi-directional (from** [37]**)**

With regard to the bracing systems: as far as seismic design is concerned, it appears that racks behave like moment-resisting frames in the down-aisle direction, where only beam-to-column joints and base-plate connections carry the lateral load, owing to the impracticability of using bracing systems in selected areas of pallet racks. Hence, most of the model of the unbraced semi-continuous frame is adopted for design. However, in some back-to-back selective rack systems, steel rope or bracing rod systems are adopted at the middle of two rack frames to provide additional seismic resistance.

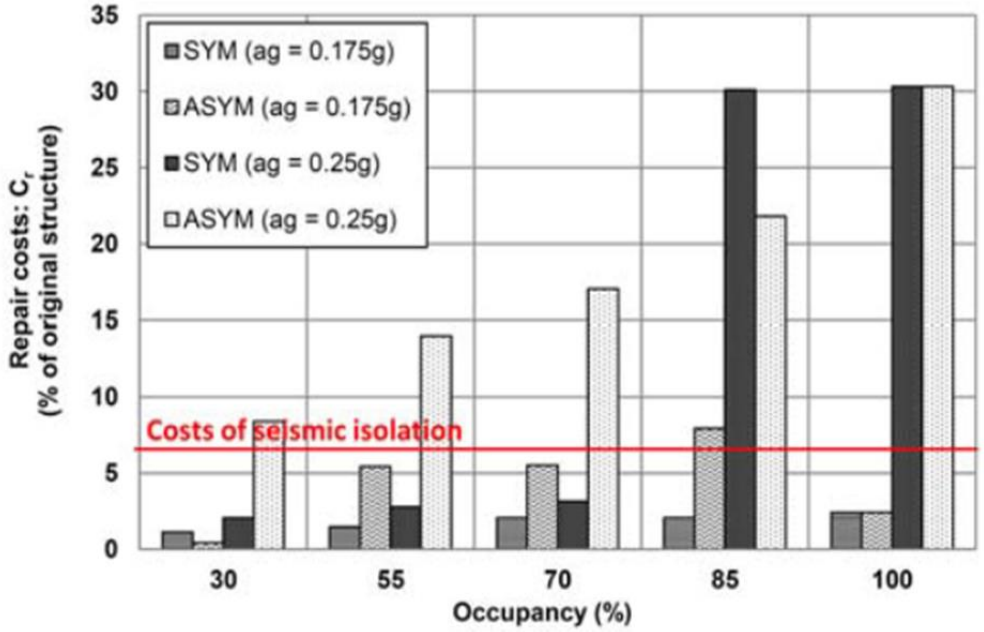

Figure 2.17: Seismic isolation costs VS structural repair costs for different occupancy levels, ground motion intensities and structure model (SYM stands for Symmetric; ASYM stands for Asymmetric) [38]

However, all these measures have their limitations. Inclined shelving does not prevent the collapse of the racking system. Beam-to-column connections and baseplate-to-upright connections are still weak spots in racking systems. Even if a racking system survives a severe earthquake, these connections can be either fractured or have too much plastic deformation, and could not be used any more. It is not cost effective to replace all the damaged racking after each earthquake. Although base isolated racking systems performed pretty well, it is too expensive and not affordable for most regular warehouses. Kilar *et al*. 2013[38] conducted research on the financial aspects of a base isolation system for a high-rack-structure. As shown in Figure 2.17, it is clear that there is a large gap between

the cost of seismic isolation and repair cost; this blocks industry adoption of this technique as a seismic measure. A low-damage and low-cost technique to improve the seismic resilience of the racking system is demanded.

2.4 Rocking / Uplifting behaviour

Conventional structures, designed to current seismic codes, are intended to prevent permanent damage or large residual deformation, for example, the use of plastic hinges in order to withstand an intense earthquake event. The associated repair cost from an event may be so high that it is more economical to demolish and rebuild the structure than to repair it. Some new concepts for earthquake-resistant systems are being developed to economically improve the seismic performance of structures. A controlled rocking steel frame is such a system. In this system, the base of a column is allowed to lift off its foundation rather than develop large tension. This behaviour is called uplift, and acts as a mechanism that limits seismic force, and reduce damage.

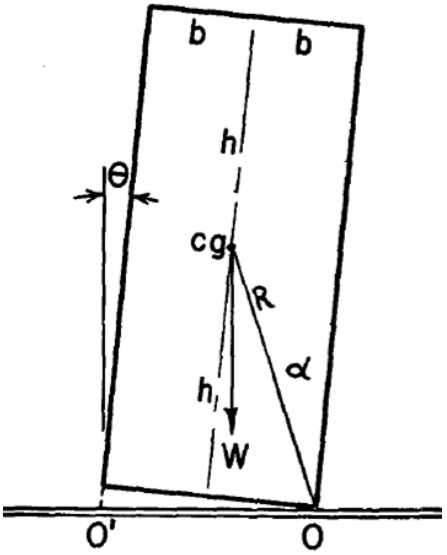

Figure 2.18: A rocking block (from [39]**)**

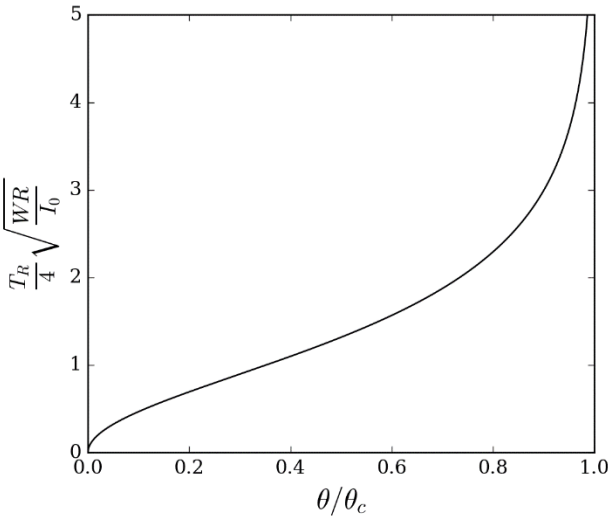

Figure 2.19: Period T of block rocking with amplitude $\boldsymbol{\theta}$

$$T_R = 4\sqrt{\frac{I_0}{WR}}\ \cosh^{-1}\left(\frac{1}{1-\theta/\theta_c}\right) \qquad \textbf{Equation 2.1}$$

Uplift was recognized as a beneficial effect by Housner 1963 [39] from his observation of some slender structures that survived the 1960 Chile earthquake. Housner analytically studied the rocking period and energy loss of a rigid rocking block as an inverted pendulum. An equation was derived to reveal the relationship between the period of the rocking block and the initial amplitude, as shown in Equation 2.1. Clough and Huckelbridge 1977 [40] concluded that the uplift phenomenon provides a type of structural fuse to reduce internal force and ductility demand on the system, providing a more rational and more economical design for a realistic seismic loading condition. Huckelbridge 1977 [41] stated that a system with uplift has a large energy absorption capacity in the form of potential energy stored by the mass because of its relative elevation, and this energy reservoir can be more

economically exploited than that of systems whose total energy absorption capacity is only from internal strain energy. Priestley *et al*. 1978 [42] compared Housner's theory of free rocking of a rigid block with an experimental result and concluded that the rocking mechanism limited the lateral accelerations to the level first inducing the rocking. Housner assumed that the impact at the end of uplift is inelastic, but Priestley concluded that this assumption makes the analysis non-conservative. Wang and Gould 1993 [43] introduced a proposed structure incorporating the mechanism of uplift and the mechanism of sliding in the foundation. Numerical analysis shows that the maximum amount of uplift for the proposed system is significantly reduced compared with that of the conventional system, even for an earthquake as severe as the EI-Centro 1940. The researchers suggested that this feature should be accepted into professional practice. Wiebe and Christopoulos 2013 [44], [45] numerically and experimentally studied the effect of multiple rocking sections on multi-storey building design. It was concluded that allowing rocking to occur at multiple locations would be advantageous. Small scale shaking table tests by Roke *et al*. 2009 [46] have shown that self-centring performance is excellent, with minimal residual drifts and minimal damage to the steel friction connection, floor slabs and framing members after massive ground excitation.

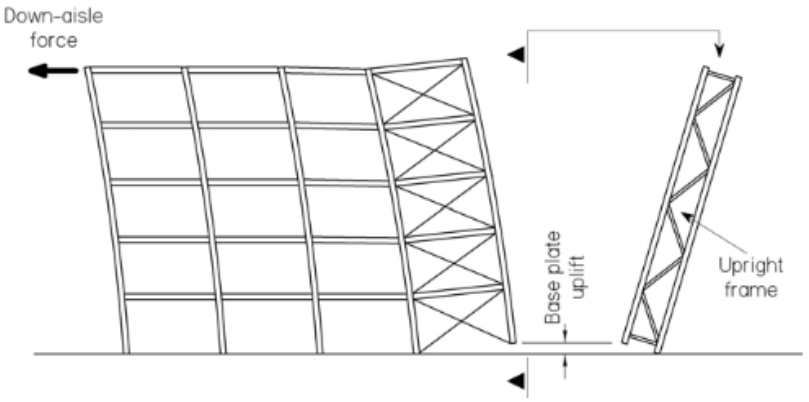

Figure 2.20: Uplift behaviour in a rack frame in the down-aisle direction (Left); the cross-aisle direction (Right) (from [47]**)**

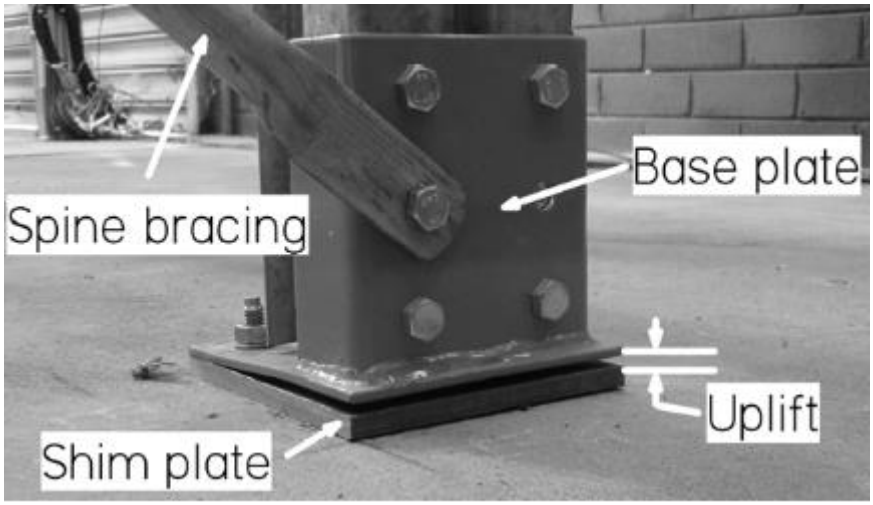

Figure 2.21: Baseplate uplift (from [47]**)**

Uplift behaviour is also observed in the racking system. Gilbert and Rasmussen 2009 [47] observed in a full-scale drive-in rack test that the baseplate lifts up at the base when the upright is subjected to a tension force, as shown in Figure 2.21. Uplift behaviour in racking systems can occur, in conjunction

with upright base rotation, from two sources. The first of these is when the down-aisle direction is strengthened with supplementary bracing to create a braced selective pallet rack. This resists the down-aisle forces mainly by axial tension and compression in the spine bracing uprights. When the axial force in the upright in tension overcomes the axial compressive force due to the pallet loading, baseplate uplift occurs, as shown in Figure 2.20 (Left). The second form of uplift is from bracing action in the cross-aisle braced frame system. The upright uplift may occur on one upright while the rack frame rotates about the upright base at the other side due to the cross-aisle horizontal seismic action, as shown in Figure 2.20 (Right). Figure 2.21 shows a typical baseplate floor plate uplift and deformation during the full-scale rack tests presented in [48]. In most rack assemblies, uplift is more common in the cross-aisle direction. Gilbert and Rasmussen 2009 [49] claim that the uplift behaviour at the upright base increases the second order P-Δ effect in both cases above. However, this behaviour may also reduce the force demand of the rack at upright-base connection and prevent structural collapse from upright buckling. As evidence, during the 2010 Darfield Earthquake, in the same warehouse, some non-anchored racks walked off their original position and survived the earthquake with no damage, while the racks that failed were anchored [4]. This uplift behaviour has been observed and reported in many other types of structure that have survived an earthquake event. This observation is inconsistent with the requirement of most racking standards and design guidelines which require baseplate anchorage for seismic resistance. This behaviour has been extensively studied in many types of regular buildings, but limited research has been conducted on racking systems.

2.5 Energy transformation and energy dissipation devices

Some buildings survived strong earthquakes with acceptable damage. It was found that some energy dissipation mechanisms have significantly contributed to their seismic performance. Equivalent static seismic design methodologies use an estimated external force to represent seismic reaction. However, in practice, an earthquake merely imparts energy into a structure and the structure reacts in terms of deformations which induce internal forces. Mendes-Victor explains that the nature of the energy taken by the structure is not restricted; it may be elastic or elasto-plastic [50]. As illustrated in Figure 2.22, the maximum reacting force is not a physical reality; it is a technical by-product; it may be large (*Fel*) or small (*Fpl*), at the expense of small or large safely exhibited deformations of the system, which is called available ductility. For a given earthquake, brittle systems are required to react with high resistance *Fel*, whereas ductile systems may be required to withstand forces as low as *Fpl*, in Figure 2.22. Instead of designing for resistance, the engineers have now to design for ductility too. This concept opened an entirely new avenue in seismic engineering. In traditional terminology, the acting seismic force could now be a function of the energy dissipation capacity of the system.

In buildings, where the self weight is typically greater than the imposed load, studies have shown that the drift envelope of the structure is largely insensitive to the shape of the hysteresis curve of the energy dissipating elements, with more important factors being the ability of the inelastically responding system to retain strength under multiple cycles of inelastic loading to the similar deformation limits and not to develop slip under load reversal. However, for pallet racking systems where the response is dictated by the dynamic movement of the pallets, the self weight of the structure

is minimal and the ductility capability of the structure itself is low, reducing the input seismic energy coming into the system through the base system is a very important way of enhancing seismic resilience.

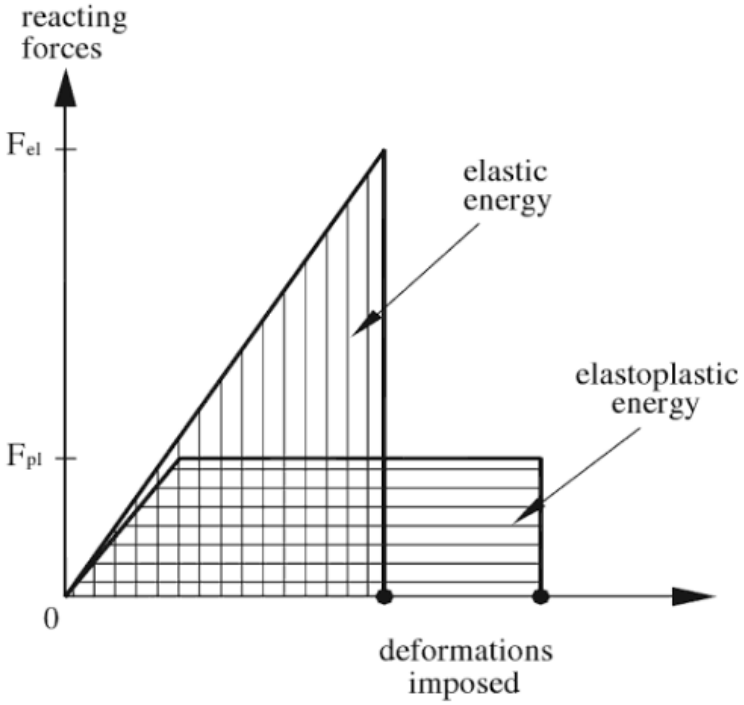

Figure 2.22 : Earthquake impart energy to the structure; the structure translates energy into reacting forces, depending on its elastic or elasto-plastic behaviour ([50]**)**

Damping is the mechanism by which energy is removed from a vibratory system; it is the property responsible for the eventual decay of free vibrations and for the fact that the response of a vibratory system excited at resonance (i.e. cyclic excitation with frequency) does not grow without limit. Sources of damping in conventional buildings include energy dissipated by non-structural elements, material damping, frictional dissipation of energy at bolted connections and yielding of structural members, , also energy dissipated by radiation damping and soil nonlinearity through the foundation.

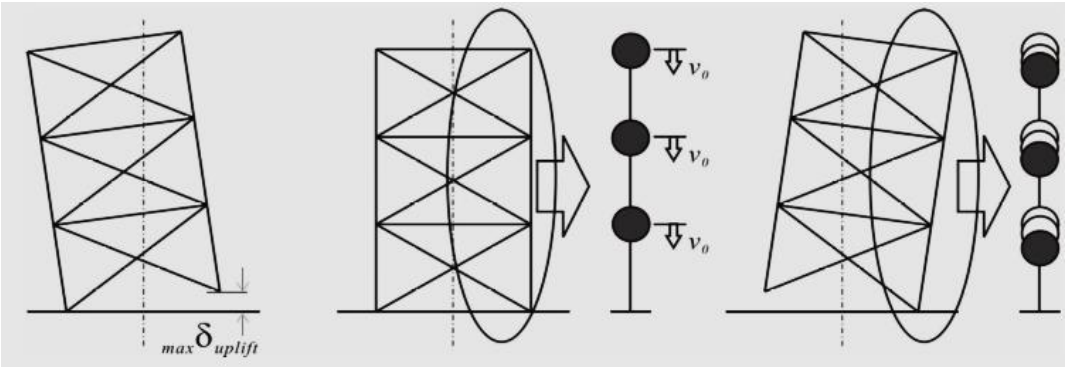

Figure 2.23: Uplift behaviour results in the lifting of the gravity centre

The energy imparted from an earthquake (E_I) has several ways of being absorbed without destroying the structure. Firstly, the energy imparted to the racking system (E_I) is converted to elastic potential energy (E_U) in the structure members to create elastic deformation; the system starts to vibrate under the seismic excitation and a portion of the energy is converted to kinetic energy (E_K). Once a column commences uplift, the gravity centre of the system lifts, the gravity potential energy (E_G) of the system

increases, as shown in Figure 2.23.

If the amount energy imparted to a structure member exceeds the yielding limit, then plastic deformation occurs, this portion of energy (E_B) is dissipated by the material yielding or fracturing. When the structure is vibrating, a small portion of energy is dissipated by material damping (E_M); if there are dampers in the system, for example, metal dampers or friction dampers, a considerable amount of energy (E_D) can be dissipated and converted to internal energy. For pallet racking system, the cold-formed thin-wall members can't sustain plastic hinge deformation without rapid decrement on their capacity, therefore, plastic deformation (E_B) is undesirable and should be avoided in the design of racking system. The material damping in a steel structure (E_M) is negligible. A controlled rocking system with a friction damper can restore some energy as elastic and gravity potential energy (E_U and E_G) to avoid excess energy getting into the system to create the plastic deformation of any member, at the same time the friction damper can dissipate a significant amount of energy (E_D) by controlled uplift behaviour at column bases.

$$\boldsymbol{E_I = E_U + E_G + E_k - E_B - E_M - E_D} \qquad \textbf{Equation 2.2}$$

Analytical study on this phenomenon is difficult because, in real engineering systems, damping is a complex mix of these mechanisms and many of these are negligible, some are desirable and some are undesirable. Various types of energy dissipation device are developed, to meet the differing needs of buildings, by increasing the energy dissipation capacity of the structures without allowing undesirable damage. For example, fluid dampers, metal yielding dampers and friction dampers are now wildly used in various types of buildings. However, most of them are very expensive and not economically feasible to improve the seismic resilience of an industrial racking system.

G. C. Clifton 2005 [10] developed a friction sliding hinge joint to replace the conventional beam-column connection for steel moment resisting frames and this has been widely used in New Zealand. As shown in Figure 2.24, instead of forming irrecoverable plastic deformation at the beam-column joints, it is designed to be rigid up to ultimate limit state and sliding under severe seismic events: dissipation of energy through the friction damper mechanism results in minimal damage. The tightness of the bolt groups connecting the bean and the column can be adjusted to achieve an optimal seismic performance. This concept is a relatively easy and cost-effective way to achieve significant seismic resistance and can potentially be used in a racking system.

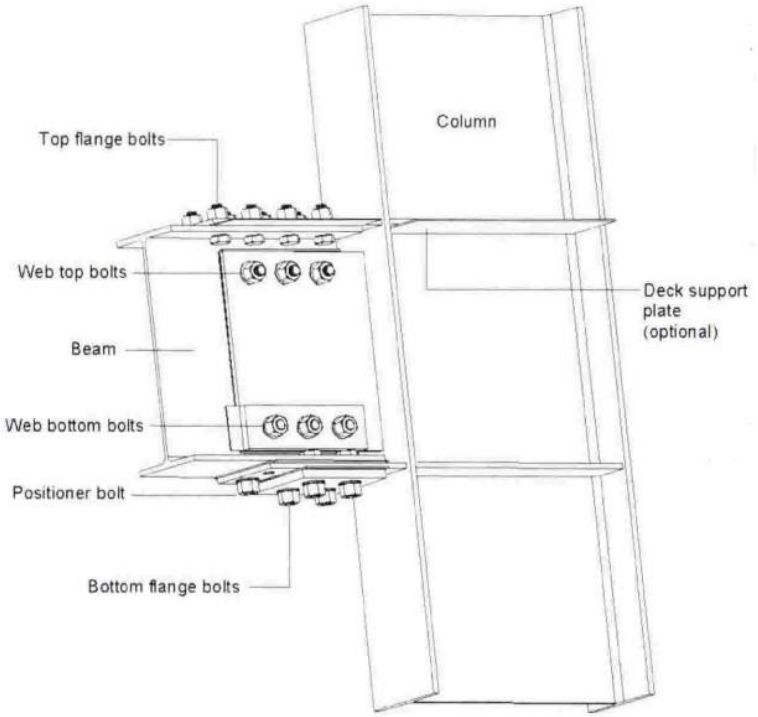

Figure 2.24: Friction sliding hinge joint for a moment frame beam-column connection (from [10])

2.6 Rocking with dampers

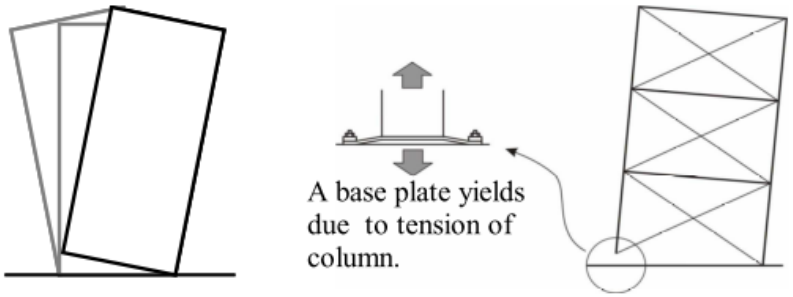

Figure 2.25 : Basic conception of rocking structural systems with yielding base plates (from [51]**)**

As both rocking behaviour and the application of seismic dampers can improve the seismic performance of a structure, some researchers have tried to combine these two measures to achieve a cost-effective and low-damage seismic-resistant structure.

To reduce the seismic response of steel buildings Azuhata *et al*. 2002-2004 [52][51] developed a rocking structural system with steel yielding baseplates which allow a rocking vibration during strong earthquakes. When the weak base plates yield due to the tension of the column during an intense earthquake ground motion, the building structure develops a rocking vibration. The basic idea of the base plate yielding systems is illustrated in Figure 2.25. This research group proposed a simplified method to predict the seismic response of the system and achieve good agreement comparing to shaking table test results. The full-scale shaking table test result demonstrated that the seismic energy dissipation by the uplifting gravity centre and the hysteresis damping of base plates are responsible for a large part of the energy dissipation corresponding to the maximum moment input energy.

Apart from this research, there are many other studies adopting this combined concept as a seismic measure. Loo *et al*. 2014 [53] adopted the slip-friction connector as the seismic energy damper for a rocking time shear wall and found it can impart ductile and elasto-plastic characteristics to what would otherwise be essentially brittle structures. Ormeno *et al*. 2015 [12] adopted the slip-friction connector in the design of the rocking liquid storage tank. A bolt group with Belleville springs was introduced to calibrate and maintain a controlled friction force to achieve a stable friction damper behaviour. A significant increase in damping ratio and reduction in axial stress was observed. The self-centring potential was also found to be excellent in all the studies. All these studies showed that the slip-friction connector gives a significant improvement in the seismic performance of the structures.

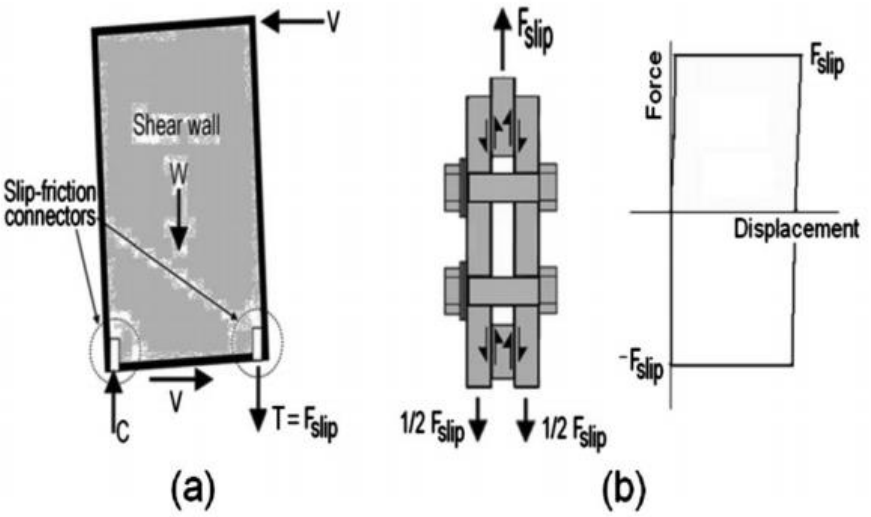

Figure 2.26: Slip-friction connectors used in a timber shear wall (from [53]**)**

By allowing frame uplift combined with energy dissipation components, the seismic resilience of a pallet racking system will significantly increase because the structure dissipates more energy in the predetermined energy dissipation component which having greater ductility and protection of key elements from premature localise. This can result in a low-cost and low-damage seismic design.

Chapter 3 Concept Development

Pallet racking systems comprise an assemblage of light gauge, thin-walled, skeletal structural systems supporting discrete pallet loads. For lateral load resistance in the down-aisle direction, selective pallet racking systems comprise an assemblage of beam-upright connections and upright-base connections in a semi-rigid configuration, while in the cross-aisle direction the lateral load resistance is from braced frames and upright-base connections.

The performance of the upright-base connection is found to significantly influence the overall behaviour of the rack system. In the cross-aisle direction, the baseplate-upright connection determines the stability and flexibility of the rack; in the down-aisle direction, it shares the moment demands with the beam-upright connections. The role of the baseplate in these two directions is very different. The design concepts for these two cases are considered separately in order to develop a baseplate which can significantly improve the seismic resilience of the rack frames in both directions.

3.1 Cross-aisle consideration

Gilbert and Rasmussen [47] observed in a full-scale drive-in rack test that the baseplate lifts up at the base when the upright is subjected to a tension force, as shown in Figure 3.1. This behaviour is called uplift, and is often observed for slender structures during earthquake events. However, this uplift behaviour is not accounted for in most of the current pallet racking system design specifications [47].

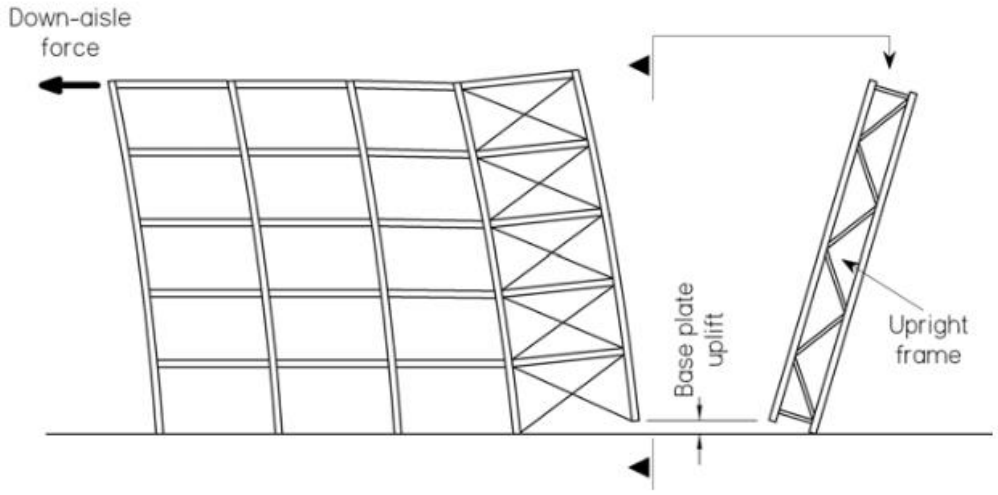

Figure 3.1 Cross-aisle deformation of a rack frame when uplift occurs (from [47]**)**

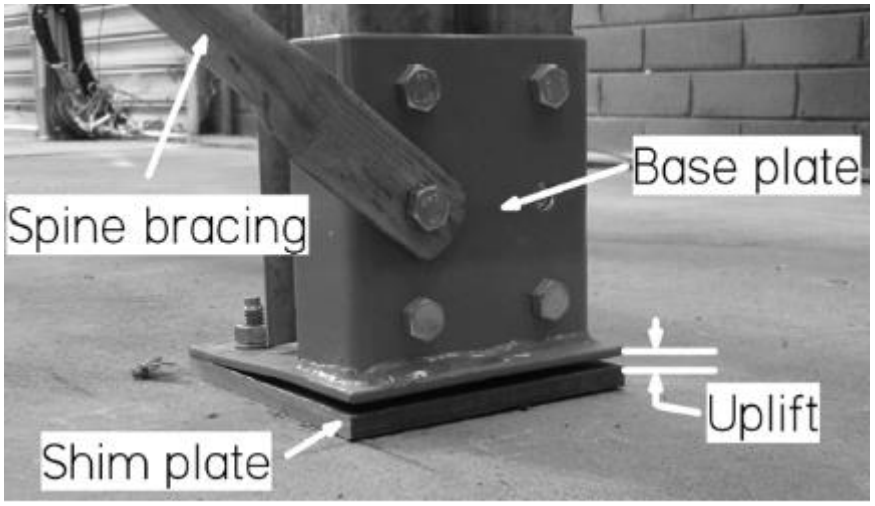

Figure 3.2 Baseplate uplift (from [47]**)**

Uplift behaviour in racking systems, in conjunction with upright base rotation, can occur from two sources. The first of these is when the down-aisle direction is strengthened with supplementary bracing to create a braced selective pallet rack. This mainly resists the down-aisle forces by axial tension and compression in the spine bracing uprights. When the axial force in the upright in tension overcomes the axial compressive force due to the pallet loading, baseplate uplift occurs, as shown in Figure 3.1 (Left). The second form of uplift is from bracing action in the cross-aisle braced frame system. The upright uplift may occur on one upright while the rack frame rotates about the upright base at the other side due to the cross-aisle horizontal seismic action, as shown in Figure 3.1 (Right). Figure 3.2 shows a typical baseplate's floor plate uplift deformations during the full-scale rack tests presented by Gilbert and Rasmussen [48]. In most of the rack assemblies, uplift is more common by the second mechanism, which is in the cross-aisle direction.

Gilbert and Rasmussen [49] claim that the uplift behaviour at the upright base increases the second order P-Δ effect in both mechanisms mentioned above. However, this behaviour may also reduce the force demand of the rack at the upright-base connection and prevent structural collapse from upright buckling under high compression. As evidence, during the 2010 Darfield Earthquake, in the same warehouse, some non-anchored racks walked off their original position and survived the earthquake with no damage, while the racks that failed were anchored [4]. This observation is inconsistent with the requirements of most racking standards and design guidelines, which require baseplate anchorage for dependable seismic resistance. However, such column rocking has been observed in many other types of structure that have survived earthquake events; the earliest reported was after the 1960 Chile M9.5 Earthquake by Housner [39]. He observed that a number of tall, slender structures survived strong earthquake shaking whereas structures appearing more stable were severely damaged. It was noted that, in each of these structures, the base of the structure lifted up from the foundation and started the rocking motion. The researchers initiated the investigation on this rocking behaviour analytically, considering it as an inverted pendulum, and found that there is a scale effect that renders tall, slender structures more stable against overturning than might have been expected. Following this work, the literature now has extensive studies in this behaviour of structures, called rocking or uplift behaviour. It provides types of structural fuse to reduce the internal force and ductility demand on the

system, and provide a more rational and more economical design for a realistic seismic loading condition [40]. Huckelbridge [41] performed 67 shaking table tests for a 9-storey eccentric steel frame, and compared the seismic response of the structure with and without supplementary anchorage of the columns. He concluded that a system with uplift has a large energy absorption capacity in the form of potential energy stored by the mass because of its relative elevation, and this energy reservoir can be more economically exploited than the systems whose total energy absorption capacity is only from internal strain energy. Priestley et al. [42] compared Housner's theory of free rocking of a rigid block with an experimental result and concluded that the rocking mechanism limited the lateral accelerations to the level inducing rocking, as well as limiting the development of the peak base shear force. These findings explain at least in part why unanchored racks survived the Darfield earthquake. These findings also suggested that this feature could be introduced into professional practice in pallet racking system design to enhance its seismic performance.

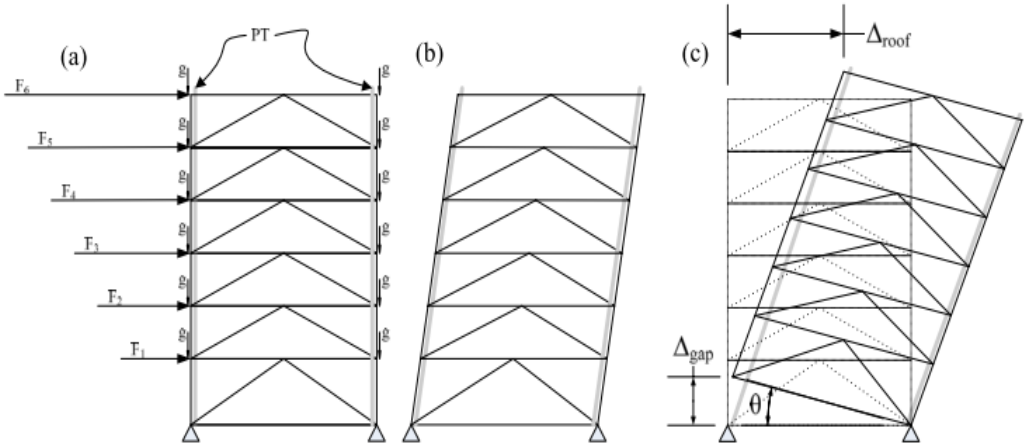

Figure 3.3: SC-CRS system: (a) schematic of members and lateral forces; (b) elastic response prior to column uplift; (c) rigid-body rotation after column uplift

A design concept of self-centring controlled rocking structures (SC-CRSs) has been investigated by a few research teams in different systems [54]–[57], Wiebe and Christopoulos [58] even started a study on multi-storey controlled rocking steel frames. In these structures, the base of selected columns is permitted to uplift from the foundation in response to severe lateral loading, as shown in Figure 3.3: the development of uplift of a typical SC-CRS. It was found that controlled rocking behaviour can reduce the seismic demand of the system and increase the seismic resilience with minimal cost.. The controlled rocking concept in which the base of the structure or selected upright is permitted to uplift from the base in response to severe lateral loading has been included in pallet racking system design,. This achieves a more cost-effective pallet racking system and improves its seismic resistance. The seismic response can be controlled using post-tensioning, and the seismic energy can be dissipated by various types of energy dissipation methods. The most frequently used energy dissipation method is by baseplate metal yielding [42], [59], [60], as shown in Figure 3.4. A ductile yielding baseplate is a mature product in New Zealand industrial, which utilises the principle of controlled rocking combining with steel yielding for energy dissipation, and does achieve a relatively good seismic performance. However, two issues limit the use of this type of baseplate. Firstly, the yielding of the baseplate would likely fracture the steel plate under the great tension uplift force. Secondly, the failure of the connection of the baseplates in a framing system would likely lead to a major loss of lateral

load resistance and end up with overturning or collapsing of the rack. In addition, even if the frame with the yielding baseplates survived a severe seismic event, the baseplates would probably be extensively damaged and have to be replaced. The replacement of the baseplates would be costly, time-consuming, affect the business continuity of the owners, and impact the insurance companies. A more robust baseplate is demanded.

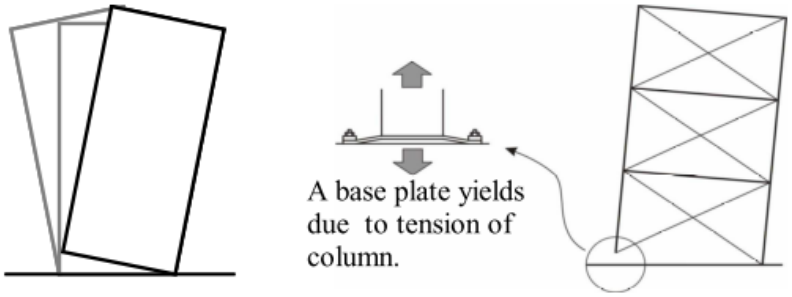

Figure 3.4: Basic conception of rocking structural systems with yielding base plates (from [16])

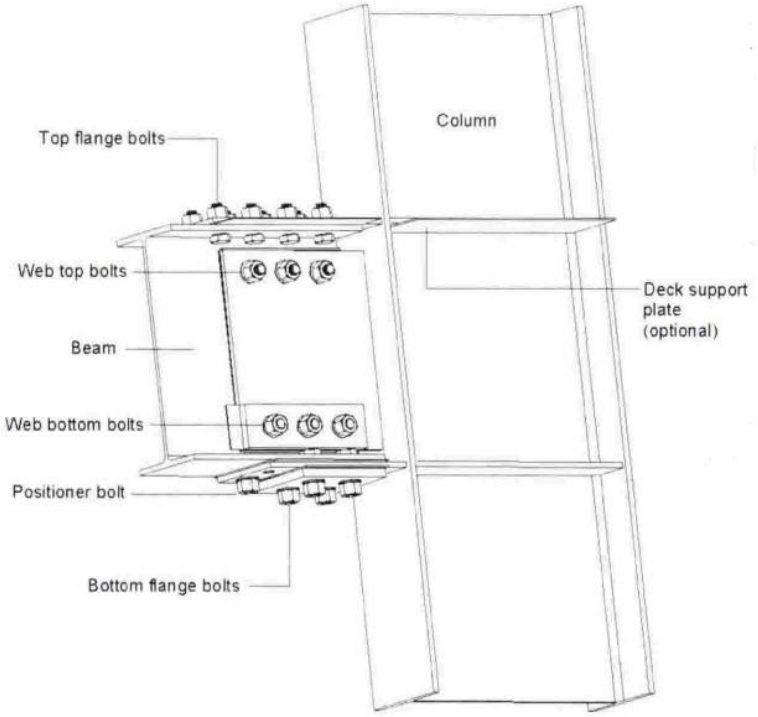

Figure 3.5: Sliding friction joint developed for steel moment resisting frames (from [10])

Clifton [10] developed an innovative sliding friction joint to replace the conventional beam-column connection for steel moment resisting frames, which has been widely used in New Zealand. As shown in Figure 3.5, instead of forming irrecoverable plastic deformation at the beam-column joints, it is designed to be rigid up to the ultimate limit state and to slide under severe seismic events. Energy is dissipated by the friction damper mechanism resulting in minimal damage to the structure. The tightness of the bolt groups connecting the beam and the column can be adjusted to achieve the optimum seismic performance. Apart from the research conducted by Clifton, there are many other studies adopting this as a seismic measure. For example, Loo et al. [53] adopted the slip-friction connector as the seismic energy damper for a rocking timber shear wall; Ormeno et al. [12] adopted the slip-friction connector in the design of rocking liquid storage tanks. All these studies showed that

the slip-friction connector has a large energy dissipation capacity and significantly improves the seismic performance of the structure.

The concept of the sliding friction joint developed by Clifton [10] fits the needs of a proper energy dissipation component for a racking system when applied to the column base. Instead of forming a yielding zone at the baseplate, the sliding friction joint dissipates energy by friction force, similar to a brake on a car.

The energy imparted from an earthquake (E_I) has a few paths it can follow, as shown in Equation 3.1. Firstly, the energy imparted to the racking system (E_I) is converted to the elastic potential energy (E_U) of the structure members to form elastic deformation; the system starts vibration under the seismic excitation and a portion of this energy is converted to kinetic energy (E_K); once a column lifts up, the gravity centre of the system lifts, the gravity potential energy (E_G) of the system increases, as shown in Figure 3.9; if the amount energy imparted to a structure member exceeds the yielding limit, then plastic deformation occurs, this portion of energy (E_B) is dissipated by the material yielding or fracturing; while the structure is vibrating, a small portion of energy is dissipated by material damping (E_M); if there are dampers in the system, for example, metal dampers or friction dampers, a considerable amount of energy (E_D) can be dissipated and converted to internal energy. For pallet racking system, the cold-formed thin-wall members can't sustain plastic hinge deformation without rapid decrement on their capacity, therefore, Plastic deformation (EB) is undesirable and should be avoided in the design of racking system. The material damping in a steel structure (E_M) is negligible. A controlled rocking system with a friction damper can restore some energy as elastic and gravity potential energy (E_U and E_G) to avoid excess energy entering the system to generate plastic deformation of any member, also it can dissipate a significant amount of energy through the friction damper (E_D) impact on the uplift behaviour at column bases.

$$\boldsymbol{E_I = E_U + E_G + E_k - E_B - E_M - E_D}$$

Equation 3.1

The concept of a baseplate with a friction damper is based on the principle described above; the drawing of the proposed baseplate is shown in Figure 3.6. The mode of operation of this joint is relatively simple and the experimental and numerical research that has been undertaken shows it delivers significantly enhanced rocking performance compared with the ductile baseplate currently used to enable rocking. The baseplate consists of two parts: a robust 150 mm high, 5 mm thick C-shape stub welded to a 10 mm thick floor plate. The thickness of these two components allows a robust weld between them. The stub is designed to fit the shape of the upright so they can tightly fit together to achieve proper grabbing and stable friction sliding, as shown in Figure 3.7. The thick stub sitting inside the upright protects the base of the upright from impact damage and also enables the upright to develop very high local stresses from unequal bearing without causing upright failure. The upright is not bolted directly to the stub. The baseplate is connected to the upright through the controlled tightening of a bolt group. The upright is clamped to the inner stub by a bolt (bolts) located partway along the stub length and tightened through the two flange lips of the upright. The friction due to sliding is controlled by the clamping force between the upright and the stub of the baseplate. According to the needs of the design, the friction force and hence the energy dissipation capacity and force demand in the uprights, can be varied by changing the number of bolts and the torque applied

to each bolt. This innovative baseplate is named the friction slipper baseplate (FS baseplate).

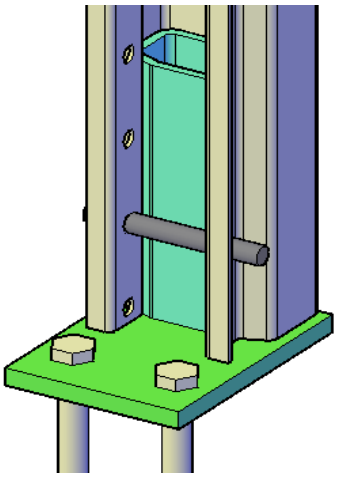

Figure 3.6: Friction slipper baseplate (FBP)

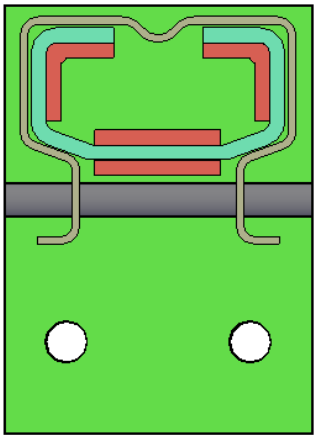

Figure 3.7: Top view of FS baseplate, the red zones are for welding

Figure 3.8 : Failure of the baseplate to upright connection [17]

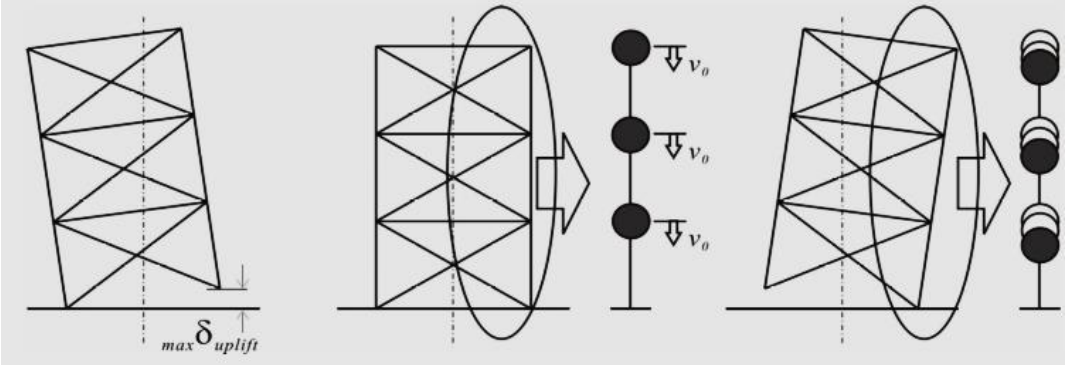

Figure 3.9: Uplift behaviour results in the lifting of the gravity centre

Conventional baseplates are fixed to uprights rigidly with bolts or welding. For these types of upright-base connection, uplift behaviour only occurs at the deformation of the floor plate relative to the base; the upright cannot move relative to the baseplate other than to a minimal extent. Tension force in the upright increases with the increasing deformation of the endplate. With an increase in uplift displacement, the tension demand on the upright, baseplate, and anchorage increase rapidly, which may eventually lead to baseplate fracture or an anchor bolt being pulled out of the concrete floor, as shown in Figure 3.8. The friction slipper baseplate allows the upright to lift up from its baseplate when the tension force exceeds the static friction force limit. The tension force is independent of the relative displacement of uprights and baseplates. With a selected friction force, the tension demand on the upright and base connection can be controlled. Also, limiting the tension uplift force, in turn, limits the increase in compression force developed in the "compression" upright on the other side of the braced frame, reducing the likelihood of failure of that upright due to a too high compression force. The relative displacement and the controlled friction force allow energy induced from ground motion to be dissipated significantly and efficiently through friction force and the impact between the uprights and the base. Both mechanisms can significantly increase the damping ratio and reduce the seismic response of the rack system.

The structural ductility factor, μ is used to evaluate the structure's ductile deformation capacity and is adopted to calculate the seismic resistance of the pallet racking system. The less ductile connection will limit the overall performance of the racking system. The principle behind the calculation of the ductility factor for a component with a plastic hinge is shown in Figure 3.10. It is expected that the friction sliding behaviour of the FS baseplate enables a racking system to exhibit extensive ductile behaviour so as to reduce the seismic demand of the system.

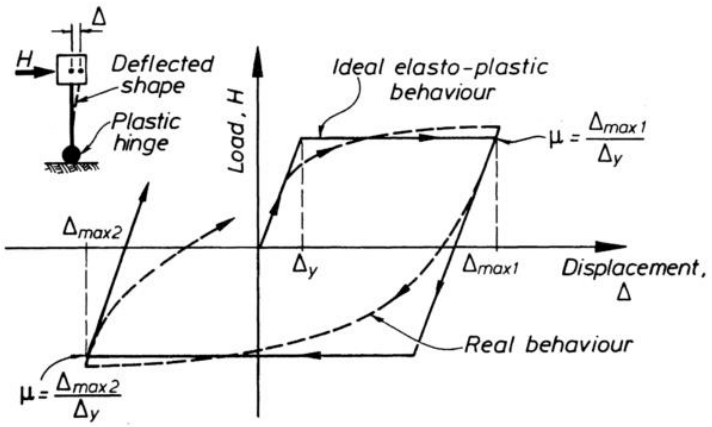

Figure 3.10: Method of calculation of ductility factor (from [7])

Another significant advantage of the friction slipper compared with the ductile baseplate is that while it permits uplift at a carefully controlled force, it prevents lateral movement of the base of the uplifting tension upright. During an earthquake, the columns are subject to high lateral shear, especially in the bottom storey. When the cross-aisle system is not rocking, this shear is resisted by both columns in each cross-aisle braced frame. However, when the system starts rocking, in a ductile baseplate or unanchored baseplate system, the uplifting tension column's ability to transfer this seismic shear reduces, causing more to go into the compression column, increasing the shear and moment demand on the compression column and leading to column failure. By preventing lateral movement of the uplifting column, the FS baseplate allows this column to fully participate in resisting earthquake shear forces when it is uplifting thus providing another layer of protection against failure of the compression column.

A final significant advantage over the ductile baseplate is that the welds between the FS baseplate stub and the baseplate are not connecting members subject to significant plastic rotation; this significantly reduces the likelihood of baseplate weld failure when the ductile baseplate is uplifting.

3.2 Down-aisle consideration

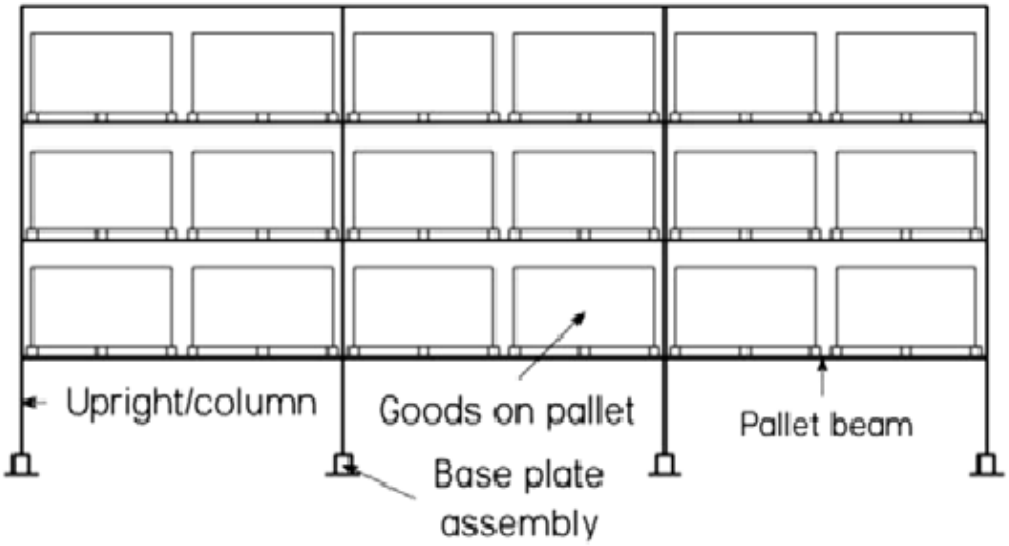

Figure 3.11: Typical storage rack elevation schematic in the down-aisle direction (from[33]**)**

For lateral load resistance, in the down-aisle direction pallet racking systems comprise two types of connections: beam-upright connections and baseplate-upright connections, both are considered to be semi-rigid connections. The stability of a storage rack in the down-aisle direction is significantly dependent on their rotational stiffness and moment resistance. Typically, the connections between the floor and the uprights are achieved by means of a baseplate assembly. The baseplates are usually fixed to the floor with multiple anchor bolts to resist shear and pull-out force. The idealized view of a typical storage rack in the down-aisle direction is shown in Figure 3.11.

In many previous earthquakes, for example, the 1987 Edgecumbe Earthquake, the 2010 Darfield earthquake and the 2011 Lyttleton earthquake, extensive failure of cold-formed steel racking systems has been observed [61][16]. In the down-aisle direction, this is typically due to the damage to one or more of the baseplate-upright or beam-upright connections. This damage arises when the peak ground accelerations are higher than the design values. Research by Hoogeveen [14], on conventional selective pallet racking systems in the down-aisle direction, has shown that the lower threshold for the collapse is peak ground acceleration (PGA) greater than 1.3 times the design PGA. This is in contrast to modern steel frame buildings, which delivered an excellent response in earthquakes with PGA of over 2.5 times the design value [16].

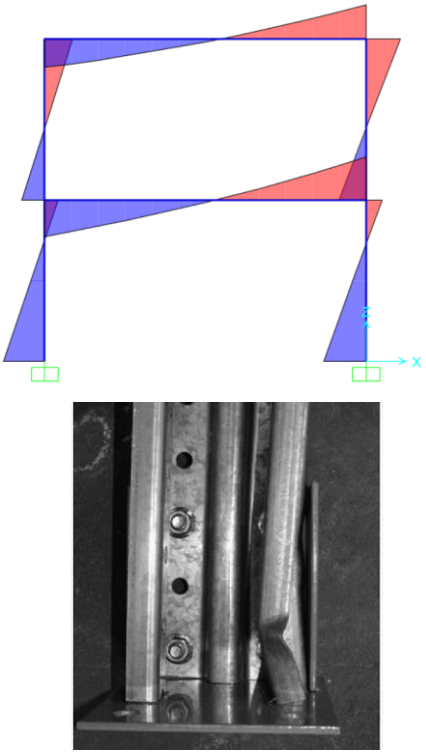

Figure 3.12: Fixed baseplate connection moment diagram and typical failure at upright column

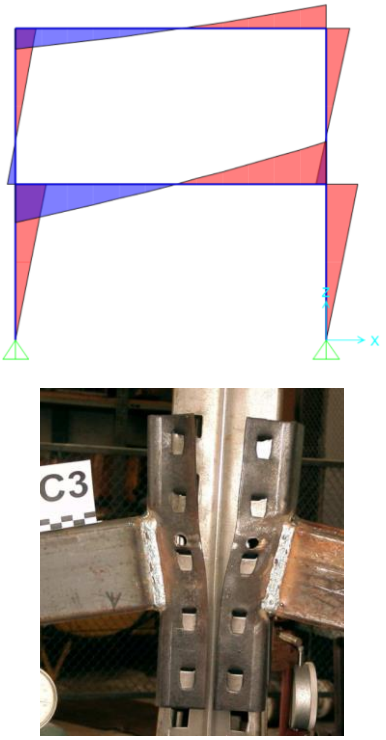

Figure 3.13: Pin baseplate connection moment diagram and typical failure at the beam-upright connection

The baseplate-upright connections are typically considered as semi-rigid connections. The rotational stiffness varies with different types of baseplate-upright connection. For conventional connections, if baseplates are designed to be sufficiently robust, they are referred to as rigid baseplates (RBP), with a large rotational stiffness approaching that of a rigid connection. Failure is initiated by the formation of local buckling at or near the base of the upright, an example of which is shown in Figure 3.12. If the baseplates are too flexible, with a small rotational stiffness which is closer to a pin connection, then the lowest beam-upright connection may suffer fracture failure due to the large moment, as shown in Figure 3.13. Both baseplate-upright and beam-upright connection failure will generate a system failure if the pallet racking system is deformed significantly into the inelastic range in a severe earthquake.

The baseplates with large rotational stiffness are well studied and are widely adopted on the world market. This type of baseplate is designed to be very rigid in both the down-aisle and cross-aisle directions. The ductile yielding baseplate (DBP), which has very small rotational stiffness, is adopted widely in New Zealand industrial storage. It gives good seismic performance in the cross-aisle direction by dissipating seismic energy through steel plate yielding under the uplift behaviour, allowing controlled rocking in the cross-aisle direction. This baseplate-upright connection with the ductile design concept can potentially lead to a low-cost and low-damage racking structure in the cross-aisle direction, as further described in Section 3.1. However, the high flexibility of this type of baseplate has the column base connection effectively pinned in the down-aisle direction, which means the down-aisle direction design will require a large moment demand at the beam-upright connections close to the base. Increasing the rotational stiffness of the baseplate in the down-aisle direction,

especially when the upright is under little or no axial compression load, will put the column in the bottom storey into reverse curvature, reducing the moment demand on the column at the bottom beam level and reducing the curvature demand on the beam to column semi-rigid connection. This will significantly raise the seismic resilience of the overall system.

The friction slipper baseplate (FBP) is developed to have sufficient stiffness and moment resistance to improve the down-aisle direction seismic performance, while having an excellent cross-aisle direction seismic performance compared with both rigid baseplates and ductile baseplates.

The drawings of three types of baseplates are shown below:

A typical rigid baseplate is shown in Figure 3.14, with a thick floor plate (10 mm thick) and a steel C-section (5 mm thick) fixed to upright with 4 bolts at the front;

A ductile yielding baseplate is shown in Figure 3.15, with a thinner (3.5 mm thick) and more ductile floor baseplate and a 3.5-mm thick C section bolted to uprights with 1 bolt at the back.

A friction slipper baseplate is shown in Figure 3.16, with a 10 mm thick floor plate and a C-shaped 5 mm thick inner stub bolted to the uprights. The clamping force is controlled by adjusting the number of bolts and the torque applied to them.

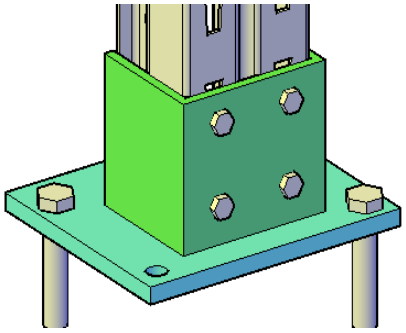

Figure 3.14: Typical rigid baseplate (RBP)

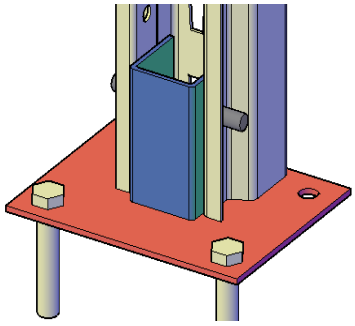

Figure 3.15: Ductile yielding baseplate (DBP)

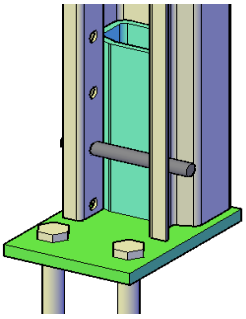

Figure 3.16: Friction slipper baseplate (FBP)

The geometric and material properties of a baseplate determine its rotational stiffness, rotation capacity, ultimate moment resistance and ductility. Several baseplate investigated in previous studies on the performance of the baseplate-upright connection in the down-aisle direction are cited in references [33][62][31][63], and shown in Figure 3.17. These baseplates perform in a rigid connection manner and do not allow uplift to occur.

All these studies indicate that rotational stiffness and moment resistance of all types of baseplate-upright connections change significantly with varying axial loading, which represents the gravity loading of pallets on a rack. Overall, when an axial load is applied, at between 0-60% of the ultimate upright axial compressive capacity, the moment resistance increases with the increase in applied axial load. However, if the axial load is so large that it is close to the upright's ultimate compressive capacity, the baseplate-upright connection is likely to fail in a small rotation angle at the upright by local buckling, as shown in Figure 3.12. The ultimate moment resistance is reached at a smaller axial loading. Experimental results from previous research [33] show that the baseplate rotational stiffness, measured as the tangential stiffness in the elastic range of behaviour, can increase 40 times from 0 kN axial loading case to 100 kN axial loading case, and the moment resistance can increase for over 10 times. For the DBP, which is designed and detailed to allow the rack frames to rock in the cross-aisle direction with uplift of the column in tension, the rotational stiffness on the tension column side drops

to zero. This leads to a significant reduction in the moment resistance of the rack frame in on the tension column side, meaning that the column in compression from cross-aisle action also must resist significant base moment developed from down aisle action. This phenomenon has been shown conceptually to lead to column failure for the rack frames with baseplates that allow uplift [16], and this has also been observed in the field.

As can be seen, the ultimate rotation capacity in most of these studies is in the range of 0.07 rad or smaller. This is because the ultimate rotation capacity of the beam-upright connection is roughly in the same range. If the rotation angle at either the baseplate-upright or beam-upright connection exceeds this range, the other connection will have to carry a much more significant moment demand, which will lead to failure on that connection.

In this research, both DBP and FBP connections allow the rack frame to uplift. They were tested with a wide range of axial loading to produce a relationship for designers between axial loading and the down-aisle moment-rotation characteristic, as further described in Chapter 4.

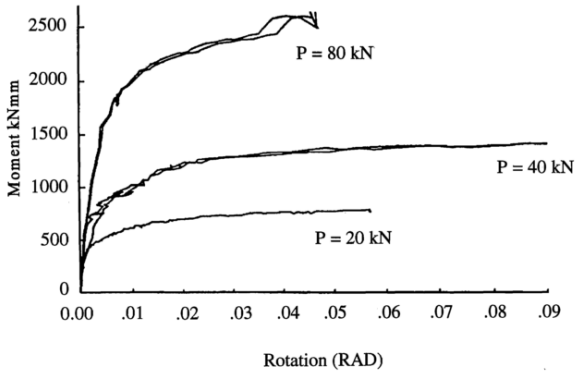

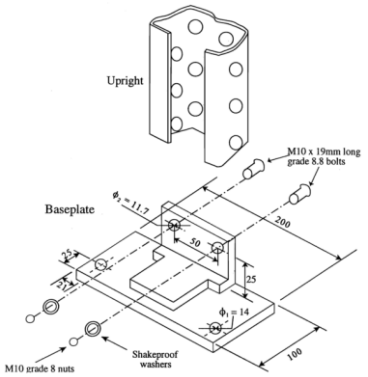

From [31]

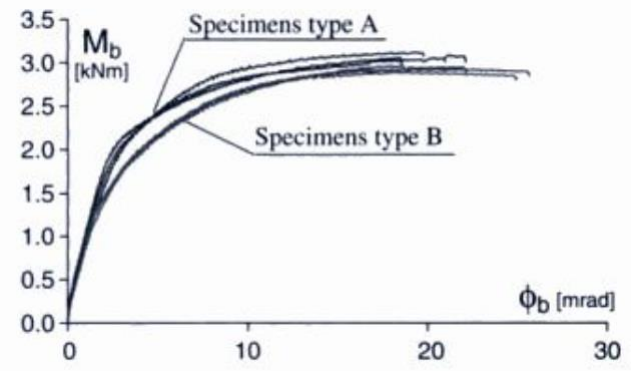

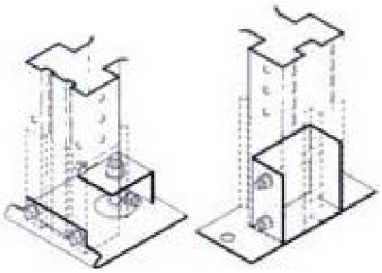

From [62]

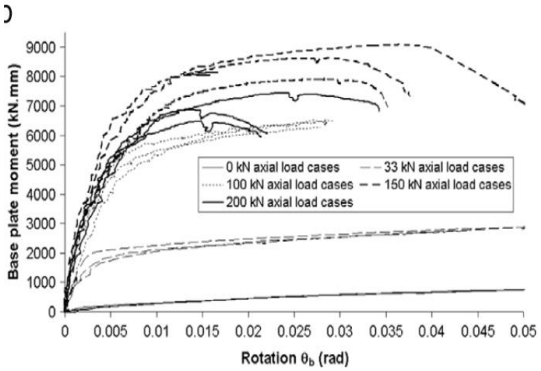

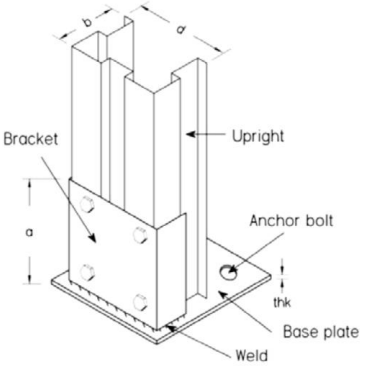

From [33]

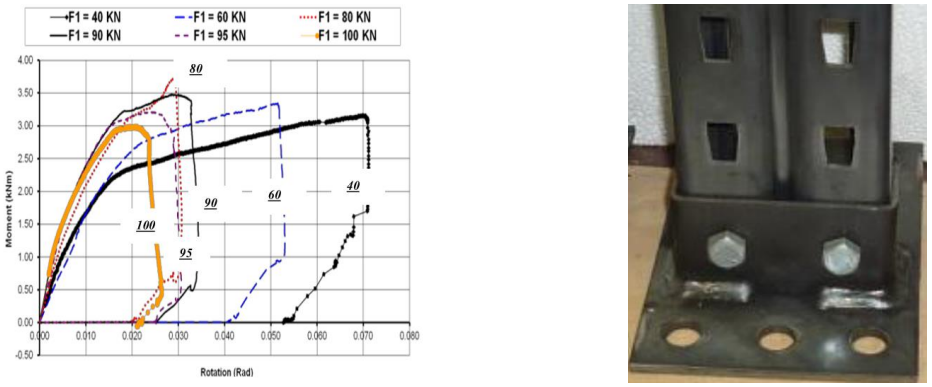

From [63]

Figure 3.17: Previous studies on the baseplate-upright connection moment-rotation tests and the baseplate drawings

3.3 Conclusions

A new, innovative type of seismic resisting system baseplate, the friction slipper baseplate, is proposed. The design concept is described. The friction slipper baseplate brings the following significant benefits to the rack system:

1. The friction slipper baseplate allows engineers to nominate a maximum uplift force which will not be exceeded under high earthquake-induced uplift demands, thus limiting the uplift forces to within the anchor bolt capacity even for a weak floor slab.
2. Use of the friction slipper baseplate can significantly increase the ductility of the racking system.
3. The friction slipper baseplate provides more protection to the column base against operational damage than any other baseplate system.
4. The friction slipper baseplate can provide a rotationally stiffer base-upright connection in the down-aisle direction, thereby putting the column into reverse curvature and significantly reducing the moment demand on the column and beam at the lowest beam level.
5. The ultimate moment capacity of a friction slipper baseplate can be significantly larger than the ductile yielding baseplate.
6. By encasing the column around a rigid stub, the friction slipper baseplate provides protection to the base of the column against section failure due to local buckling or yielding at the base and also against in-service damage from impact loading during operation. While the latter is not a direct benefit in terms of enhanced seismic resilience, it is in terms of reducing the operational costs of the racking system in service.

Chapter 4 Component tests

4.1 Baseplate cross-aisle cyclic tests

A series of component tests have been conducted to determine the uplift behaviour of the friction slipper baseplate. The influence of different bolt configurations, i.e., torque values & number of bolts, on the friction force, and different loading rates on the uplift stiffness are investigated. The test results show that the friction slipper baseplates can develop a wide range of bolt tightened friction forces with different bolt configurations and that this is controllable and stable under a wide range of loading rates.

4.1.1 Introduction

To improve the seismic resistance for a pallet racking system, a design concept of controlled rocking structures has been developed in which the base of the structure or selected upright is permitted to uplift from the base in response to severe lateral loading. A friction damper mechanism has been adopted in order to dissipate energy and to deliver significantly enhanced rocking performance compared with the ductile baseplate currently in use. Friction due to sliding between the baseplate and the upright is introduced via a controlled clamping force between the upright and a stub welded to the baseplate. The clamping force is related to the tightening torque and the number of bolts connecting the baseplate to the upright. Figure 4.1 illustrates the concept. A 150-mm-high 5-mm-thick C-shaped inner stub is welded to a 10-mm-thick floor plate. The thickness of these two components allows a robust weld between them. The upright is clamped to the inner stub by the bolt located partway along the stub length and tightened through the two flange lips of the upright. The upright is not bolted directly to the stub. The thick stub sitting inside the column protects the base of the column from impact damage and also enables the column to develop very high local stresses from unequal bearing without causing column failure. According to the needs of the design, the friction force can be varied by changing the number of bolts and the torque applied to each bolt. By adjusting the tightening torque of the bolts, using a torque wrench, the energy dissipation capacity and force demand in the uprights can be suited to the design needs. This innovative baseplate is named as the friction slipper baseplate.

Conventional baseplates are fixed to uprights rigidly with bolts or welding. For this type of upright-base connection, uplift behaviour only occurs at the deformation of the floor plate relative to the base; the upright is not able to move relative to the baseplate other than to a very limited extent. Tension force in the upright increases with the increasing deformation of the endplate. With an increase in uplift displacement, the tension demands on the upright, baseplate and anchorage increase rapidly, which may eventually lead to baseplate fracture or the anchor bolt being pulled out of the concrete floor, as shown in Figure 4.3. The friction slipper baseplate allows the upright to lift up from its baseplate when the tension force exceeds the static friction force limit. The tension force is independent of the relative displacement of uprights and baseplates. The tension demand on the

upright and base connection can be controlled by selection of the proper friction force. Also, limiting the tension uplift force, limits the increase in compression force developed in the "compression" upright on the other side of the braced frame, reducing the likelihood of failure of that upright due to too high compression force. The relative displacement and the controlled friction force between the uprights and the base enables the energy induced from ground motion to be dissipated significantly and efficiently; this then significantly increases the damping ratio and reduces the seismic response of the rack system.

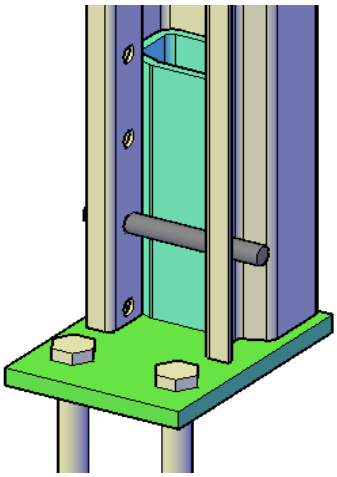

Figure 4.1: Friction slipper baseplate

Figure 4.2: Cross-aisle direction collapse of pallet racking system [5]

Figure 4.3: Failure of baseplate to upright connection [17]

Another significant advantage of the friction slipper compared with the ductile baseplate is that while it permits uplift at a carefully controlled force, it prevents lateral movement of the base of the uplifting tension column. During an earthquake, the columns are subject to high lateral shear, especially in the bottom storey. When the cross-aisle system is not rocking, this shear is resisted by both columns in each cross-aisle braced frame. However, when the system starts rocking, in a ductile baseplate or unanchored baseplate system, the uplifting tension column's ability to transfer this seismic shear reduces, causing more to go into the compression column, increasing the shear and moment demand on the compression column and leading to column failure. By preventing lateral movement of the uplifting column, the FS baseplate allows this column to fully participate in resisting earthquake shear forces when it is uplifting, thus providing another layer of protection against failure of the compression column.

A final significant advantage over the ductile baseplate is that the welds between the FS baseplate stub and the baseplate are not connecting members subject to significant plastic rotation; this would significantly increase the likelihood of baseplate weld failure when the ductile baseplate is uplifting.

In order to achieve the design concept, the uplift behaviour of the friction slipper baseplate and the behaviour of the friction damper mechanism must be known. The relationship between the friction force and the number & torque of bolts applied, and the influence of the loading rate needs to be experimentally determined. Additionally, the effect of bolt torque decay is discussed.

4.1.2 Methods

This test has comprised a series of component tests to determine the uplift behaviour of the friction slipper baseplate. Component tests with a wide range of bolt configuration have been conducted with a wide range of loading rate. The bolt configuration for each test was selected in sequence from a set of combinations of 1, 2, 3 bolts and 25, 30, 35 Nm of torque, respectively. Each of the 9 bolt configurations was tested under 5 loading rates of 1, 4, 8, 16, 32 mm/s and repeated for 3 cycles in a maximum uplift displacement of 64 mm.

The test setup is shown in Figure 4.4. A 500 mm long, 90 mm wide, 2 mm thick upright was adopted for this component test. The upright was rigidly fixed to an actuator with four bolts at the top and connected to the friction slipper baseplate with the selected bolt configuration at the bottom. The baseplate was then bolted to a steel block with two M10 bolts.

Vertical cyclic loading was applied along the neutral axis of the upright and vertical displacements are recorded at both sides of the upright using two Linear Variable Differential Transformers (LVDTs) ($\delta_1 \; and \; \delta_2$) were symmetrically positioned about the upright neutral axis. An averaged displacement value was taken for analysis. One LVDT was placed in front of the upright to measure the deformation of the floor plate. A load cell was embedded in the actuator to monitor the force response during the testing. After a set of 5 loading rates was completed, with 3 cycles for each rate, the bolt configuration was adjusted for the next test. A temperature sensor was attached on the outer surface of the upright to measure the change of the temperature of the specimen during the friction sliding.

After the above test series were completed, a group of 5 sets of 10 cycles of cyclic loading under 32 mm/s of loading rate were applied to the specimen without re-tightening the bolts during the loading. The decay of the friction force was monitored and reported.

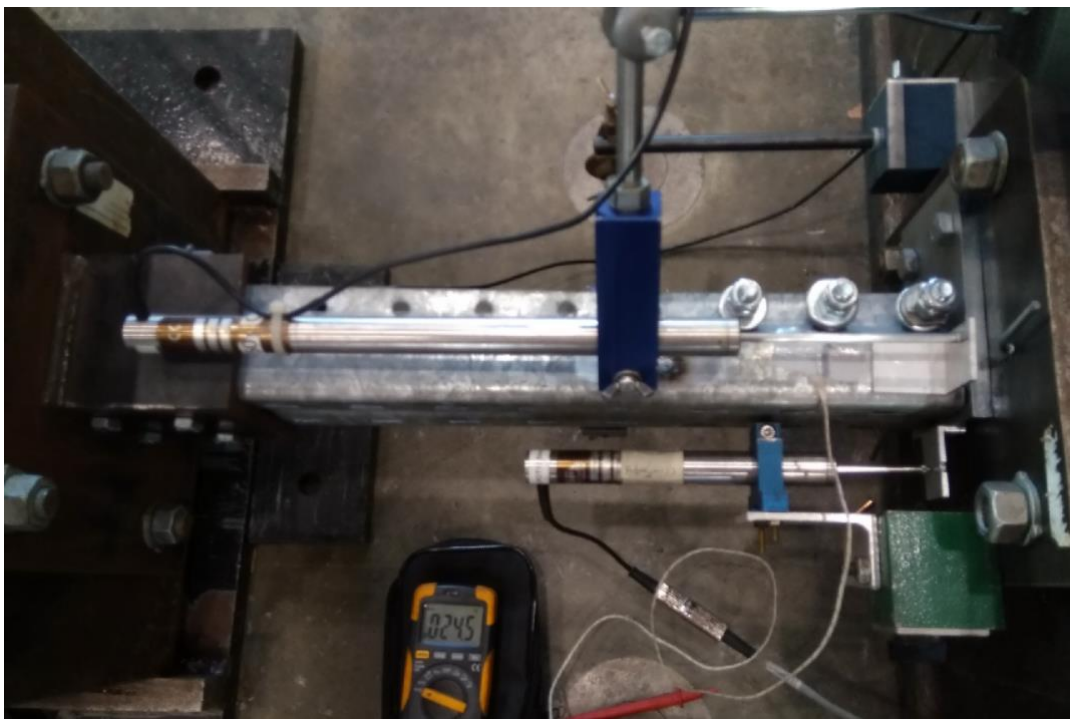

Figure 4.4: A photo of the test setup

4.1.3 Results

After all the cyclic loadings were conducted, the upright and baseplate were disassembled and inspected for damage. As shown in Figure 4.5: Specimen after the testing: contact surface of the (a) friction slipper baseplate; (b) inside of upright , three regions of scratches can be found at the contacting surface of both the upright and the baseplate at the front, side and back surface, the thicknesses of the steel are marked on the figure. The severest abrasion is on the front of the baseplate (0.2 mm or 4%) and the back of the upright (6.5%). It is important to note that these abrasions are from an accumulated result of more than 200 cycles of uplift; whereas a severe earthquake will typically generate less than $1/10^{th}$ of this number. No noticeable permanent deformation is found at the floor plate.

The force-displacement curves for a series of cyclic tests conducted with one, two and three bolts tightened to a torque of 30 Nm are shown in Figure 4.6. It can be seen that the friction force for all the cases is effectively stable with changing of displacement within the range of uplift tested. The test results show clearly that the friction force of the friction baseplate can be developed to a selected value by changing the number of bolts and torque applied to each bolt. The performance of the friction slipper baseplate is stable and repeatable over several cycles within the testing range.

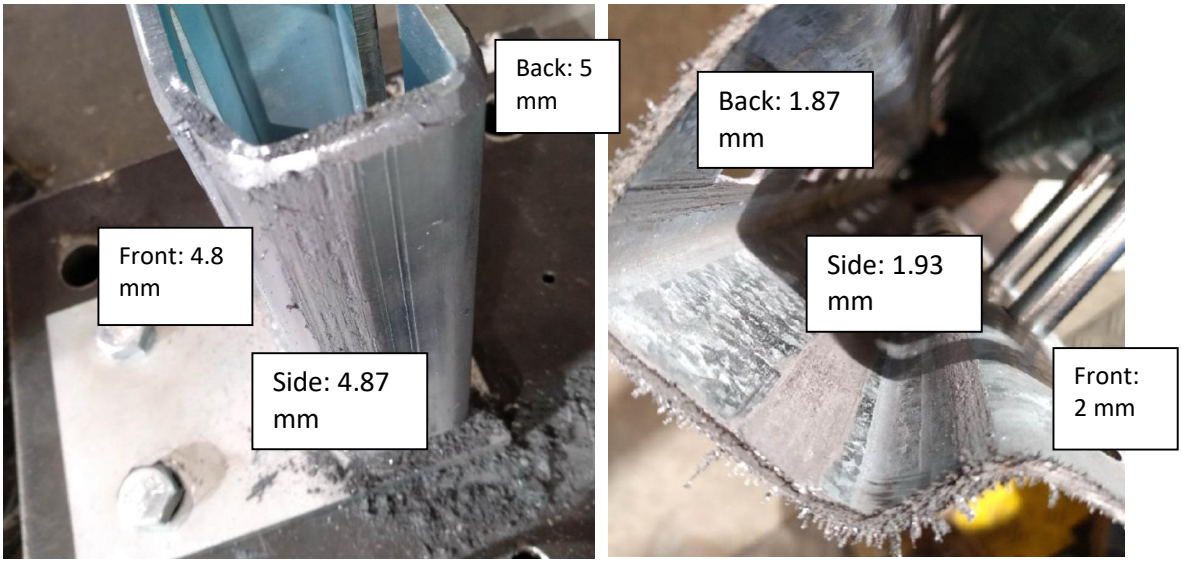

Figure 4.5: Specimen after the testing: contact surface of the (a) friction slipper baseplate; (b) inside of upright

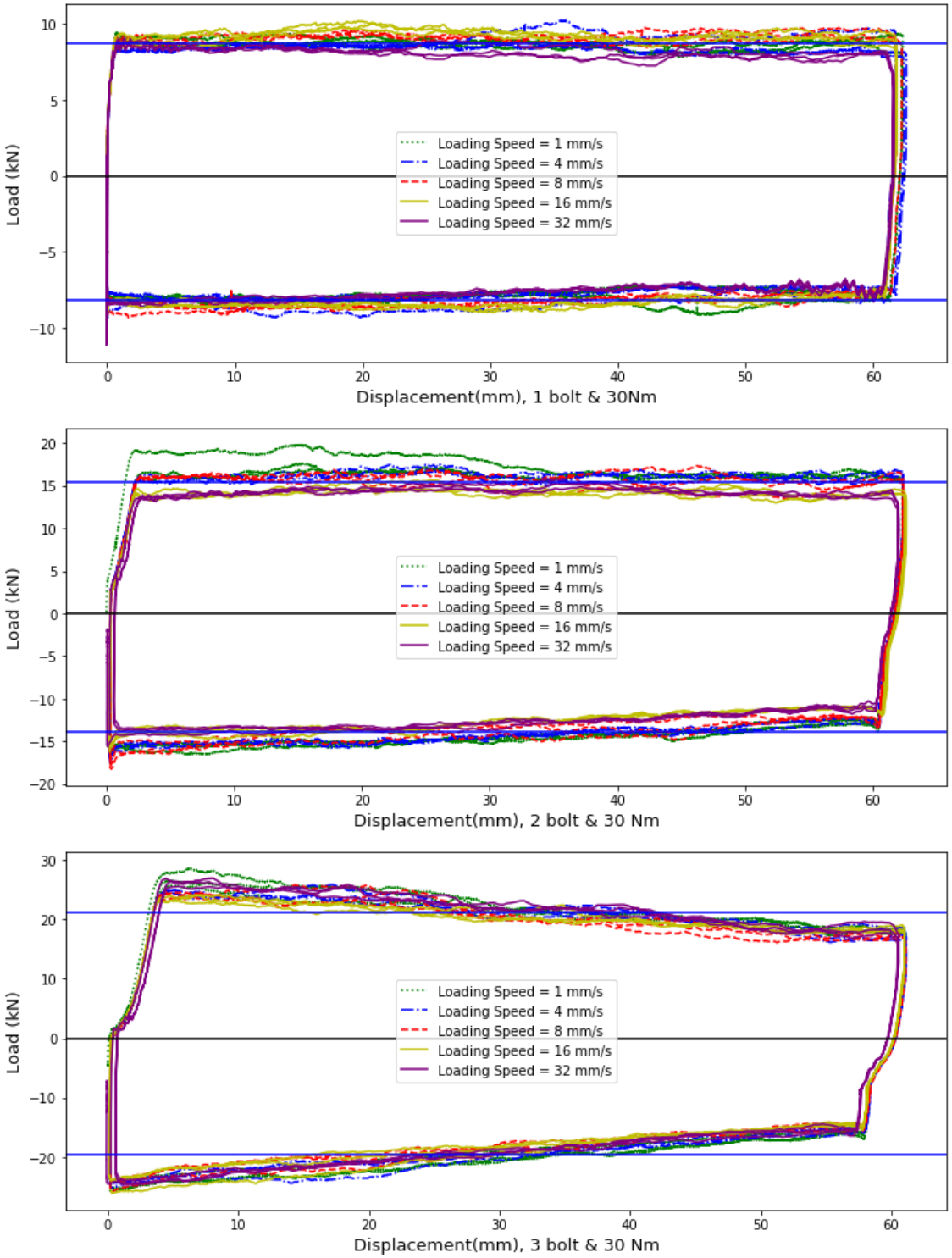

Figure 4.6: Load-displacement curves for varying loading speed with different bolt configurations: (a) 1 bolt & 30 Nm; (a) 2 bolts & 30 Nm; (a) 3 bolts & 30 Nm;

The load-displacement curves can be divided into 5 stages:

Stage 1, the floor plate deforms elastically due to the upright pull-up force and a very small uplift develops between the baseplate and the floor.

Stage 2, the pull-up force reaches the static friction limit, the upright starts to slide along the inner stub with a stable friction force provided by the bolt clamping, the uplift between the baseplate and the floor remains unchanged, and the uplift between the upright and the baseplate starts to develop.

Stage 3, the uplift reaches the maximum value, and then the actuator starts to reduce the pull-up force and then applies a compression force instead. The very small uplift between the baseplate and the floor closes and a compression force develops.

Stage 4, the upright starts to slide again when the friction force reaches the static friction limit, reducing the uplift between the upright and the baseplate.

Stage 5, the upright returns to bearing on the baseplate and foundation, with all the uplift closed. If the compression force continued to increase, the upright would carry a rapidly increasing compression load.

Figure 4.7 gives a comparison between 3 typical bolt configurations with the same loading rate. Interestingly there is a slight negative slope to the load with increasing displacement, especially at the higher installed bolt friction. The reason for this is not known but is probably due to the area of the contact surfaces decreasing as the uplift increases, especially at the top of the inner stub, which generates the friction sliding resistance. Reduced contact surface means less stress and hence less friction force with increasing uplift. Despite this, it is clear that the greater the installed bolt friction, the larger is the area enveloped, which means that larger energy dissipation capacity can be provided by the connection.

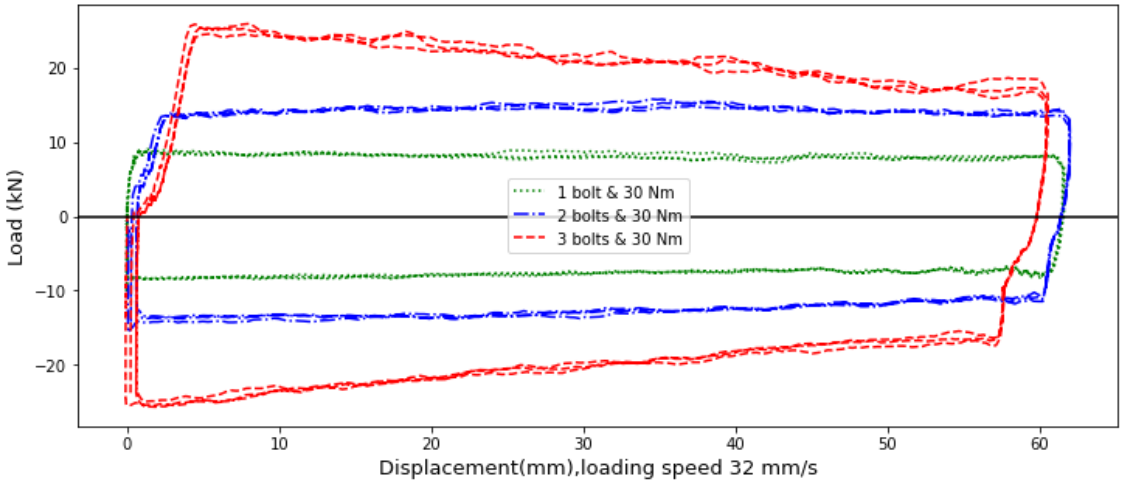

Figure 4.7: Load-displacement curve for loading speed = 32 mm/s with different bolt configurations

The uplift stiffness is depending on the geometry properties of a baseplate assembly, i.e. the thickness of the floor plate, the distance between the anchor bolt to the upright and the bolt configuration, etc. The uplift stiffness k_{uplift} is defined as:

$$k_{uplift} = \frac{F}{\frac{\delta_1 + \delta_2}{2}}$$

Where F is the force measured by the load cell embedded in the actuator and δ_1 and δ_2 are the recorded displacements of LVDT 1 and 2 for both sides of the upright respectively. The baseplate uplift stiffness is around 5 kN/mm $\pm$20% in its elastic range i.e., at Stage 1 above.

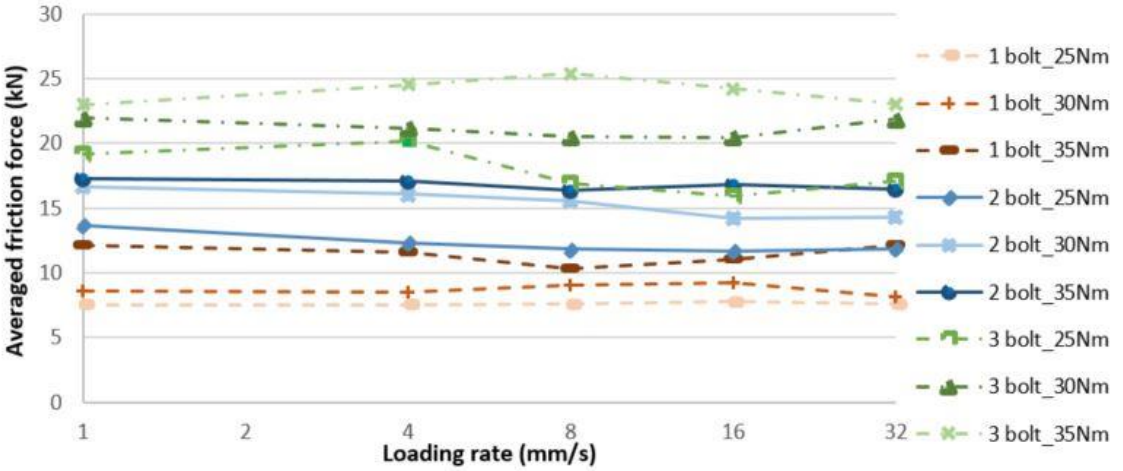

Figure 4.8: The influence of loading rate on the averaged friction force for all bolt configurations

Figure 4.8 demonstrates the influence of the loading rate on the friction force for all 9 bolt configurations. An averaged tension friction force is taken for each loading rate and bolt configuration. As can be seen, the averaged friction force does not change significantly with changes in loading rate.

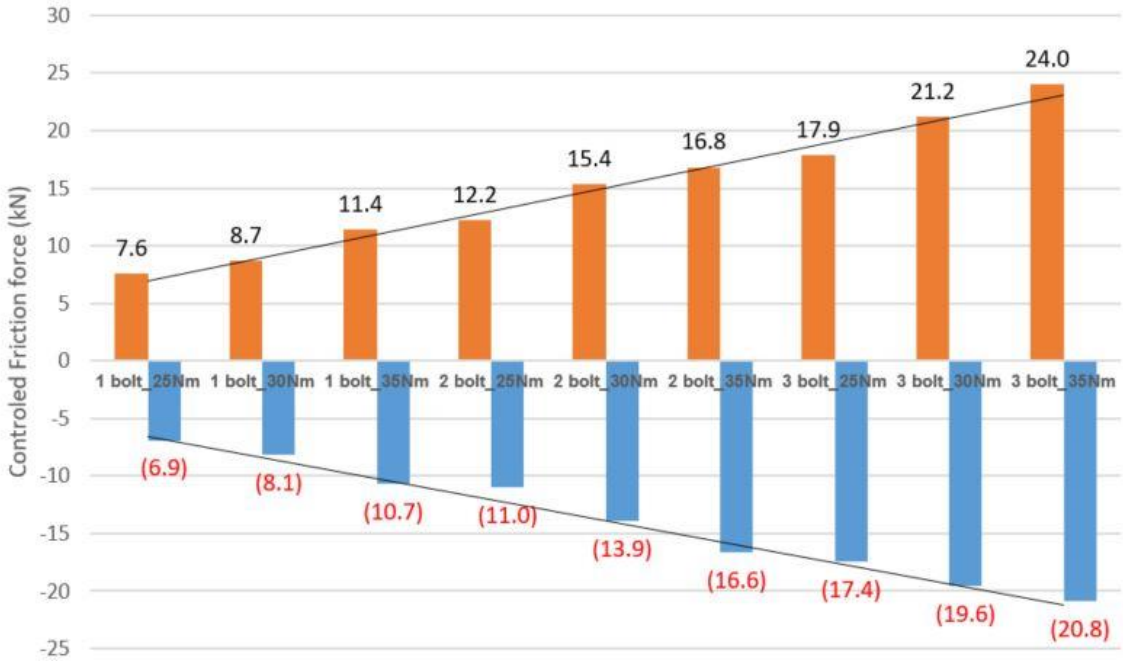

Figure 4.9: Bolt configuration VS Friction force

Figure 4.9 plots the controlled friction force corresponding to each bolt configuration. The 9 combinations of the numbers of bolts and the torque applied to the bolts provide an extensive controlled friction force range, from 7.6 kN to 24 kN that engineers can choose from when designing racking systems with friction slipper baseplates. It should be noted that the difference between two adjacent controlled friction forces is reasonably small and the overall changing slope is reasonably smooth. It is interesting to observe that the tension friction force is always slightly larger than the compression friction force. The main reason for this phenomenon is the geometry of both the upright and the baseplate inner stub. When the upright is being pulled away from the baseplate, the tension force is tending to close the C-section opening of the upright, which will increase the friction force; however, when the upright is being compressed to the baseplate, the compression force is tending to

open up the C-section. Additionally, the surface condition was found to be important to the controlling of the friction force. The tests conducted in this section was on the friction slipper baseplates with electroplating surface. The tests conducted in Chapter 5 was on the friction slipper baseplates with black steel finish surface. It is found that the electroplating surface is smoother and results in slightly smaller friction force with slightly more stable friction sliding behaviour.

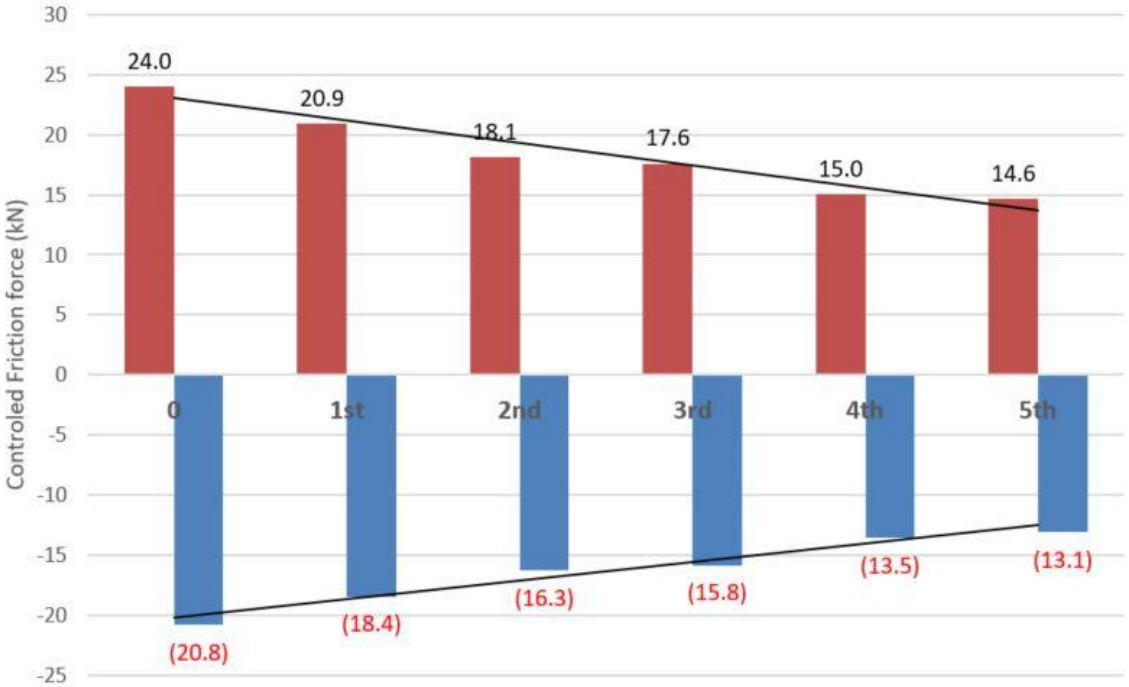

Figure 4.10: Friction force decaying without re-tightening the bolts after each loading

Since the friction force is provided by the bolt torque applied to the uprights, the decay of the torque may reduce the friction force, especially after a severe earthquake. A concern has been raised about the influence of torque decay on the bolts after a set of cyclic loading. Figure 4.10 plots the controlled friction force corresponding to each set of cyclic loading, repeated without retightening the bolts. As can be seen, the decay of the controlled friction force is noticeable but not structurally significant. Even after 5 sets of 10 cycles of uplift, the friction force remains over 60% of capacity. In practice, this means that the bolts would not need to be retightened after one severe earthquake or severe earthquake series, but this might be considered after two or three severe earthquakes or severe earthquake series. Such an occurrence is statistically highly unlikely for any given pallet racking system.

As a friction damper, the temperature effect from the controlled sliding was measured to determine whether it is significant. It was observed that in 10 cycles of loading with 3 bolts & 35 Nm of torque, the upright surface temperature increased by up to 30 degrees C, which will not influence the load-deflection response.

4.1.4 Conclusions

This report presents the key findings of an experimental investigation to determine the uplift behaviour of the innovative friction slipper baseplate. The following conclusions can be drawn:

1. The friction slipper baseplate can generate stable, controlled friction within the range of uplift tested.
2. The damage or abrasion on the baseplates and the uprights tested, after a massive amount of cycles of uplift, is still reasonably small.
3. The baseplate uplift stiffness is around 5 kN/mm in its elastic range.
4. A wide range of controlled friction force can be generated by changing the bolt configuration. Additionally, since the friction force can be selected from a reasonably wide range, according to engineers' needs, the application of the friction slipper baseplate allows those warehouses with a fragile concrete floor to install a racking system with a much larger capacity.
5. The influence of the loading rate on the friction force is found to be negligible.
6. The decay of the controlled friction force after a set of cyclic tests is reasonably small, which means no urgent retightening is required after an earthquake. The retightening work can be done in the next annual inspection.

4.2 Baseplate down-aisle moment-rotation tests

Both the ductile yielding baseplate and the friction slipper baseplate, have been tested to determine the moment-rotation characteristics between uprights and baseplates in the down-aisle direction of rotation. The tests were in accordance with Eurocode EN 15512:2009 [64], with test setup modification to the support conditions for one of the actuators as described in Section 4.2.3; as per the test method proposed by *Gilbert and Rasmussen 2011* [33]. The rotational stiffness, ultimate moment resistance, moment-rotation curves and failure mode of both types of baseplates are reported. The test results show that the moment resistance and the rotational stiffness of the ductile baseplates change significantly with the pre-loaded axial compression on the uprights. The friction slipper baseplate shows larger moment resistance as compared to ductile baseplates for all levels of axial loading, with the rotational stiffness being neither too rigid nor too flexible to adversely affect the frame performance in the down-aisle direction.

4.2.1 Introduction

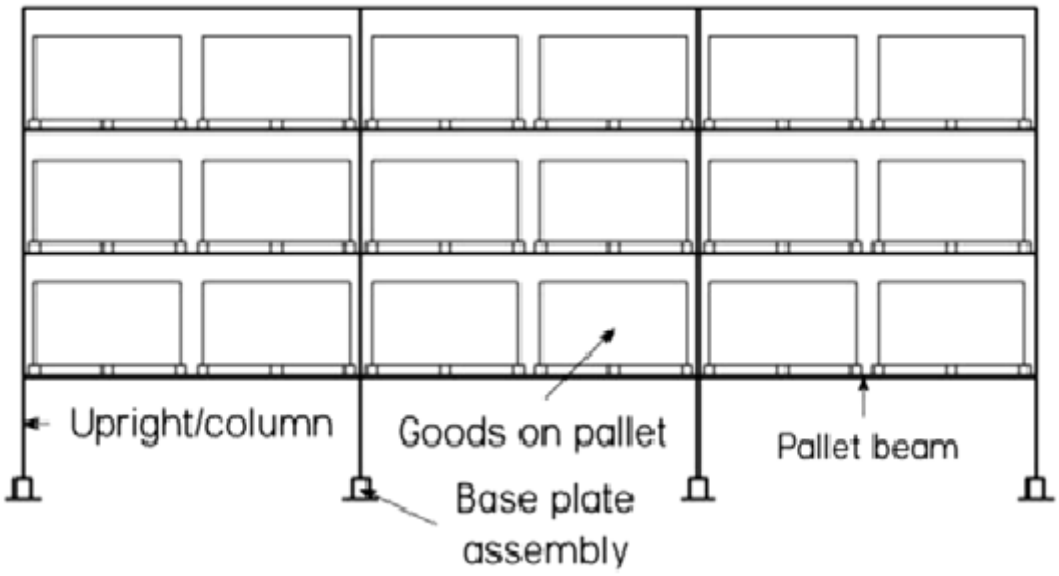

Figure 4.11: Typical storage rack elevation schematic in the down-aisle direction (from [33]**)**

Storage racks are mainly made from light gauge, thin-walled cold-formed steel profiles. There are two principal directions considered for designing pallet racking systems: the down-aisle direction and the cross-aisle direction. For lateral load resistance in the down-aisle direction, pallet racking systems comprise two types of connections: beam-upright connections and baseplate-upright connections, both are considered to be semi-rigid connections. The stability of a storage rack in the down-aisle direction is significantly dependent on its rotational stiffness and moment resistance. Typically, the connection between the floor and the upright is achieved by means of a baseplate assembly. The baseplate is usually fixed to the floor with multiple anchor bolts to resist shear and pull-out force. In this study, the research interest focuses on the performance of baseplate assemblies in their down-

aisle direction. The idealized view of a typical storage rack in the down-aisle direction is shown in Figure 4.11.

Extensive failure of cold-formed steel racking systems has been observed [61][16] in many previous earthquakes, for example the 1987 Edgecumbe Earthquake, the 2010 Darfield earthquake and the 2011 Lyttleton earthquake. In the down-aisle direction, this is typically due to the damage to one or more of baseplate-upright or beam-upright connections. This damage arises when the peak ground accelerations are higher than the design values for the structure. Research on conventional selective pallet racking systems in the down-aisle direction, has shown that the lower threshold for collapse is peak ground acceleration (PGA) greater than 1.3 times the design PGA [5]. This is in contrast to modern steel frame buildings, which delivered an excellent response in earthquakes with PGA of over 2.5 times the design value [16].

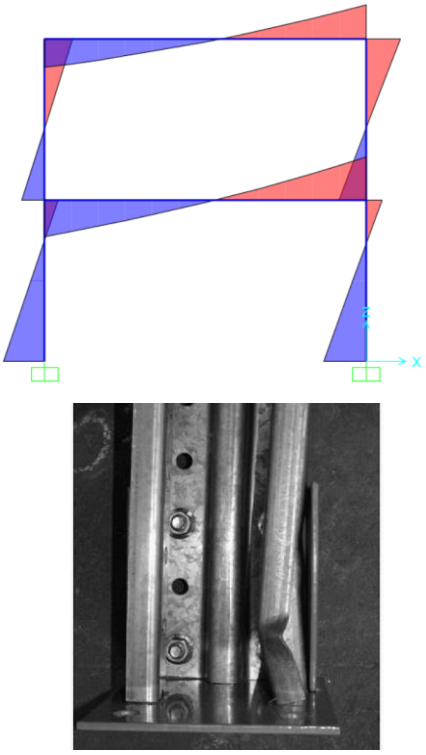

Figure 4.12: Fixed baseplate connection moment diagram and typical failure at upright column

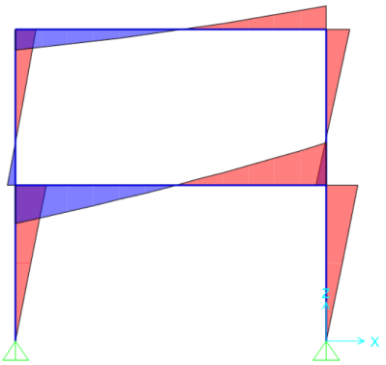

Figure 4.13: Pin baseplate connection moment diagram and typical failure at beam-upright connection

The baseplate-upright connections are typically considered as semi-rigid connections. The rotational stiffness varies with the different types of baseplate-upright connection. For conventional connections, if baseplates are designed to be sufficiently robust, with a large rotational stiffness approaching that of a rigid connection, failure is initiated by the formation of local buckling at or near the base of the upright, as shown in Figure 4.12. If the baseplates are too flexible, with a small rotational stiffness, closer to that of a pin connection, then the lowest beam-upright connection may suffer fracture failure due to the large moment, Figure 4.13. The result of either baseplate-upright or beam-upright connection failure will generate a system failure if the pallet racking system is deformed significantly into the inelastic range in a severe earthquake.

Baseplates with large rotational stiffness are well studied and are adopted by the market world-wide.

This type of baseplate is designed to be very rigid in both the down-aisle and cross-aisle directions. The ductile yielding baseplate, which has very small rotational stiffness, is adopted widely for industrial storage in New Zealand, due to its good seismic performance in the cross-aisle direction. This is achieved by considerable seismic energy dissipation capacity through yielding of the ductile steel plates from the uplift behaviour, allowing controlled rocking in the cross-aisle direction. This baseplate-upright connection with the ductile design concept can potentially lead to a low-cost and low-damage racking structure in the cross-aisle direction. However, the high flexibility of this type of baseplate means that the column base connection is effectively pinned in the down-aisle direction, which induces a large moment demand at the beam-upright connections close to the base in the down-aisle direction. Raising the damage threshold may limit the seismic performance of the overall system. The friction slipper baseplate, has been developed to have sufficient stiffness and moment resistance to improve the down-aisle direction seismic performance; whilst also having excellent cross-aisle seismic performance when compared to both rigid baseplates and ductile baseplates. For a dependable design process, the rotational stiffness and moment-rotation characteristics in the down-aisle direction, must be known for both the ductile yielding baseplate and friction slipper baseplate. This is the main aim of this part of the research.

This section presents details on the down-aisle direction performance of these two types of baseplate connection; by simulating the principal seismic actions that cause baseplate-upright connections to rotate and fail.

The drawings of three types of baseplates are shown:

A typical rigid baseplate drawing as shown in Figure 4.14, with a thick floor plate (10-mm-thick) and a steel C-section (5-mm-thick) fixed to upright with 4 bolts at the front;

A ductile yielding baseplate is shown in Figure 4.15, with a thinner (3.5-mm-thick) and more ductile floor baseplate and a 3.5-mm-thick C-section bolted to uprights with 1 bolt at the back.

A friction slipper baseplate as shown in Figure 4.16, with a 10-mm-thick floor plate and a C-shaped 5-mm-thick inner stub, fixed to the uprights with various number of bolts via a controlled clamping force by adjusting the amount of the bolts and the torque applied to them.

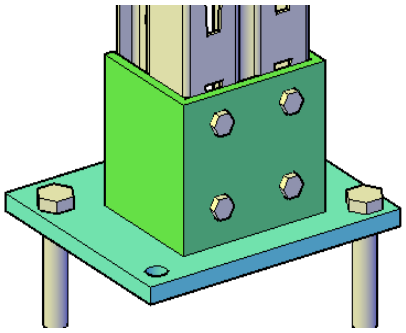

Figure 4.14: Typical rigid baseplate

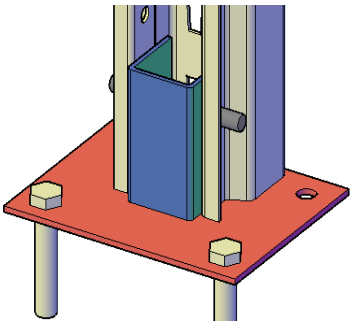

Figure 4.15: Ductile yielding baseplate

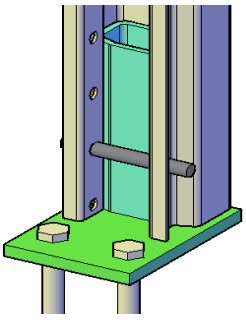

Figure 4.16: Friction slipper baseplate

4.2.2 Literature review

The geometric and material properties of a baseplate determine its rotational stiffness, rotation capacity, ultimate moment resistance, and ductility. A few types of baseplate investigated in previous studies on the performance of the baseplate-upright connection in the down-aisle direction are shown in Figure 4.17, [33][62][31][63]. Most of these perform as a rigid connection and do not allow uplift. All these studies indicate that the rotational stiffness and moment resistance of all types of baseplate-upright connections change significantly with varying axial loading, which results from the loading of pallets on a rack. Generally, the rotational stiffness increases with increasing axial compression loading, which means that the more the rack frame is loaded, the stiffer the frame behaves. Experimental results from previous research [33] show that the baseplate rotational stiffness, measured as the tangential stiffness in the elastic range of behaviour, can increase 40 times from 0 kN to 100 kN axial loading, and the ultimate moment resistance can increase by over 10 times. For the ductile baseplate, which is designed and detailed to allow the rack frames to rock in the cross-aisle direction with the uplift of the column in tension, the rotational stiffness on the tension column side drops to zero. This leads to a significant reduction in the moment resistance of the rack frame on the tension column side; this means that the column in compression from cross-aisle action also must resist significant base moment developed from the down aisle action. This phenomenon has been shown, conceptually, to lead to column failure in rack frames with baseplates that allow uplift [16], and this has also been observed in the field [33]. In this research, both the ductile yielding baseplate and the friction slipper baseplate connections allow the rack frame to uplift. They were tested with a wide range of axial loading to produce a relationship between axial loading and the down-aisle moment-rotation characteristic for designers.

Overall, when an axial load is applied, in the range between 0 and 60% of the ultimate upright axial compressive capacity, the moment resistance increases with the increase in the applied axial load. However, if the axial load is so large that it is close to the upright's ultimate compressive capacity, the baseplate-upright connection is likely to fail in a small rotation angle at the upright under local buckling, as shown in Figure 4.12. Therefore, the ultimate moment resistance will not be reached and its maximum capacity will occur at a smaller axial loading.

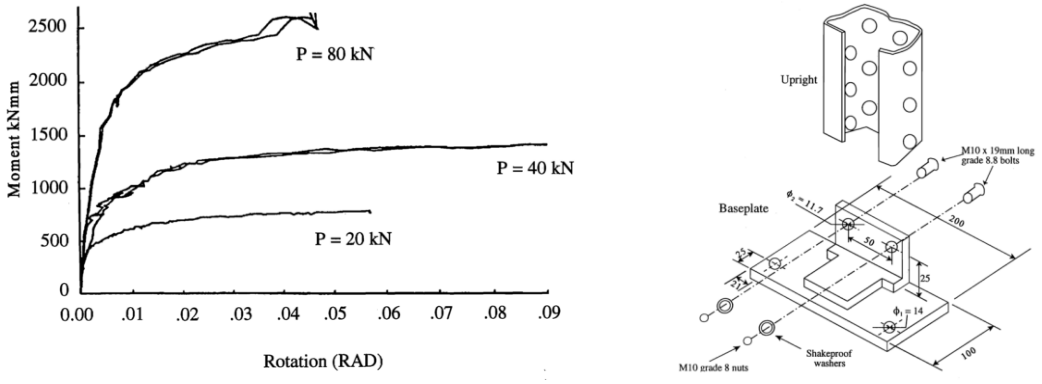

From *Feng et al 1998* [31]

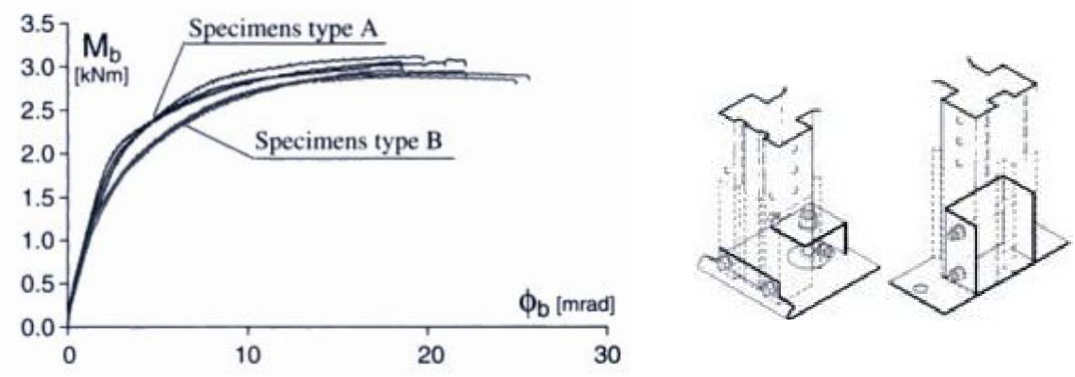

From *Baldassino and Zandonini 2003* [62]

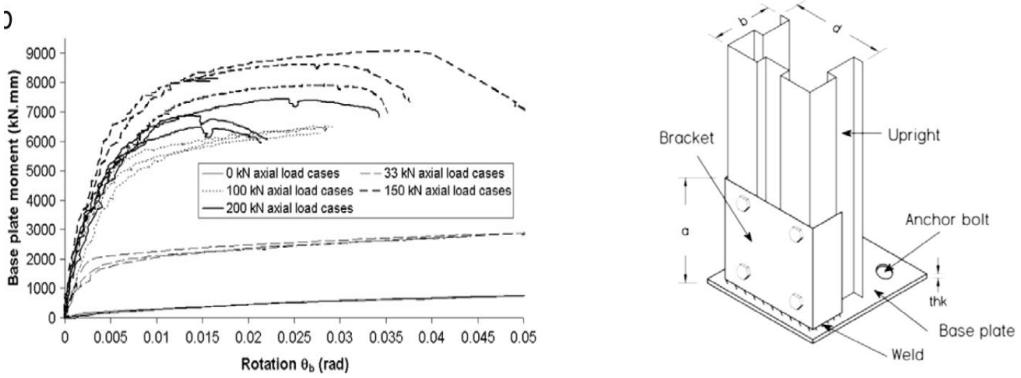

From *Gilbert and Rasmussen 2011*[33]

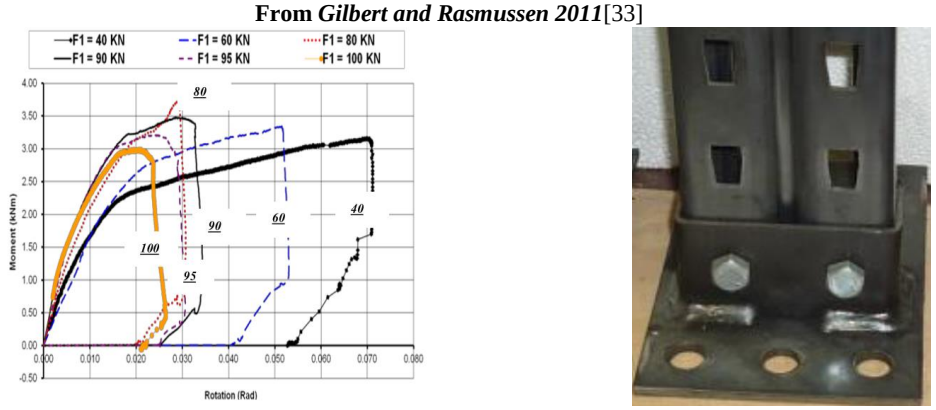

From *Firouzianhaji et al. 2014*[63]

Figure 4.17: Previous studies on moment-rotation tests of different baseplate-upright connections

As can be seen that, the ultimate rotation capacity of most of those studies are in the range of 0.07 rad or smaller. This is because the beam-upright connection ultimate rotation capacity is roughly in the same range. If the rotation angle at either the baseplate-upright or beam-upright connection exceeds this range, the other connection will have to carry a much larger moment demand, which may lead to failure on either of the connections. With a large axial loading because of the significant *P-Δ* effect, the ultimate rotation capacity decreases and failure occurs at an earlier stage, as shown in Figure 4.17(c) and (d).

The structural ductility factor, μ is used to evaluate the structure's ductile deformation capacity and adopted to calculate the seismic resistance of the pallet racking system, as recommended in *BRANZ Design Guide 2012* [65] for design in accordance with *NZS 1170.5* [66]. For the whole racking system, this factor is affected by the rotation capacity and the moment resistance of both the baseplate-upright and beam-upright connections. The less ductile connection will limit the overall performance of the racking system. The principle behind the calculation of the ductility factor for a component with a

plastic hinge is shown in Figure 4.18. The baseplate-upright connection component ductility factor can be derived from the component moment-rotation curve, drawn from experimental results. This is also an aim of this research.

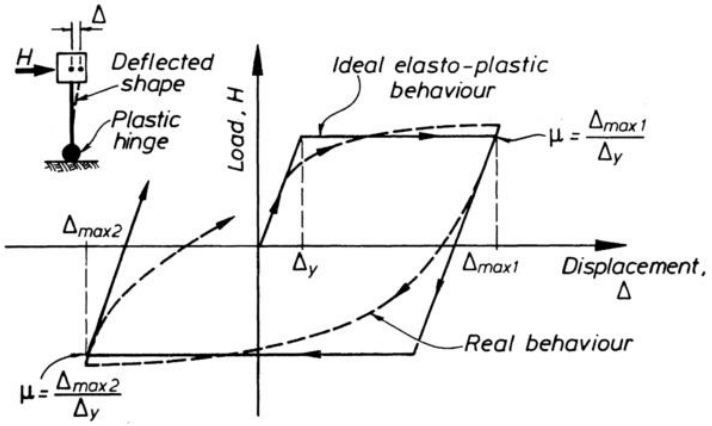

Figure 4.18: Method of calculation of ductility factor (from [7])

4.2.3 Methods

Baseplate assemblies have been tested for their moment-rotation behaviour following the requirement of EN 15512:2009 [64], with an important change proposed by Gilbert and Rasmussen 2011 [33]. This change is to the connection of the transverse loading jack 2, which is changed from the pinned connection recommended by EN 15512:2009 to a rigid connection, as shown in Figure 4.20. This generates a more stable setup and permits more accurate and effective tracking of the baseplate behaviour well into the inelastic range [33].

The test setup is shown in Figure 4.19 and Figure 4.20. A dual actuator setup is used. Two pieces of 500 mm long, 90 mm wide upright fitted with the baseplates are bolted at one side of the baseplate with anchorage bolts, to each side of a concrete block. After a selected axial loading was applied by the Jack 1 (J1) to simulate the gravity loading of pallets, another jack (J2) applies the lateral load to the concrete block to create a moment in the baseplate assembly. The load at Jack 2 is gradually increased until the load reaches a maximum; there is no significant change to the loading on Jack 1 which remains at its selected level. While Jack 2 is loading, the relative displacements to the concrete block at c1 to c4 are recorded as δ_1 to δ_4 These are measured at the interface between the baseplate assemblies and the uprights, at both sides of the uprights, using two portal gauges symmetrically positioned about the upright neutral axis. The horizontal movement of the concrete block is also recorded by two LVDTs at c5 and c6. Two LVDTs (c7 and c8) are placed at both pinpoints to measure the lateral deformation of the whole system, which was subtracted from the averaged value of c5 and c6, the result is taken as Δ, the lateral deformation of the baseplate assemblies. The loads applied to Jack 1 and Jack 2 are recorded as F1 and F2. It is important to note that roller bearings under the concrete block base act in both directions.

Note this shows a rigid connection at the specimen end of jack 2, which has been changed from a pinned which is shown in Figure 4.19.

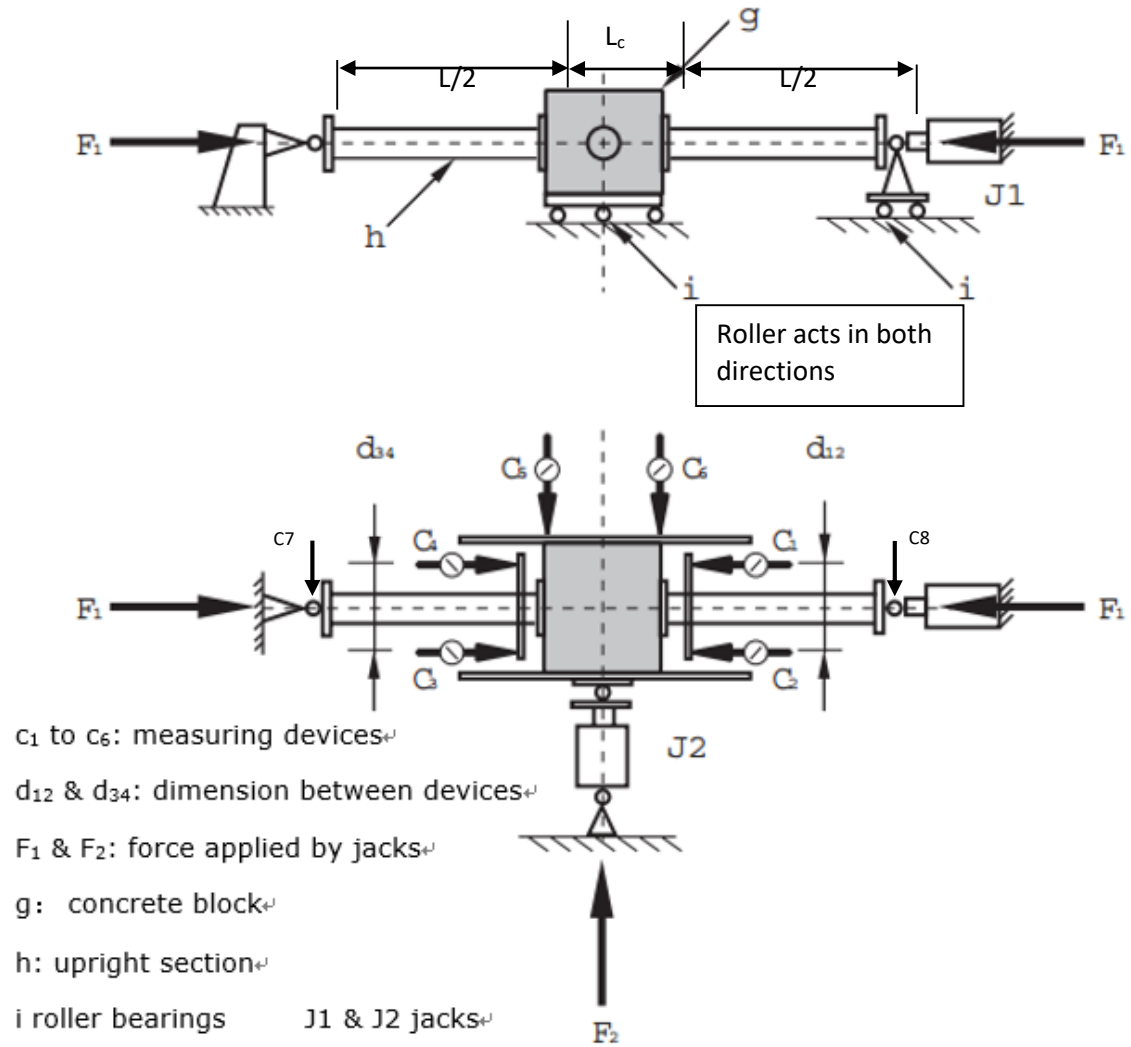

Figure 4.19: A sketch of the test setup (from [64]**)**

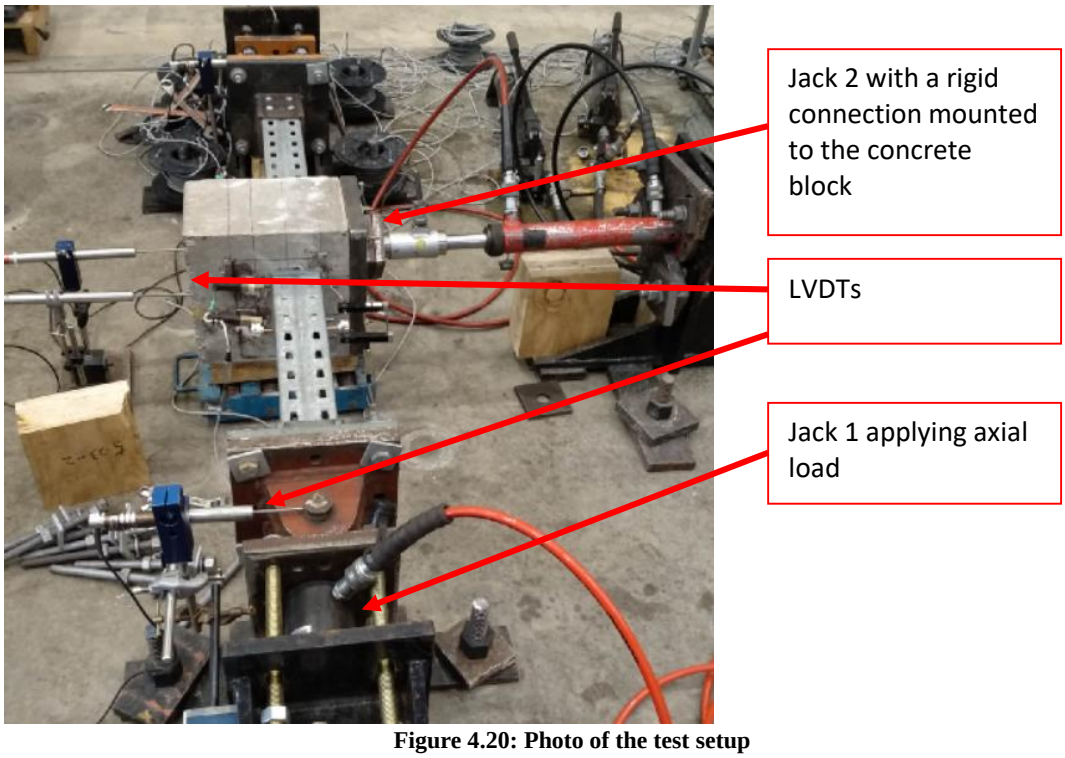

Figure 4.20: Photo of the test setup

The baseplate rotation angle at both sides can be calculated as the following equations:

$$\theta_{b,12} = \theta_{12} = \frac{\delta_1 - \delta_2}{d_{12}}$$

$$\theta_{b,34} = \theta_{34} = \frac{\delta_4 - \delta_3}{d_{34}}$$

Equation 1 (from [33]**)**

The baseplate moment for each side can be calculated as Equation 2:

$$M_{12} = \frac{F_2 L}{4} + \frac{M_R L}{4(L + L_C)} + F_1 \Delta$$

$$M_{34} = \frac{F_2 L}{4} - \frac{M_R L}{4(L + L_C)} + F_1 \Delta,$$

Equation 2 (from [33]**)**

Where M_R is the moment exerted by the rigid connection restraining system since the pinned connection at Jack 2 was changed to a rigid connection, as shown in Figure 4.20.

The average baseplate rotation θb and moment M_b applied to the baseplates can be calculated as the following equations, respectively:

$$\theta_b = \frac{1}{2}(\theta_{12} + \theta_{34}) = \frac{1}{2}\left(\frac{\delta_1 - \delta_2}{d_{12}} + \frac{\delta_4 - \delta_3}{d_{34}}\right)$$

Equation 3 (from [33]**)**

$$M_b = \frac{1}{2}(M_{12} + M_{34}) = \frac{F_2 L}{4} + F_1 \Delta$$

Equation 4 (from [33]**)**

At least 4 tests were carried out for each type of baseplate, at each axial load. For the ductile baseplate, axial load tests were performed at 5 kN, 15 kN, 30 kN, 60 kN, 90 kN and 100 kN. For the friction slipper baseplate, axial load tests were performed at 0kN, 15kN, 30kN and 60 kN. The 5 kN load test for the ductile yielding baseplate and 0 kN load test for the friction slipper baseplate were conducted to simulate the situation where the upright frame is lifting up and then the axial load drops to zero. Because the ductile yielding baseplate is very flexible, in the current setup it was very difficult to conduct the test with no axial loading, hence the small amount of axial loading at 5 kN was applied for the test and produce stable moment-rotation curves. The actual rotational stiffness and moment resistance of the ductile yielding baseplate is expected to be an even smaller value for the 0 kN load case.

4.2.4 Test Results

Figure 4.21 and Figure 4.22 show the "average" curves of the baseplate moment against rotation for all loading cases for both baseplates, in accordance with EN 15512:2009. An example of the derivation of the "average" moment-rotation curve is given for the 30 kN load case in Figure 4.24.

For ductile yielding baseplates, in axial load cases 5, 15 and 30 kN, the connection moments increased until the actuator stroke limit was reached at 0.1 radians. The same phenomenon was reported by *Gilbert and Rasmussen 2011* [33]. One side of the baseplate deformed and lifted up while Jack 2 was pushing the concrete block outwards, as shown in Figure 4.25. After each test, significant plastic

deformation was observed at the inner C-section and the floor plate of the tested baseplates, as shown in Figure 4.26. There is no damage observed in the uprights. For the axial load cases of 60, 90 and 100 kN on ductile yielding baseplates, the baseplate assemblies reached the maximum moment resistance and then the moment resistance decreased marginally, with increasing rotation until the *P-Δ* effect was so significant that the system collapsed suddenly at the middle, like the buckling of a long-slender steel bar. No damage to the uprights was observed for the 60 kN load case. An inward-bend was found at one side of the edge of the upright at the side contacting the baseplate, as shown in Figure 4.26(c). Anchorage bolts were not visibly affected in any of the above tests.

For friction slipper baseplates, during the tests, the floor plate rotated about one edge of the baseplate and formed a gap of a few millimetres. After each test, the baseplates were inspected for any potential failure or permanent deformation. However, except for ignorable deformation at the corner of the baseplates, these were smaller than 1 mm, and there were some scratches on the surface of the baseplates, no other damage was observed, Figure 4.27. This result indicates that the friction baseplate performs in an elastic manner in down-aisle direction rotation, which can also be observed from the linear response recorded and plotted in Figure 4.22. With the increase of loading and deformation, the system failed at the anchor bolts fixing the baseplate to the concrete block. The anchor bolts were pulled out slowly or sometimes produced cracks on the concrete block, which indicated that the moment resistance of the friction slipper baseplate is limited by the anchor bolt pull-out resistance. Despite this, the friction slipper baseplates are capable of rotating 0.08 rad with no significant permanent deformation and no decrease in moment resistance, as shown in Figure 4.28.

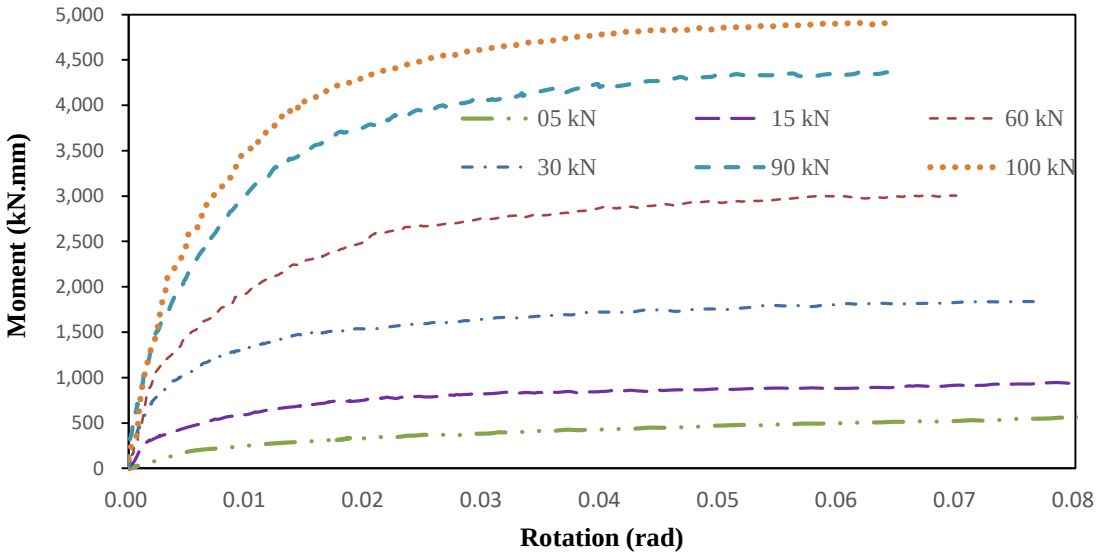

Figure 4.21: The "average" moment-rotation curves for the ductile yielding baseplates

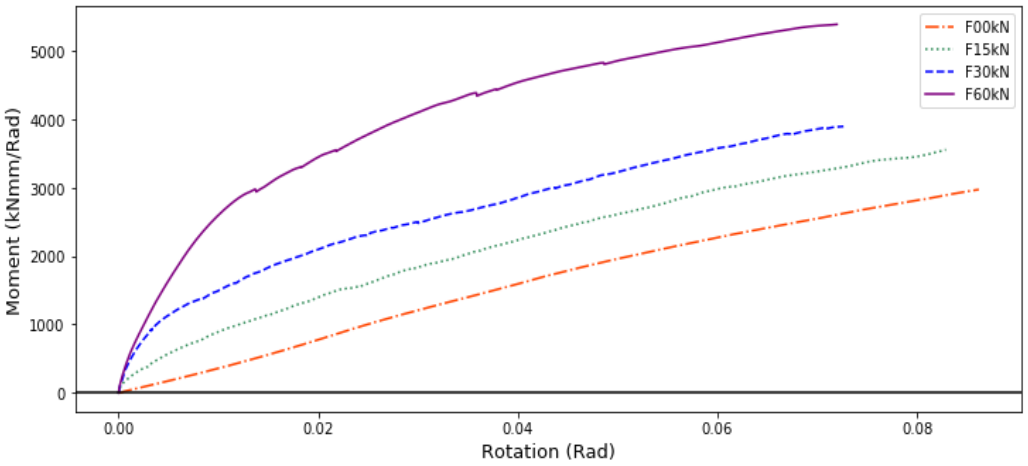

Figure 4.22: The "average" moment-rotation curves for the friction slipper baseplates

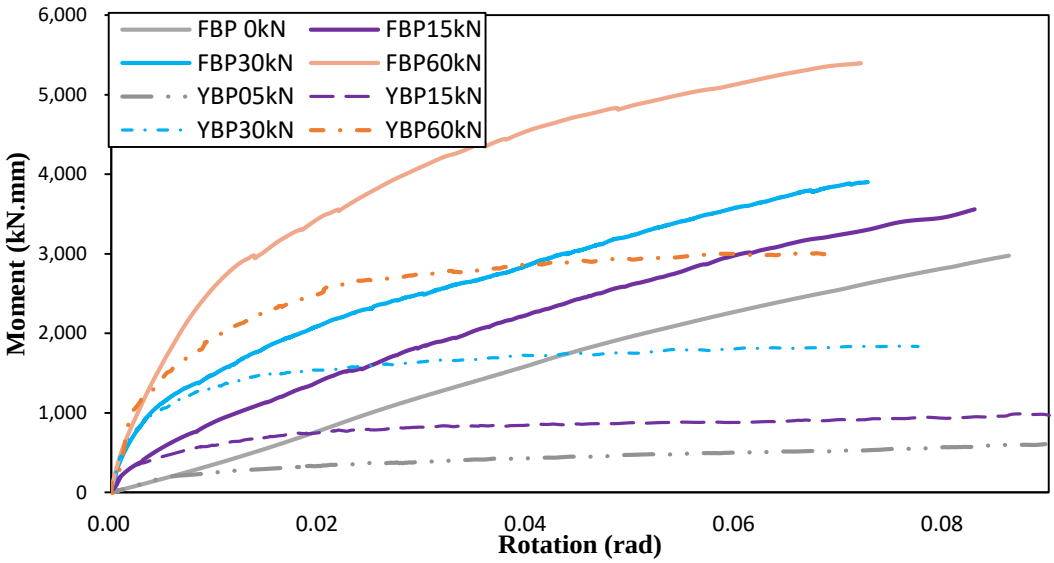

Figure 4.23: Comparison: Friction slipper baseplate V.S. Ductile yielding baseplate

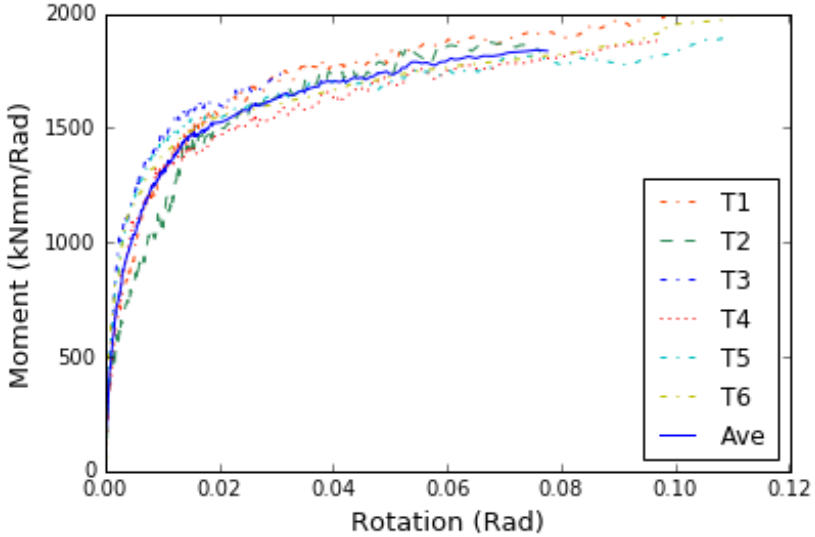

Figure 4.24: An example of the derivation of the "average" moment-rotation curve from 6 experimental curves for 30 kN load case

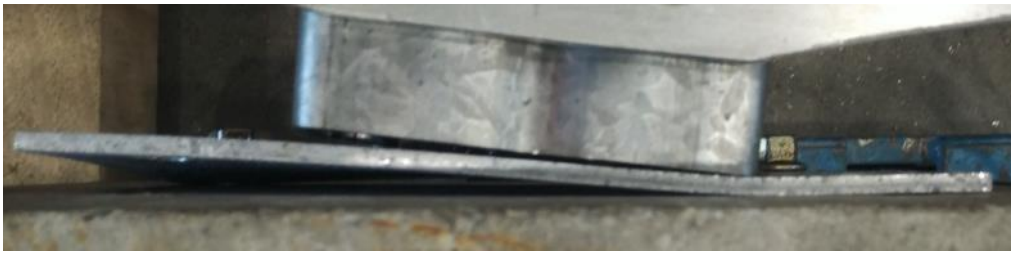

Figure 4.25: Ductile yielding baseplate deformation during the test

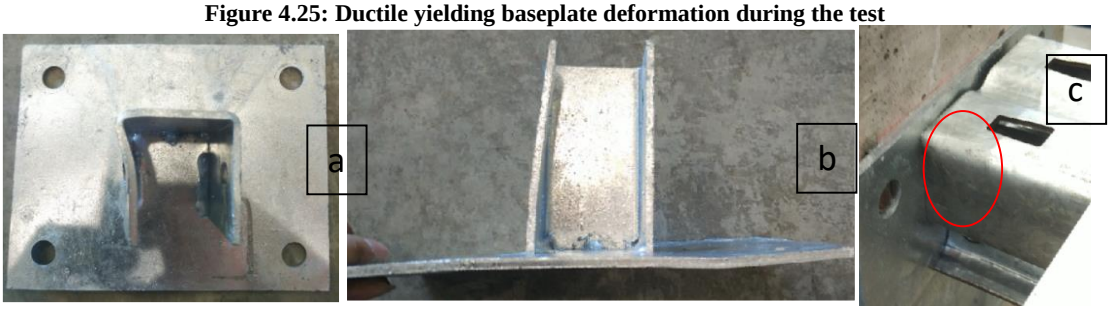

Figure 4.26: Yielding at the inner C-section (a), floor plate (b) and the damage found at the edge of the upright (c).

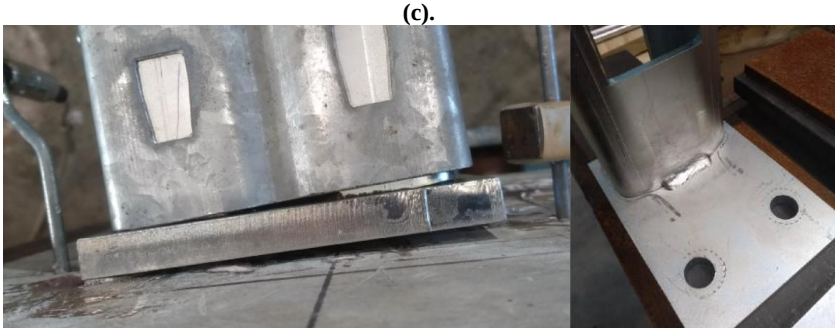

Figure 4.27: Friction slipper baseplate deformation during the test (left) and no damage found after the test (right)

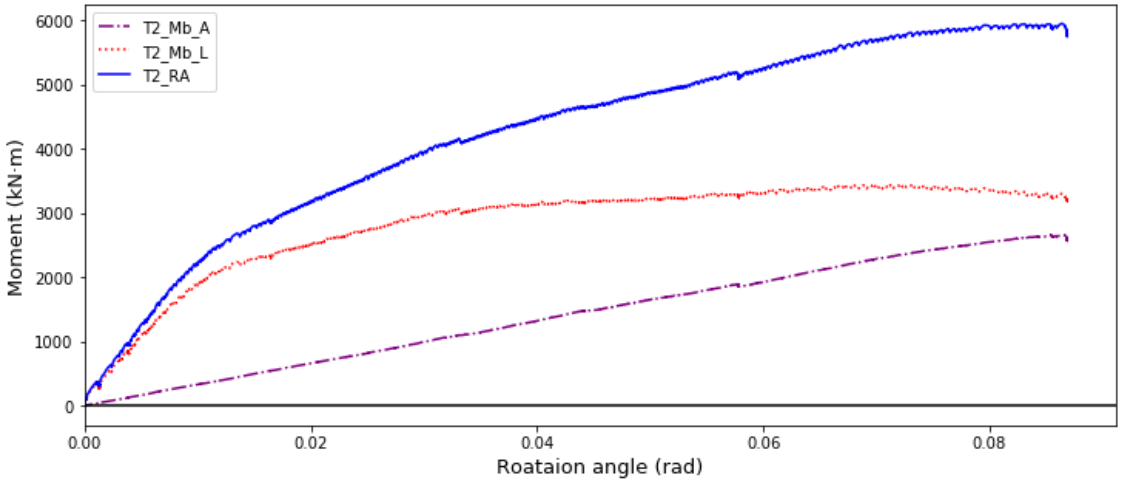

Figure 4.28: An example the two components of moment resistance of friction slipper baseplate for 60 kN axial load case, blue line = purple line + red line

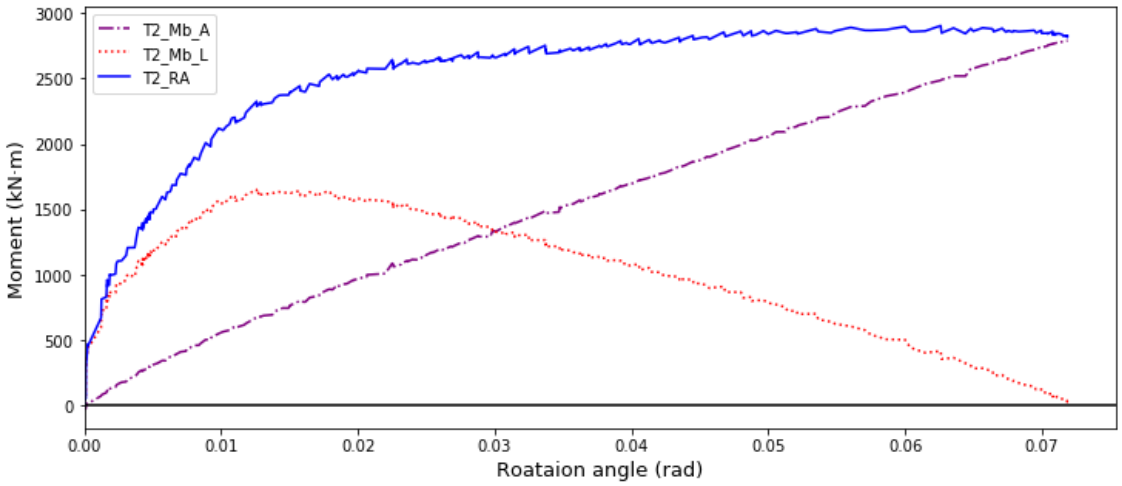

Figure 4.29: An example the two components of moment resistance of ductile yielding baseplate for 60 kN axial load case, blue line = purple line + red line

$$M_b = \frac{1}{2}(M_{12} + M_{34}) = \frac{F_2 L}{4} + F_1 \Delta$$

Equation 5

As mentioned in Section 2 (Equation 5), the moment resistance of the baseplate is the sum of two components: $F_1\Delta$ and $F_2L/4$, in which, F_1 is the axial load and F_2 is the lateral load applied to the baseplate. The axial load F_1 was controlled to be a constant value through the testing process. Therefore, the change in the moment component $F_1\Delta$ is proportionate to the increase in displacement of the concrete floor (Δ). As represented by the purple lines in Figure 4.28 and Figure 4.29, this moment component is roughly the same for both types of baseplate. However, for the other moment component $F_2L/4$, $L/4$ is a constant, and the lateral load $F2$ is determined by the baseplate geometry and material properties. For ductile yielding baseplates, the thin ductile steel floor plate is designed to be very flexible and deform easily so it can dissipate energy by steel yielding. As shown in Figure 4.29, the red line is the moment component generated by the lateral load, which gradually dropped to zero after reaching its maximum at around 0.012 rad of rotation. The overall moment resistance (the blue line) remains reasonably constant for quite a long rotation period. However, for the friction baseplates, the thick 10 mm steel floor plate allows the baseplate connection to deform almost elastically for a large rotation while retaining a reasonably large amount of lateral moment resistance, as shown in Figure 4.28 in the red line. The ultimate moment resistance (The blue line in Figure 4.28) of the friction slipper baseplate connection did not reach its maximum until the anchor bolt became loose or pulled out. The ultimate moment resistance of the friction slipper baseplate connection can be double of that of the ductile yielding baseplate.

These test results indicate that the rack frame with friction slipper baseplates can take a much larger lateral load compared to the rack frame with ductile yielding baseplates. Therefore, although the rotational stiffness of each loading test for both types of baseplate, because of the much larger and stable moment component $F_2/L4$ the moment resistance of the friction slipper baseplate is much larger than that of the ductile yielding baseplate for each loading test, respectively, as shown in Figure 4.23. It should be noted that when one side of the rack frame is lifting up and the upright axial load drops to zero, the ductile yielding baseplate will lose most of its moment resistance, but the friction yielding baseplate can retain a reasonably large amount of moment resistance, as shown by the two grey lines

in Figure 4.23.

In EN 15512:2009, a bi-linear curve is required to be derived from the experimental average curves. The design rotational stiffness of the baseplate-upright connection shall be obtained as the slope of a line through the origin which isolates equal areas between it and the experimental curve below the moment corrected, as shown in Figure 4.30. M_{Rd} is the design moment for the connection, calculated by:

$$M_{Rd} = \eta \frac{M_k}{\gamma_M}$$

Equation 6

Where γ_M is the safety factor for the baseplate-upright connection, a value of 1.1 for ultimate limit state and serviceability limit state; η is the variable moment reduction factor selected by the designer ≦ 1.

Another form of the stiffness of the connection is taken from the elastic range of the moment-rotation curve, which was suggested by *Gilbert and Rasmussen 2011*[33] could be used for determining global serviceability deformations.

The design moment M_d, design rotational stiffness k_m and the elastic range stiffness k_e of both types of baseplate-upright connection for all load cases are listed in Table 4.1 and Table 4.2. An example of determining the properties of the baseplate-upright connection from its average experimental curve, and the comparison between k_m and k_e for a 100 kN load test is shown in Figure 4.31.

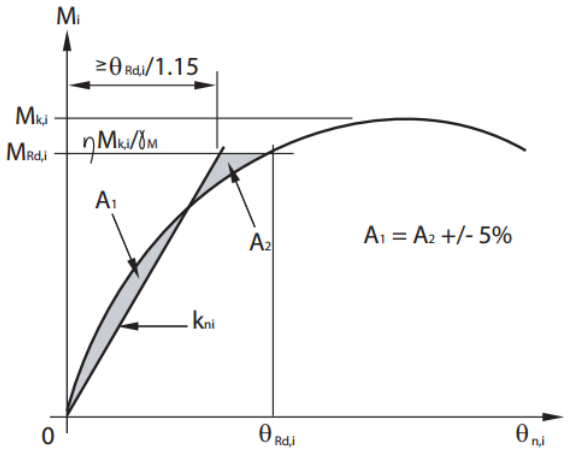

Figure 4.30: Derivation of baseplate assembly rotational stiffness

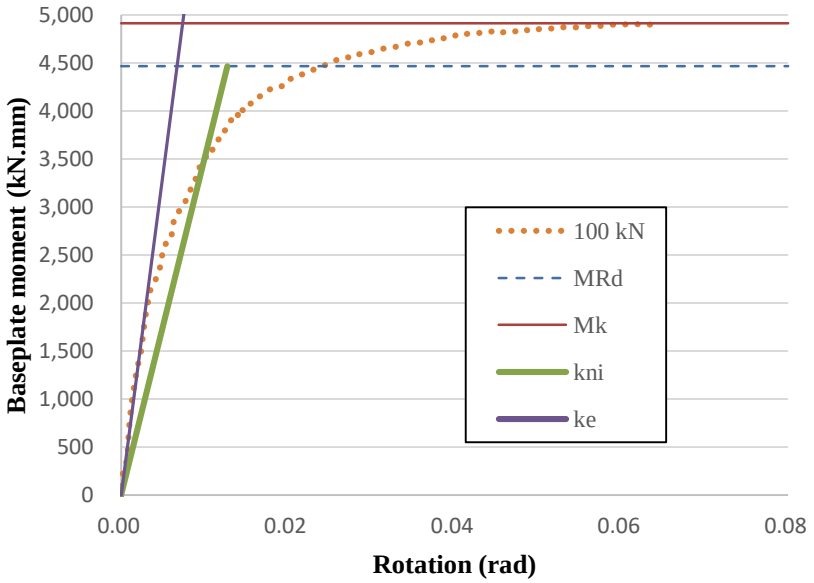

Figure 4.31: An example of determining the properties of the baseplate assembly

Table 4.1 Properties of the ductile yielding baseplate connection

Axial load (kN)	ke(kN·m/rad)	km(kN·m/rad)	Md (kN·mm)
5	40	15	564
15	150	55	865
30	230	123	1672
60	330	195	2734
90	450	315	3972
100	650	350	4466

Table 4.2 Properties of the friction slipper baseplate connection

Axial load (kN)	ke (kN·m/rad)	km (kN·m/rad)	Md (kN·mm)
0	37	37	2727
15	159	62	3182
30	260	104	3636
60	427	175	4909

As listed in Table 4.1 and Table 4.2, the rotational stiffness k_e and k_m for both types of baseplate are close to each other. However, the design moment resistance of the friction slipper baseplate is much larger than that of the ductile yielding baseplate, especially for small axial loadings.

The component ductility factors may have a value of 3 based on the test results obtained for the ductile yielding baseplates. For the friction slipper baseplates, because of their linear elastic performance at low axial loads, the structural ductility factor of the whole rack frame will be determined by its beam-upright connection performance. The average curve of the 60 kN axial load test can produce a component ductility factor of over 4.5.

4.2.5 Conclusions

This report presents a comparison of experimental test results undertaken to determine the down-aisle

baseplate-upright connection moment-rotation behaviour of steel storage racks with ductile yielding baseplate and friction slipper baseplates.

According to the experimental results, the following conclusions can be drawn:

1. The ductile yielding baseplates are easily subject to plastic deformation whereas the friction slipper baseplates deformed in elastic range.
2. The ductile yielding baseplate-upright connection failed in collapse under the significant *P-Δ* effect.
3. The friction slipper baseplate-upright connection's capacity was limited by the anchor bolt resistance.
4. The lateral load resistance contributes the most of the difference on the moment resistance comparing two types of baseplates.
5. The moment resistance of the friction slipper baseplates is much larger than that of ductile yielding baseplates for all axial loading cases.
6. The component ductility factor of the ductile yielding baseplate maybe 3 and the friction slipper baseplate maybe 4.5.
7. The ductile yielding baseplate lose most of its moment resistance when there is not sufficient axial load while the friction slipper baseplate remains a considerable large amount of moment resistance.
8. For both types of the baseplates, rotational stiffness varies widely with the change of axial load, the same for the moment resistance.

The last two finds, in particular, could have a significant influence on the overall pallet racking system behaviour, as the upright axial load will vary considerably during an earthquake due to truss action in the cross-aisle direction. The influence of this needs to be considered in the design.

Chapter 5 Pull-over and snap-back tests

5.1 Introduction

Traditionally, criteria for design and construction of industrial racks have been developed by their manufacturers and have been directed primarily at gravity loading, with little attention given to earthquake loading. As a result, there is a lower level of design and performance of steel racking system compared with steel buildings as evidenced by severely damaged racks observed in steel buildings of similar age with no damage [4]. Also, a minor collision with a rack can result in the total collapse of the rack system due to the dynamics of pallets falling; one rack frame collapse may fall on its adjacent racks and result in the collapse of racks in the whole warehouse, just like dominos, as shown in Figure 5.1. Heavy economic loss due to the collapse of pallet racks and loss of contents has been experienced in many past earthquakes, for example, the 1987 Edgecumbe Earthquake, the 2001 Nisqually Earthquake, the 2010 Darfield Earthquake and the 2011 Lyttleton Earthquake [5][6][7][8][9]. The seismic resilience of racking systems is now a much more important consideration in design.

Figure 5.1: A minor collision can result in total collapse due to the dynamics of pallets falling

The commonly observed collapse modes of racking systems in the cross-aisle direction during earthquake events are: (**a**) collapse, by upright buckling under high compression force, as shown in Figure 5.2 and Figure 5.3; (**b**) overturning, due to large tension force in uprights, insufficient ground anchoring or poor weld quality between the baseplates and the uprights, as shown in Figure 5.4.

Figure 5.2: Cross-aisle direction failure by column buckling [9]

Figure 5.3: Cross-aisle direction collapse of pallet racking system [5]

Figure 5.4: Fracture of baseplate connection [17]

The weak link in the cross-aisle direction is in the upright-base connection [67]. An upright-base connection consists of an upright, a baseplate and a set of anchor bolts. The behaviour of an upright-base connection is mostly determined by the type of baseplate chosen. Conventional baseplates can be divided into two types: rigid baseplates and flexible baseplates. A rigid baseplate is generally designed to be very robust and resists the seismic load by its material and section properties. However, with an excessive increase of the seismic energy imparted to the structure, the seismic load can be too large for the racks to resist, resulting in the collapse and overturning shown in the above figures. Flexible baseplates have been developed to increase the efficiency of seismic energy dissipation of racking frames by allowing rocking behaviour and steel yielding. This has been found to be a more cost-effective solution [68]. However, even if a robust and well-anchored, or a flexible rocking frame racking system survives a severe earthquake, the rack component or connections will often be either fractured or plastically deformed to the extent of requiring replacement. This outcome means dismantling the rack, leading to significant rehabilitation costs and the lose of business continuity.

Some researchers have introduced base isolation techniques to racking systems[34], [69], [70]. The concept has been verified by a large number of experiments, including full-scale shaking table tests and appears to be successful. However, the use of base isolation techniques significantly increases the cost of racking systems. A minimal-damage and low-cost solution to improve the seismic resilience of the racking system is required which demands a more robust baseplate that dissipates energy but that does not require replacement after a severe earthquake.

To increase the seismic resistance of pallet racking systems, the design concept of controlled rocking in the cross-aisle direction has been developed, in which the base of the structure or selected upright are permitted to uplift from the foundation in response to severe lateral loading. A friction damping mechanism has been introduced to the system to dissipate energy. The Friction Slipper (FS) baseplate is the resulting development to implement this design concept.

Previous studies have experimentally investigated the local quasi-static behaviour of the friction slipper baseplate when it is uplifting. It was found to be able to have large ductility, high energy dissipation capacity, and adjustable upright uplift force by changing its bolt configurations, achieving the potential of a low-damage or damage-free design.

In order to further investigate and prove the benefit of the design concept and the friction slipper

baseplate, especially for determination of its ductility and dynamic free-vibration behaviour, in this development full-scale pull-over and snap-back tests are used for evaluating the rack performance. This report presents a series of full-scale pull-over and snap-back tests that were performed to assess the quasi-static and free-vibration behaviour of the racking systems fitted with the friction slipper baseplate and other types of baseplate for comparison. The load-displacement curves and free vibration curves of the rack frames with different baseplate assemblies are used for evaluating the rack performance.

The objectives of this research are to:

1. Determine the ductility of rack frames with friction slipper baseplates;
2. Determine the racks cross-aisle structural period and rocking period;
3. Determine upright axial forces on impact during rocking motion;
4. Determine the energy dissipation capacity for each baseplate type.

(a):Frame configuration **(b) The test setup**

Figure 5.5: Frame configuration and a photo of the test setup

5.2 Test setup

As shown in Figure 5.5a, each of the tested rack frames had 3 levels (1.4-m height per level) and 2 bays (1.35 m per bay) and was 0.9-m deep, erected on concrete slabs fixed to the strong floor. Each pallet was 783 kg, clamped to the beams with steel sections and bars, so that pallet slip was suppressed. Previous studies have shown that pallet slippage can be beneficial in reducing the response of the rack unless the pallets slide off the rails and start to fall off. The frame bracing consists of two X-braces at the bottom then K-bracing to the top at 600-mm pitch. The uprights were fitted with 4 types of baseplate configurations connected to the concrete slabs with anchorage bolts:

I: Rigid baseplate, which does not allow uplift, as shown in Figure 5.6a. It dissipates around 38J of

energy per cycle, as calculated according to the area enveloped in the hysteresis curves shown in Figure 5.7, within the range of about 20 mm of displacement and 15 kN of axial load. The Rigid baseplate has demonstrated a small (3mm) of platform at around 5 kN, which is from the friction force of the 4 bolts bolted at the front. The 3 mm platform is because of the M8 bolts fitting into the 11 mm diameter pre-opened holes on the baseplates. As can be seen, once the bolts reached the top of the gap between the pre-opened holes and the bolts, the axial load rapidly and linearly increased. Once the baseplate is unloaded, the load-displacement curve returns following the same path. It is important to note that the linearly increment will not provide damage-free energy dissipation capacity. With the rapid increment of axial load, the Rigid baseplate will reach its anchor bolt pull-up resistance quickly.

II: Ductile Yielding baseplate, which allows the frame to uplift at the base and dissipate energy through yielding, as shown in Figure 5.6b. It dissipates around 156 J of energy per cycle within the range of about 20 mm of displacement and 15 kN of axial load. As can be noted that, the Ductile Yielding baseplate dissipates energy in not only the pull-up stage but also the press-down stage, which is contributed by its metal plate yielding. This type of baseplate should be made of very ductile steel with good anti-fatigue performance. With further increment of the axial load, the Ductile baseplate will keep developing its uplift and metal plate yielding until either the baseplate reaches its deformation capacity or anchor bolts reach their pull-out resistance.

III: Friction baseplate without bolt tightening**,** which can be considered to be a free-to-rock connection with horizontal shear resistance. Since there is no clamping force, the energy dissipation through the baseplate cannot be quantified, but it should be reasonably small compared to the bolt tightened case. The energy dissipation is mainly due to the friction between the uprights and the inner stub of the baseplate while it is rocking.

IV: Friction baseplate with one **bolt tightened** to 30 N m**,** as shown in Figure 5.6c. It dissipates around 329J of energy per cycle within the range of about 20 mm of uplift displacement. The friction force is very stable and almost independent to the uplift in this bolt configuration. As discussed in Chapter 4, the friction force can be adjusted by the bolt configurations (amount of bolts, arrangement, torque applied) and the surface condition of both the baseplates and the uprights. In this test, one bolt with 30 N m of torque was applied to generate roughly 10 kN of friction force.

The component behaviour of each type of baseplate configuration is shown in Figure 5.7.

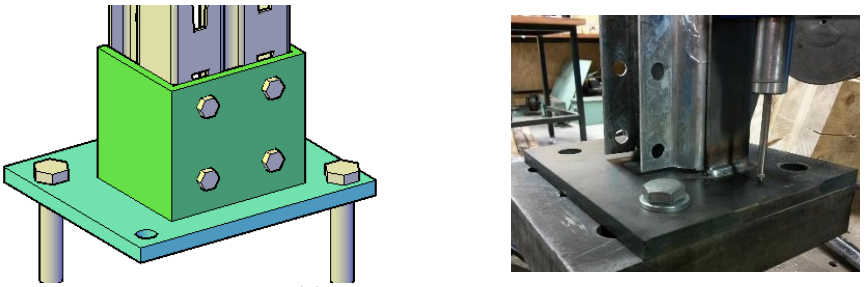

(a) **Rigid baseplate**

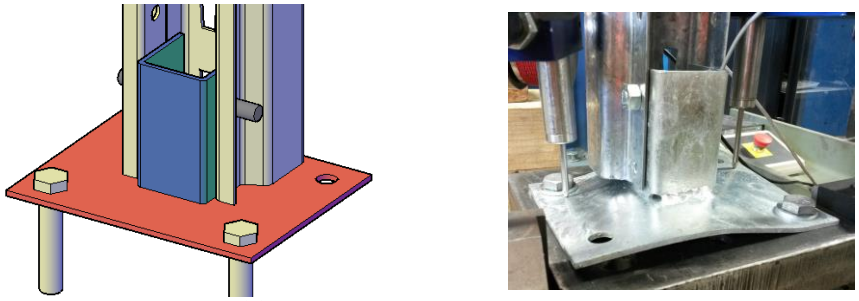

(b) Ductile yielding baseplate

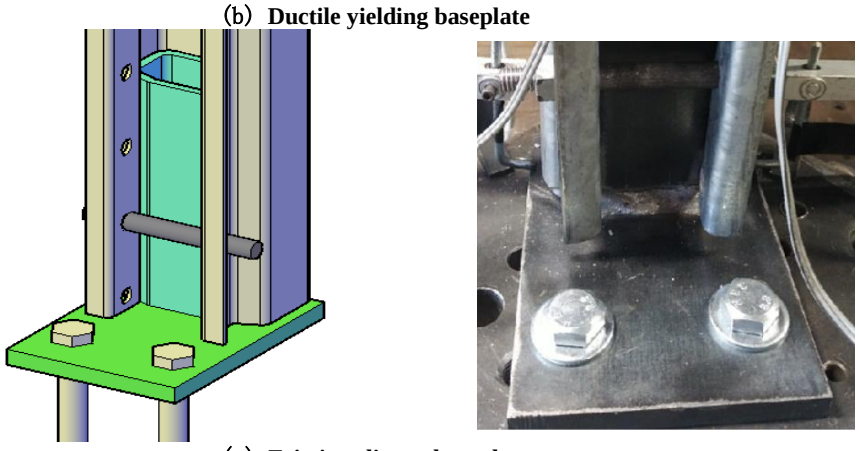

(c) Friction slipper baseplate

Figure 5.6: Drawing and photo of each type of baseplates

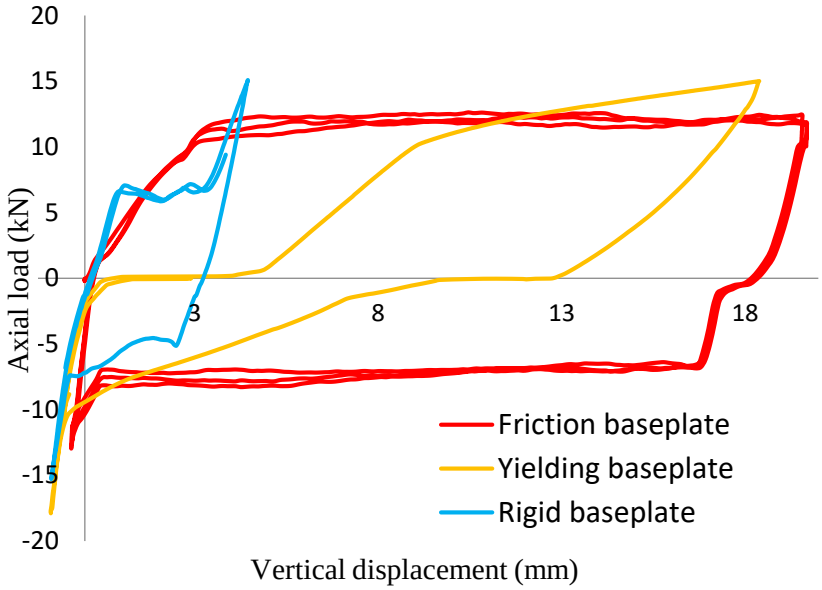

Figure 5.7: Component behaviour of rigid baseplate, ductile yielding baseplate, and friction slipper baseplate with 1 bolt tighten to 30 Nm

A photo of the test setup is shown in Figure 5.5b. Pull-over and snap-back tests were conducted to the following procedures:

1. Loading the centre of the top level of the rack frame with a design vertical loading, then hooking a hydraulic actuator mounted on a strong wall to the top and slowly pulling the rack sideways until a target displacement is reached in the cross-aisle direction. In Figure 5.5b, the actuator providing the lateral pulling force is shown to the left of the rack and the top of the rack is being pulled to the left. During this process, the load and displacement of the rack frame are monitored and recorded for a load-displacement curve.

2. Once the target displacement is reached, the actuator is released through a quick release mechanism

and the rack responds in free vibration, returning to it is at rest position in a series of dynamic cycles of motion. The test is good for determining the monotonic and the cyclic ehavior of the rack when subjected to an initial imposed lateral displacement and the frequency and damping associated with its cyclic motion. The structure's free vibration ehavior is monitored and recorded for its dynamic response.

The upright uplift displacement was measured by portal gauges, the longitudinal normal strain at the upright base was recorded with strain gauge sets, and the displacements of the frame at different beam levels were recorded by wire displacement transducers. The load applied to the frame was monitored by the load cell mounted to the actuator.

5.3 Observations and Discussion

Subsequent to the snap-back tests, there was no upright damage observed for the frames fitted with ductile yielding baseplates or friction baseplates (with or without bolt tightening), while a permanent local deformation was observed at one upright fitted with rigid baseplates. Likewise, no significant residual displacement was observed for ductile baseplates or the friction baseplates, those tended to self-centre, while a large residual displacement was observed for rigid baseplates, as shown in Figure 5.10.

It is worth noting that the anchor bolts of the rigid baseplates were loosened from the concrete foundation at the application of the horizontal displacement (time zero), although no damage was found in the baseplates themselves.

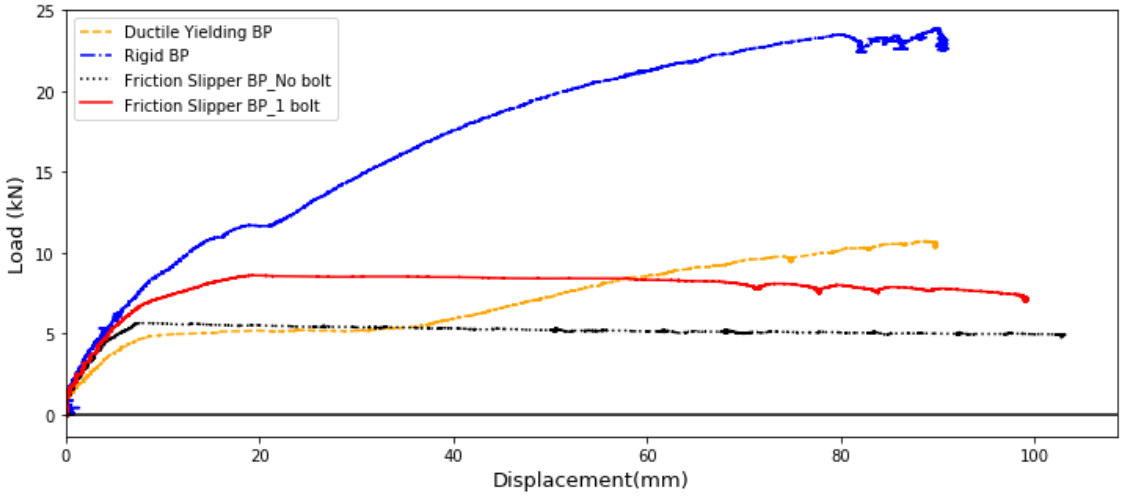

Figure 5.8: Pull-over load-displacement curves for rack frames with 4 baseplate assemblies

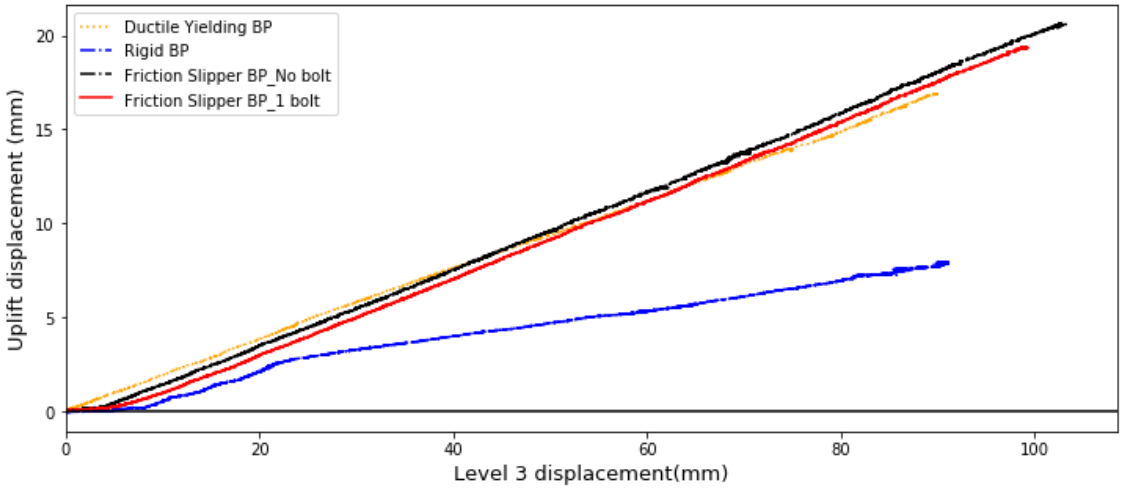

Figure 5.9: Base uplift displacement against Level 3 beam level displacement

Figure 5.8 shows the pull-over curves recorded for all frames in the initial static, monotonic part of the test. It can be seen that the rack frames with friction slipper baseplates with and without bolt tightening force give a very similar performance. After a similar initial stiffness, the load keeps increasing to the point where friction sliding uplift commences. The friction force is very stable. In the actively sliding range, the overall load decreased slowly due to the P-Δ effect, but over 85% of the peak uplifting force is maintained up to 2.5% of top drift. Interestingly the slope of the sliding part of the curve is the same for the friction slipper baseplates with and without bolt tightening. In the full-scale rack test, the uplifting upright is describing a shallow arc, rather than being uplifted vertically, and this balances out the reduced capacity due to the reduced contact area. It means that the load-deflection characteristics of the sliding part of the curve are defined by the P-Δ effect. This effect is linear up to a certain point then becomes non-linear as the point where lateral instability is reached. The curves in Figure 5.8 do not show non-linear behaviour up to the 2.5% drift imposed, meaning that the rack is still operating in the linear large displacement range up to that drift limit. This observation also shows that the friction baseplate can keep the upright uplift force within the nominated range, throughout the design uplift, associated with reaching 2.5% lateral drift. Based on a bilinear approximation, the yielding displacement of the rack with bolt tightening was at approximately 16 mm and the maximum displacement was approximately 100 mm. The ductility factor of the frame can be calculated as $\mu = \mu_{max}/\mu_{Yield} = 6.25$. From the methodology used to determine the ductility factor it is clear that with a smaller friction force applied, an even larger ductility factor can be obtained, while both the ductile yielding baseplate and the rigid baseplate have much smaller ductility.

The ductile yielding baseplate demonstrates a three-stage behaviour. After travelling 10 mm with a relatively small initial stiffness, which is due to its thin floor plate, a force plateau at around 25 mm of uplift is developed, followed by a typical decaying slope with the increase of the load and displacement, which shows a yielding behaviour on the floor plates. The plateau is due to the sliding of the bolt connection uprights and baseplates, which are travelling in a 17 mm slot pre-opened at the inner C-section of the baseplate. The slot has been designed to have enough tolerance for connecting bolts to be installed easily between the opened holes on the upright and the baseplate. The bolt is 10-mm in diameter, so the free travelling uplift displacement in the slop range is around 4-7 mm

depending on the tolerance of both components. After the bolt reached the top of the slot, the bolt started to pull the baseplate up with the increment of the upright uplift. As can be seen at the end of the curve, the load is almost flat, which means that the curve is about to reach its ultimate capacity.

A very different load-displacement behaviour is found for the rigid baseplate curve. It does not allow upright uplift, which generates much higher loading for a given lateral displacement. Large plastic deformation can be observed from the curve. Larger damage was formed with larger lateral load resistance. The top of the curve is flat, similar to the ductile yielding baseplate case, indicating that it was close to its ultimate resistance. This is supported by the observed anchor bolt partial pull out from the concrete.

Figure 5.9 shows the relationship between the base uplift displacement against the Level 3 beam level displacement of 4 types of baseplate assembly. The baseplates' behaviour can be divided into two types, depending on whether uplift is allowed or not. It is clearly indicated that, at each displacement stage, the larger the plastic deformation, the smaller the uplift displacement. Also, since the rack frames with baseplate assemblies allowing uplift have rigid block rotation behaviour, they have a similar uplift displacement/Level 3 displacement ratio, which is close to the ratio of the width of the rack frame by the height of the Level 3 displacement measuring point, which is roughly 900/4400 mm ≈ 0.205.

The load was released at around 90-100 mm of displacement at the level 3 beam level. The top-level displacement time-history of the frames with 4 types of baseplate configurations are plotted in Figure 5.10.

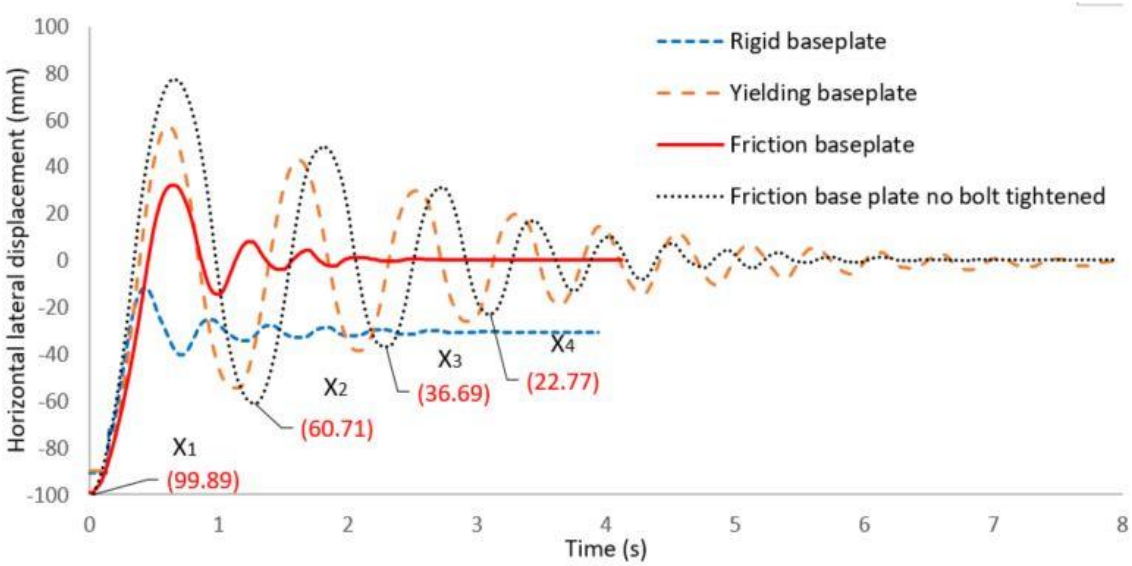

Figure 5.10: Time-history of horizontal displacements of the top of the middle upright frame with 4 types of baseplate configurations

$$\delta = \frac{1}{2\pi n} \ln \left| \frac{X_1}{X_{1+n}} \right| = \frac{1}{6\pi} \ln \left| \frac{X_1}{X_4} \right|$$

Equation 1

Rocking was observed for the frames fitted with yielding and friction baseplates. The upright frames rocked in a manner similar to a rigid block, but with the whole rack frame block demonstrating noticeable elastic flexibility. In contrast, the frame fitted with the rigid baseplates underwent significant bending and shearing.

As can be seen in Figure 5.10, the frame with bolt-tightened friction slipper baseplates came to rest in about 5 cycles in 2.5 seconds, while that with the yielding baseplates took more than 12 cycles and 8 seconds. The periods of the first 5 cycles of the free-vibration response of each frame are listed in Table 5.1. Only the first 4 cycles can be clearly identified for the bolt-tightened friction baseplate configuration, and the maximum displacement at the 4th cycle was only 1.38 mm without uplift.

The equivalent damping ratios were estimated to give an estimate of the energy dissipation capacity of the types of baseplates. However, it is important to note that the method of estimating the equivalent damping ratios is based on the viscous damping assumption, not friction damping. The logarithmic decrement method was applied, as shown in Equation 1, and only the first three cycles are considered for the damping ratio calculation. The damping ratio of the yielding baseplate was found to be 6.6%, which is higher than the 0.5% to 3%, computed for some conventional baseplates in the cross-aisle direction [19][71]. The rigid baseplate had an estimated damping ratio of 16.3%, which is quite high. However, there was a significant residual sway displacement of 30 mm. The bolt-tightened friction baseplate had an estimated damping ratio of 20%, which is the highest of all; it comprised an initial cycle in the rocking range with a final cycle in the non-rocking range. The damping is lower in the non-rocking cycles but still well above 5%. Surprisingly, the friction baseplates without tightened bolts had a damping ratio of 7.9%, which is higher than that of the yielding baseplates. It may be caused by the small friction force existing between the upright and the baseplate.

Table 5.1：Snap-back test results：period of the first 5 cycles and damping ratio of the first 3 cycles

Base plate configuration	Period of cycles (s)					Equivalent damping ratio %
Cycle number:	1	2	3	4	5	
Rigid baseplate	0.61	0.47	0.45	0.40	0.37	16.3%
Ductile yielding baseplate:	1.04	0.94	0.87	0.70	0.63	6.6%
Friction base plate with no bolt tightened	1.30	1.00	0.82	0.65	0.53	7.9%
Friction base plate with bolt tightened	0.97	0.47	0.39	0.42	N/A	20.0%

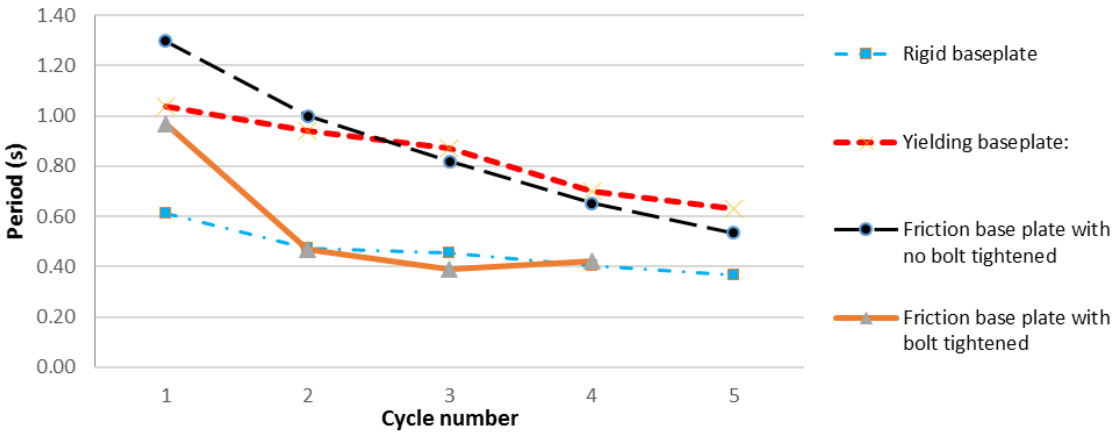

Figure 5.11: Oscillation periods of test frames

Figure 5.11 shows that in general, the oscillation periods of each frame subjected to the snap-back test decreased from one cycle to the next. However, it may be noted that the oscillation period of the frame fitted with the friction slipper baseplate increased between the third and the fourth cycle. The exact reason is unknown to the authors at this stage. The rapid drop of the second cycle for the friction baseplate shows how quickly the vibration energy was dissipated by the friction damper. The first 5 cycles of the ductile yielding baseplate and the friction slipper baseplate without bolt were still in rocking motion, but the period of the friction slipper baseplate with bolt tightening dropped down to a similar level as the rigid baseplates, which indicates elastic vibration dominates the free vibration from the second cycle, unlike the yielding baseplates and the unbolted friction slipper baseplates, which rocked for many cycles.

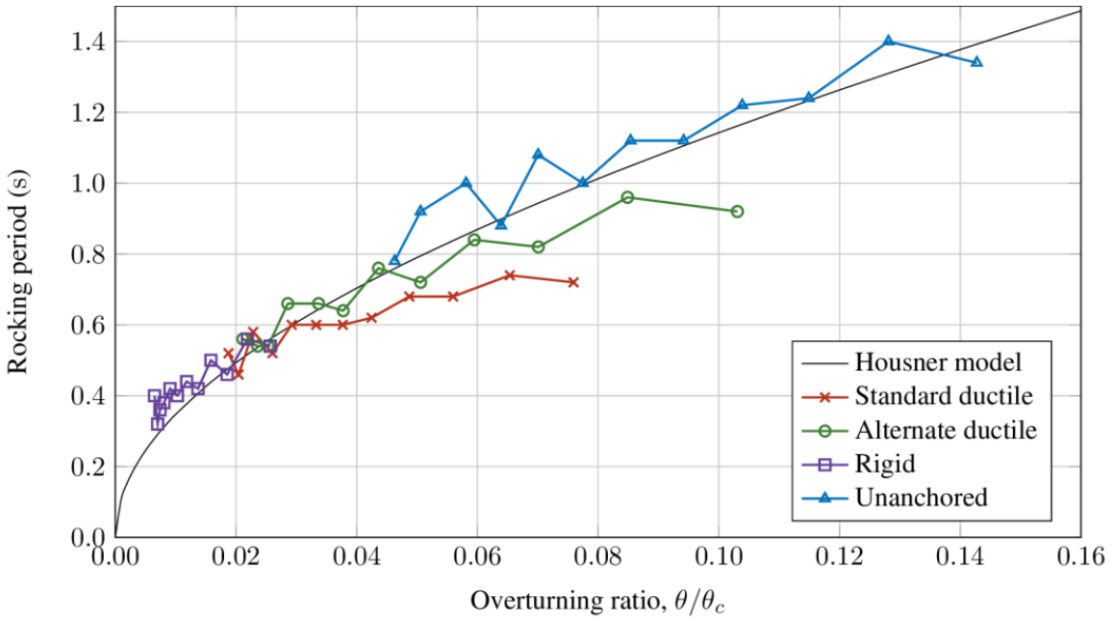

Figure 5.12： Vibration period of the structure during snap-back analysis (from [72])

Maguire *et al. 2016* [72] compares the vibration period of the structures during free rocking motion for different types of baseplates with the numerical model raised by *Housner 1963* [39], as shown in Figure 5.12. The experimental results match the numerical model very well. It indicates that when the rocking motion is initialed, the rocking period is not constant and is a function of the overturning ratio.

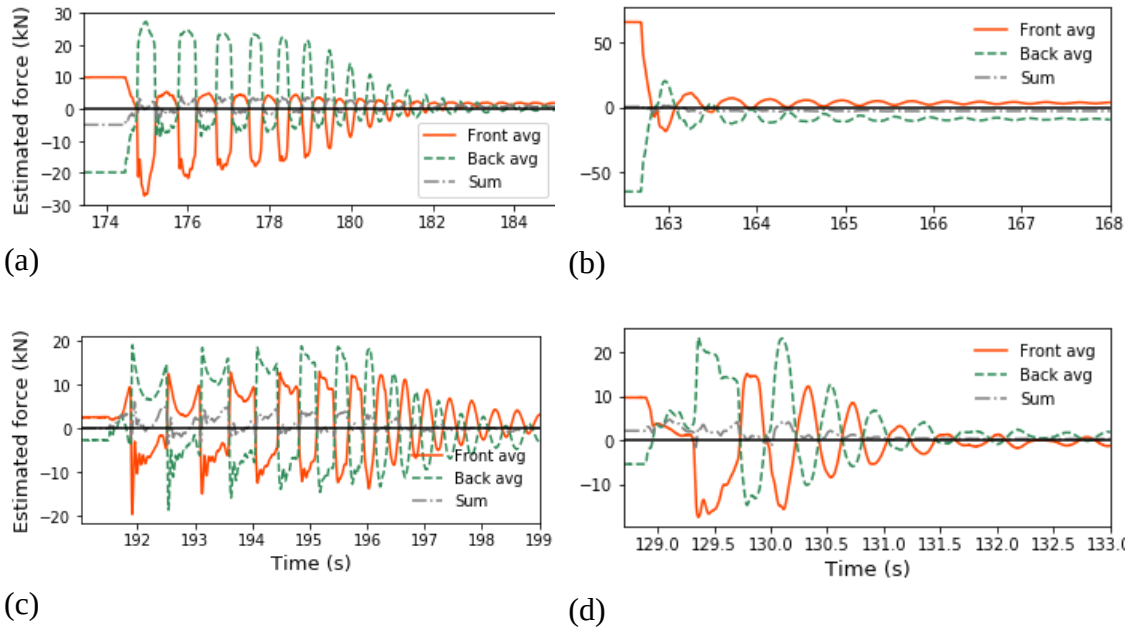

Figure 5.13: Estimated upright axial force: positive is tension, negative is compression. (a) Ductile Yielding Baseplate; (b) Rigid Baseplate; (c) Friction Slipper Baseplate without tightened bolt; (d) Friction Slipper Baseplate with bolt tightened

Figure 5.13 plots the estimated axial force in the upright, plotted from the end of the pull-over stage, release, followed by the free-vibration of the rack. The positive reading is tension, negative is compression. The front (orange line) and the back (green line) represent the front upright reading and the back upright reading from two uprights of the middle upright frame. The rack was pulled to the back during the pull-over procedure, therefore, the flat lines at the beginning of each plot, the front upright reading is always under tension, and the back upright is under compression. As can be seen from the figure, the upright with rigid baseplates suffered the largest force demand in both tension and compression, which is in accordance with the frame load-displacement curves shown in Figure 5.8. The after test inspection revealed the damage caused by the large force demand: in the compression upright, permanent local deformation was found at the side of the upright; in the tension upright, the anchor bolt was loosened due to the large pull-up force. The sum (grey line) is the sum of the front and back upright load readings, as can be seen, it stayed close to zero over time and rested at 0 at the end of free vibration. A small residual strain was found for the rigid baseplate upright as shown in Figure 5.13b, which maybe because of the large load developed in the pull-over process.

It is important to note that the estimated axial force is converted from the strain gauge readings. Therefore, it may not exactly represent the force response of the upright. Rather it is intended to give a general determination of the magnitude of the force. Also, the strain gauges are measuring the change of the strain once testing commenced; prior to this, the racks have been loaded with 5 tons of mass resulting in all the uprights being subjected to a certain compression load prior to the start of measuring. Therefore, the actual upright load should be subtracted by an axial compression loading from the estimated force, which is approximately 12 kN, but which varies for different uprights and different racks.

After being released, the rack frame immediately snapped back from its deformation and rotation, the load on both uprights first dropped to the minimum, and then the front upright started to impact on

the concrete foundation, simultaneously, the back upright started to suffer the peak tension force. The tension and compression forces in turn loaded both uprights, until the vibration ceased. The impact motion and its influence on the upright lasted for a very short period of time, around 0.2 seconds, but it was very clearly demonstrated in the strain gauge recording, especially in Figure 5.13c. The clear pulse and the vibration after it shows the energy dissipation process. The pulse and vibration can also be observed in the other plots.

It can be seen in the free-vibration period that for both compression and tension, the uprights with friction slipper baseplates had a smaller force demand than to the ductile yielding baseplates. For the rigid baseplates, since the anchor bolt was loosened during the application of the initial sway, the amount of tension force was not significant. However, the maximum compression force was slightly larger than that of the friction baseplates. It is important to note that in Figure 5.13d, the tension force was limited to a stable level which was controlled by the bolt tightening force.

Figure 5.14 illustrates the uplift time-history and the strain-uplift curves at both upright bases of the middle upright frame for all baseplates allowed to uplift. The orange line in the figure is the uplift displacement measured at the front upright of the frame, the green line is the uplift measured at the back upright of the frame. The uplift associated with the bolt-tightened friction baseplates decayed much faster than that of the other two uplifting baseplates. The second uplift was only slightly more than a quarter of the first. This excellent performance indicates that the energy input was rapidly dissipated by the friction baseplates in the first half cycle, which is advantageous for increasing the seismic resilience of pallet racking systems.

Since the strain readings were linearly proportional to the upright force, the area enveloped in each loop illustrates the amount of energy dissipated by either yielding (Figure 5.14a) or friction (Figure 5.14b, c) in each cycle of rocking. It can be seen that the amount of energy dissipated by the bolt-tightened friction baseplate is much higher than that by the other two uplifting baseplates. Also, it is important to note that, while the tightened friction baseplates dissipated much more energy during rocking, the deformation of the baseplate was lower than with the other two systems.

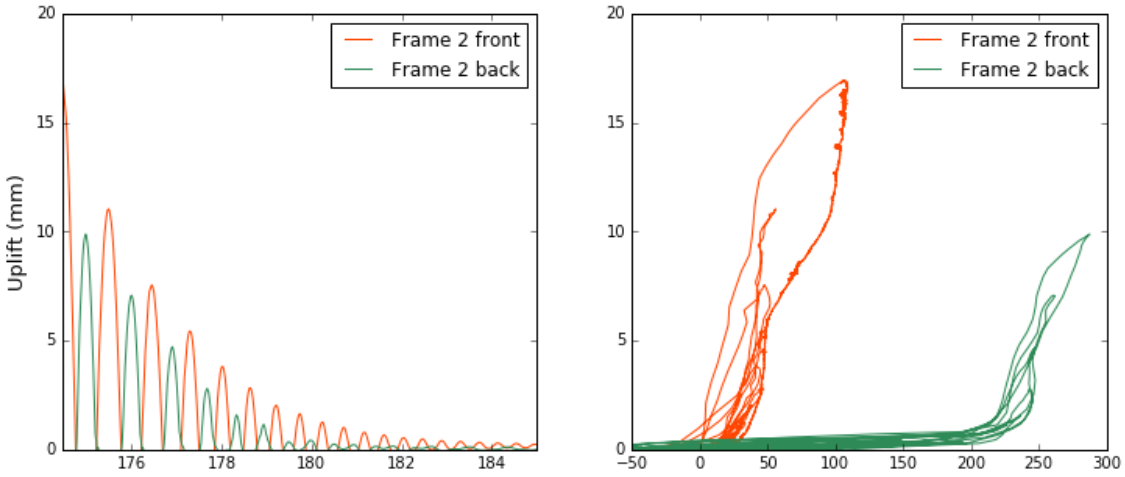

(a)

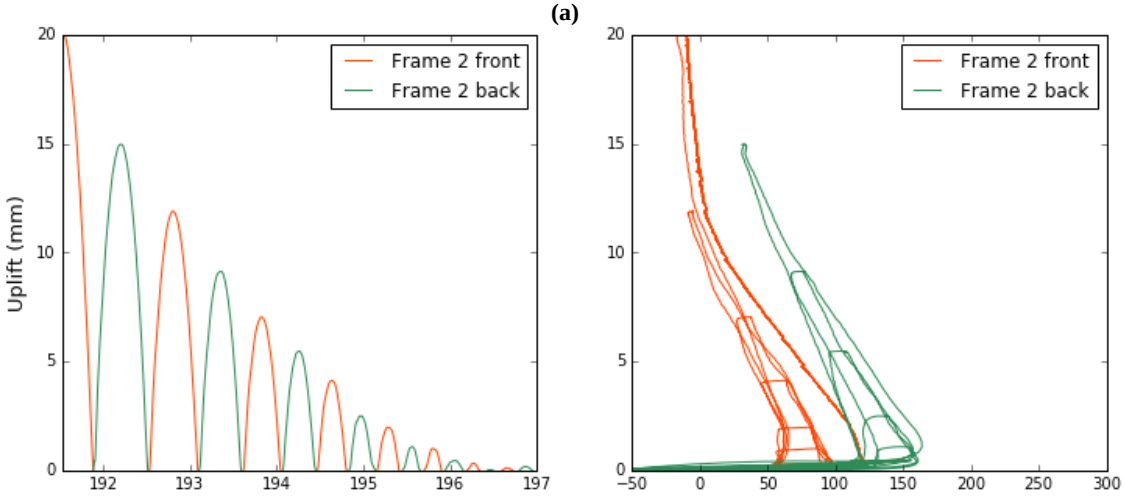

(b)

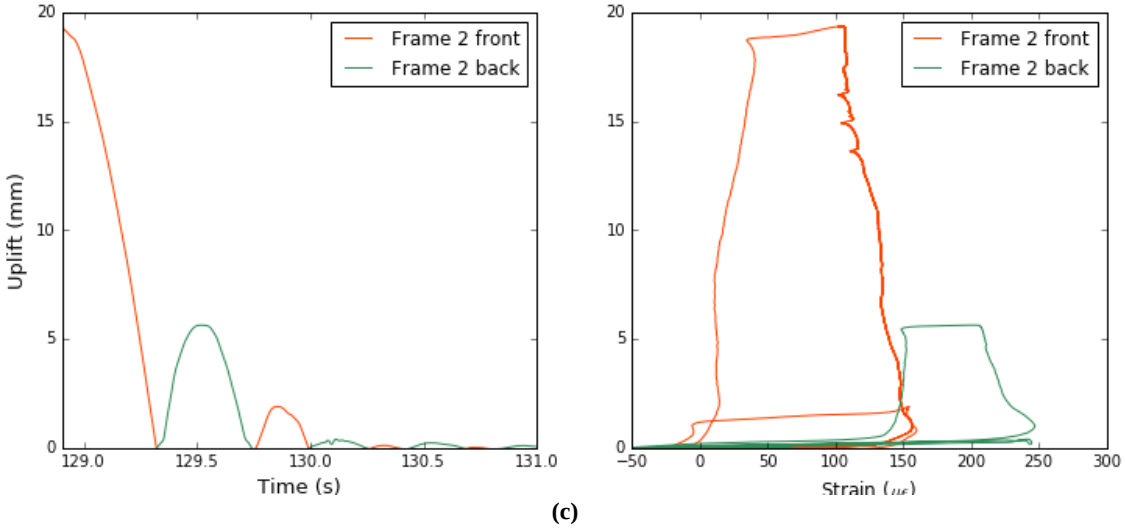

(c)

Figure 5.14: Uplift time-history at the upright base (left) and strain-uplift curves (right) of (a) Yielding baseplate; (b) Friction baseplate without tightened bolt; (c) Friction baseplate with 1 tightened bolt.

5.4 Conclusions

Through pull-over and snap-back testing, the seismic performance of the friction slipper baseplate has been compared to that of the ductile yielding and the rigid baseplates commonly used in the storage racking industry. It has been found that the bolt-tightened friction slipper baseplate gives much greater seismic resilience due to its larger energy dissipation capacity and smaller force demand. Specifically, the experimental testing programme on the pallet racking systems with friction slipper baseplates shows that the use of this baseplate has the following advantages and attributes compared with the other baseplates tested in this research:

1. It allows a lateral drift limit of 5% to be reached in the cross-aisle direction with stable, bi-linear behaviour and no damage to the baseplate or to the racking system, while the ductile yielding baseplate has significant permanent deformation at the baseplate and the rigid baseplate frame was found to have damage at its upright and loosening of its anchor bolts.
2. It enables the use of a ductility factor of over 5 in the cross-aisle direction using the Equivalent Static Method of design, which is much larger than that of the other two types of baseplates.
3. The energy dissipation capacity of the friction baseplate with bolt tightening is much larger than the other two types of baseplates.
4. It limits the tension uplift force to a predictable and stable level, meaning that the anchor bolts on both the tension the compression sides of the upright are protected from overload damage.
5. It protects the upright base from damage during severe earthquake action.
6. While not directly in the scope of this research, it also protects the column from damage due to operational impact during service much better than the ductile baseplate does.

Chapter 6 Shaking table tests

6.1 Introduction

Experimental investigations on the component behaviour, full-scale rack frame pull-over tests and free-vibration response tests have been conducted, as described in the previous chapters. The experimental results have revealed that in the cross-aisle direction the friction slipper baseplate delivers large energy dissipation capacity as well as a stable, controllable friction force. This means that the rack frame with the friction slipper baseplate can behave in an extremely ductile manner with a high damping ratio. In the down-aisle direction, the friction slipper provides significant moment-rotation capacity to the column base. Those quasi-static and short-term dynamic characteristics mean that a rack frame with friction slipper baseplates has significant potential to perform well in an actual earthquake event. To examine this potential, a series of shaking table tests were conducted to obtain the actual performance of a full-scale rack frame with the friction slipper baseplates under a range of simulated ground motions. Shaking table tests were carried out, using the same pallet rack and range of earthquake motions, on frames with other baseplate configurations for comparison with the friction slipper results

6.1.1 Shaking table

The shaking table in the Structural Test Hall of the University of Auckland was used for this test. It is a single degree of freedom shaking table with dimensions 4.5 x 3.6 m, and it is capable of a maximum displacement of +/- 180 mm, a maximum velocity of 0.987 m/s and a maximum acceleration of 16.7 m/s^2 (1.7 g), when supporting a payload of 10 tonnes.

6.1.2 Test suite

Nine rack frames were shaken under three different ground motions, in three loading directions with gradually increasing scale factor on the earthquake motions ranging from 0.25x ULS design level to 2.3x design level.

The first four racks were shaken in the cross-aisle direction with four different baseplate configurations, i.e., ductile baseplates, unanchored baseplates, rigid baseplates, and friction slipper baseplates with one or two bolts tightened to a selected torque value. Additionally, after each shake, all the clamping bolts of the friction slipper baseplates were re-tightened to the selected torque value to retain a consistent clamping force.

The 5^{th}, 6^{th} and 7^{th} racks were shaken in the down-aisle direction with three different baseplate configurations i.e., ductile baseplates, base isolators and friction baseplates.

The 8^{th} and 9^{th} racks with the ductile baseplates and the friction baseplates, were shaken at an angle of 20 degrees to the perpendicular of the shaking table movement direction.

The test suite detail is listed in Table 6.1.

Table 6.1: Test suite

Orientation	Rack frames	Baseplate configuration	Details
Cross-aisle	No. 1	Ductile yielding baseplate	A common baseplate used in New Zealand which allows the frame to uplift at the base and dissipate energy through steel yielding
	No. 2	Unanchored baseplate	Rigid baseplates, but not being anchored to the foundation, allowing free uplift of the rack
	No. 3	Friction slipper baseplate	An innovative baseplate design allows the frame to uplift at the base and dissipates energy through a friction damper mechanism
	No. 4	Rigid baseplate	A common type of baseplate in worldwide use. Anchored to the foundation and does not allow a rack to uplift
Down-aisle	No. 5	Ductile yielding baseplate	Relatively flexible in down-aisle direction rotation, acts as a pin after around 0.03 rad of rotation
	No. 6	Friction slipper baseplate	Relatively stiff in down-aisle direction rotation, its moment capacity is much larger than that of the ductile baseplate
	No. 7	Base isolator	Very flexible in down-aisle direction rotation
20 degrees	No. 8	Ductile yielding baseplate	Tends to lose its moment capacity when uplifting
	No. 9	Friction slipper baseplate	Retains a reasonable amount of moment capacity when uplifting

6.1.3 Rack assemblies

The tested rack frame assembly design remained constant for all the shaking table tests, and a new rack was used for each test. Additionally, the rack frame assembly for the shaking table tests was the same design as used for the pull-over and snap-back tests conducted in the previous chapters.

The rack frame assembly tested had three levels with two one-pallet-wide bays, having six pallet places in total. The assembly was made from the following cold-formed steel components: 4.8 m high, 90 mm wide, 2 mm thick uprights, 1.35 m long 80x40 box-section beams, and 30x25x1.8 mm lipped C-section bracing members. The frame braces had two levels of X bracing, followed by K bracing up the full height, as shown in Figure 6.7. Bracing was at 600 mm pitch.

The pallet rack was considered located in Wellington for determining the design seismic load.

Figure 6.1: A rack frame installed on the concrete foundation slabs

The rack assemblies were placed on a set of three concrete foundation blocks to provide a representative baseplate to foundation connection with these blocks rigidly connected into the shaking table, as shown in Figure 6.1.

The blocks each had cast in ducts to enable rigid clamping to the shaking table. The anchored baseplates were anchored directly into the concrete foundation blocks as they would be into the reinforced concrete floor slab of an industrial or storage building.

The foundation blocks were 1700 mm long and 150 mm thick. The two outer blocks had a width of 700 mm, and the centre block has a width of 600 mm. Each block weighs approximately 410 kg. These blocks were cast in 40 MPa commercial concrete with steel mesh cage reinforcement to represent an actual warehouse ground condition.

After each test, the concrete foundation blocks were carefully inspected for damage. The epoxy injection technique was used to repair any cracks found and any holes drilled in the blocks.

6.1.4 Structure loading/pallet mass

The rack frame was loaded with six pallet masses. Each pallet consisted of four steel billets, each billet weighing 175 kg. Total pallet mass was around 800 kg.

Figure 6.2: The pallet mass tightened to the beams and interlocked in between them so it cannot slide out

The steel billets were placed on top of a lattice of hollow steel sections which act to increase the centre of mass distance of the pallet above the beam level to what it would be in a typical pallet in practice. Two smaller hollow sections welded on the bottom fitted inside the rack beams and acted as an interlocking key. Threaded bars and bolts were used to tighten the pallet mass and sections together as a whole rigid body to prevent the masses from jumping off the rails. Two ratchet straps were used to tighten the pallet mass to the beams, working together with the interlocking keys to prevent the pallet masses from sliding and toppling off the rack. There was a gap of around 10 mm between the interlocking key and the rack beam. Therefore, although the pallet mass could not slide out of the range of the beams, it was allowed to slide in the range of the gaps in between the rack beams, as shown in Figure 6.2.

6.1.5 Instrumentation

The response of the structure was monitored by a group of instruments, at a sampling rate of 100 Hz, and recorded by a data logger connected to a computer.

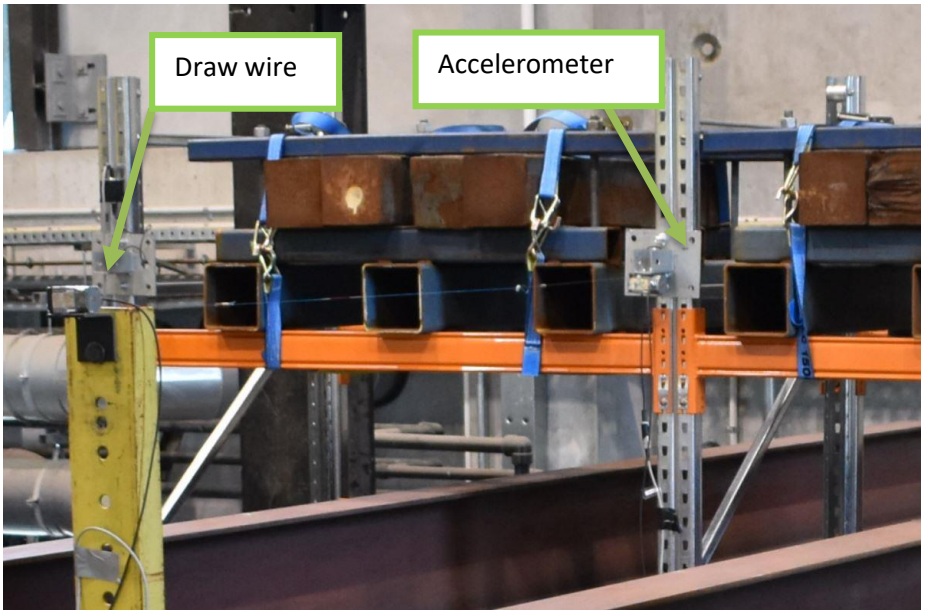

Figure 6.3: A draw wire installed at the top level of the rack frame for displacement monitoring; an accelerometer attached at the same height and protected by a channel section

The following measuring instruments were attached to the test setup:

- Draw wires were used to monitor the horizontal displacement at each level of the rack frames as show in Figure 6.3.
- One LVDT was embedded in the shaking table to record its actual output displacement.
- Accelerometers were attached to monitor the horizontal acceleration change at each level of the rack frame. The vibration caused by the impact between pallet masses and beams was also monitored by the accelerometers. One accelerometer was installed on the shaking table to record its actual output acceleration.
- A set of strain gauges was attached to both sides of each upright base, as shown in Figure 6.8, to monitor the strain change. The change of strain at the upright's base was used to determine the change of axial loading, in either compression or tension.

6.1.6 Target spectrum & selection of ground motions:

The following design criteria were used to develop the design ULS seismic spectrum.

Table 6.2: Target ULS design spectrum design criteria

Criteria	Value
Design working life	50 years
Importance level	2
Location	Wellington
Hazard factor	0.4
Site subsoil class	C (Shallow soil)
Distance to nearest fault	4 km
Structural ductility factor	3.0
Structural performance factor	0.7

Based on the requirement of NZ 1170.5 [66] and the BRANZ design guideline [65], three strong motion records were selected from the New Zealand Strong-motion Database published by GeoNet, considering only sites with subsoil class "C" and meeting the other target spectrum design criteria mentioned above. They are also selected to fit within the ultimate capacity of the shaking table. The details of these three ground motions are listed in Table 6.3.

The loading sequence applied is as follows: The 1st selected ground motion (Kaikoura 2016) was scaled to 0.25, 0.5, 0.75 and 1.0 x the ultimate limit state design level intensity of the target spectrum. After these four, gradually increased Kaikoura 2016 ground motions were applied, the structure was then loaded alternatively by gradually increased Northridge 1994 and Kobe 1995 ground motions, up to the ultimate capacity of the shaking table, which is 1.75 x design level for the Northridge Earthquake and 2.3x that for the Kobe Earthquake. In total, 12 ground motions were prepared to reach the ultimate intensity that the shaking table could generate. It is important to note that in each round of 12 earthquake loadings, the rack frame damage accumulated until the final failure or the end of each test round. The exact loading sequence and intensity of the ground motions are listed in Table 6.4. The displacement-time history of the three ground motions with a scale factor of 1.0 is shown in Figure 6.4. The comparison between the pseudo-acceleration spectra of 3 selected ground motions and the target spectrum is shown in Figure 6.5.

Table 6.3: Details of selected ground motions

Earthquake event	Event magnitude	Event fault type	Reason for being selected	The best fit scale factor	PGA (m/s2)
Kaikoura 2016 earthquake	M7.6	Oblique-slip	It is the best fit with the target spectrum in the period ranging from 0.5 s to 1.5 s which was observed in the free vibration response with a scale factor of 2.468.	2.46	1.38
Northridge 1994 earthquake	M6.7	Blind thrust	Its dominant period is the closest to those baseplates which have no uplift at the base (around 0.5s), with a scale factor of 0.988, this ground motion is at the design target level intensity	0.99	3.97
Kobe 1995 earthquake	M6.9	Strike-slip	Its considerable energy release in a long period range (1-1.5 s) which is a vulnerable period for the baseplates that enable racks to rock. With a scale factor of 0.983, this ground motion is at the design target level intensity.	0.98	2.35

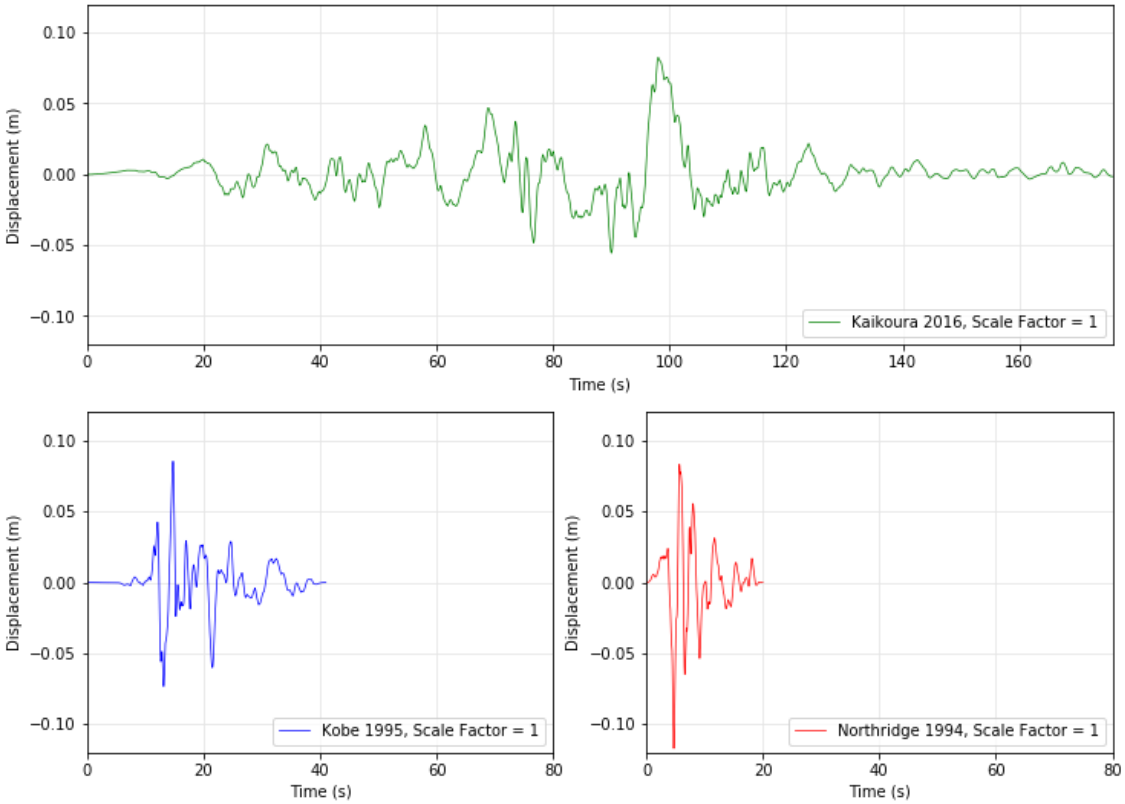

Figure 6.4: The displacement-time history of three selected ground motions with the scale factor = 1.0

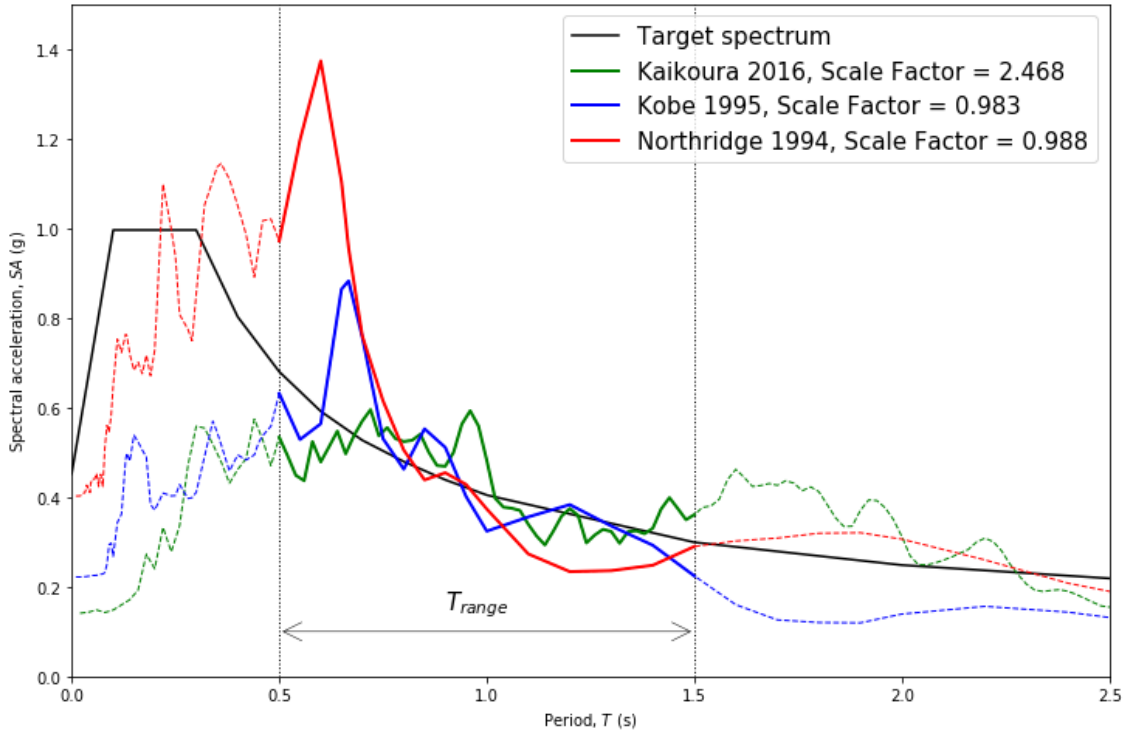

Figure 6.5: Comparison between the target spectrum and the pseudo-acceleration spectra of the three selected ground motions

Table 6.4: Test order, scale factor and the PGA of the generated ground motions

Test order	Scale factor	Ratio of design level	Ground motion	Max acc. (m/s^2)	g
1	0.617	0.25	Kaikoura2016	0.345	0.035
2	1.234	0.5	Kaikoura2016	0.689	0.070
3	1.851	0.75	Kaikoura2016	1.034	0.105
4	2.468	1	Kaikoura2016	1.379	0.141
5	0.988	1	Northridge1994	3.912	0.399
6	0.983	1	Kobe1995	2.17	0.221
7	1.235	1.25	Northridge1994	4.89	0.498
8	1.475	1.5	Kobe1995	3.256	0.332
9	1.482	1.5	Northridge1994	5.868	0.598
10	1.966	2	Kobe1995	4.34	0.442
11	1.729	1.75	Northridge1994	6.846	0.698
12	2.261	2.3	Kobe1995	4.992	0.509

6.2 Racking frame cross-aisle direction shaking

Test racks No.1-No.4 provided the seismic performance of the rack frames in the cross-aisle direction with four different baseplate configurations, which enabled a direct comparison of their seismic and rocking behaviour.

- Rigid baseplate, which does not allow the rack frame to rock, and therefore for which the whole system behaves rigidly.
- Unanchored baseplate, which allows the rack frame to rock freely.
- Friction slipper baseplate and ductile yielding baseplate. The behaviour of these two is in between the above two. They allow the rack frames to rock in a controlled manner, either by controlling its friction clamping force (friction slipper baseplate) or its thickness of floor plate (ductile yielding baseplate). The seismic energy can be dissipated through the rocking by either mechanism.

For friction slipper baseplates, if there is no bolt tightened, the rack frame acts effectively as a free rocking frame but with increased damping. If the clamping force is too strong, the upright is not allowed to slide along the baseplate, then the rack frame would act as a rigid base frame. Therefore, to achieve the optimal seismic performance, it was important to select the correct friction clamping force. In this test, two bolt configurations were conducted for comparison: the one-bolt tightened case and the two-bolt tightened case, as shown in Figure 6.6.

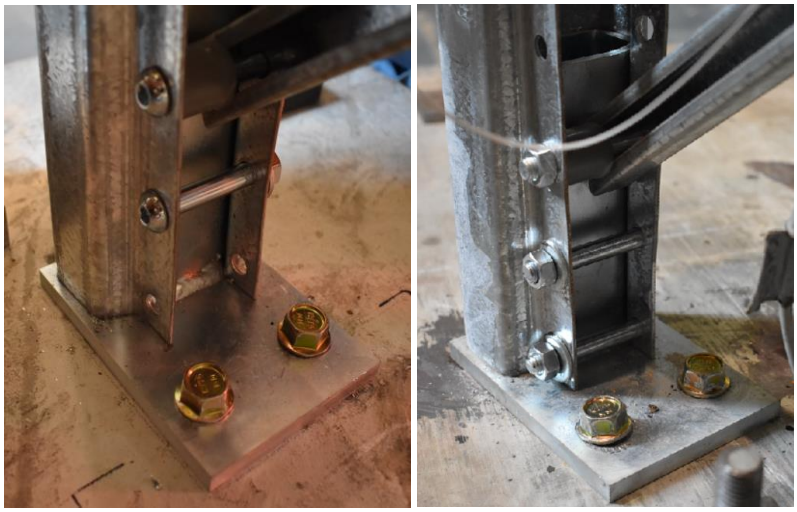

Figure 6.6: Friction slipper baseplate setup: 1 bolt tightened (Left), and 2 bolt tightened (Right)

For the ductile yielding baseplate, if its floor plate is thin enough, the rack frame would act as a free rocking frame, and the baseplate would be fractured easily; if its floor plate is too thick, the rack frame will act as a rigid base frame (not considering the sliding slot in the ductile yielding baseplate, which would allow the rack to rock freely in the range of the slot). In this case, the proper thickness of the ductile baseplate is critical. The ductile yielding baseplate has been a mature industrial product for years. The commercial version of the ductile yielding baseplate was adopted for conducting this shaking table test.

Figure 6.7: Rack frame in the cross-aisle direction

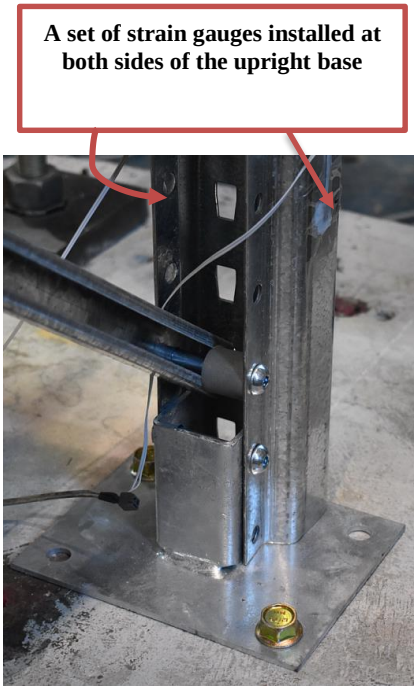

Figure 6.8: Ductile baseplate assembly

The objectives of this series of tests were to:

- Determine the peak upright axial force under three different earthquake ground motions, with

four gradually increased ratios of design level loading intensity.

- Determine the rack failure mode for each type of baseplate.
- Determine the rack resilience to earthquakes above design level.

The side view of a tested rack frame installed on the shaking table for cross-aisle direction excitation is shown in Figure 6.7. The ductile yielding baseplate assembly is shown in Figure 6.8, with two anchor bolts bolted diagonally to the concrete floor. A set of strain gauges is attached to both sides of the upright to monitor the strain changes during the testing.

6.2.1 Observations

After each shake, the rack frame was carefully inspected for damage. The observations are summarised below:

Ductile yielding baseplate

(a) Ductile baseplate permanent deformed

(b) Bolt loosened & pulled out a little

(c) Ductile baseplate fracture at welding

(d) Fracture through the floor plate

Figure 6.9: Ductile yielding baseplate damage after all 12 ground motions

The rack frame with the ductile yielding baseplate survived all the 12 ground motions with no structural failure; as described in Table 6.4, the ultimate ground motion intensity was up to 2.3x design level earthquake.

The damage observed was concentrated at the baseplate-floor connection. From 1.25 x design level ground motion, the floor plates were found to have a slight permanent bend . Some uprights were found to twist or bend locally 1-2 mm relative to the floor plates. Some cracks were found at the corners of the welds between the stub and the floor plates from 1.5 x design level ground motions. With the further increment of the ground motion intensity, the bending at the floor plate, twisting between uprights and baseplates, and fractures at the weld kept developing. The level of damage kept accumulating. After conducting all the 12 ground motions , the floor plates were extensively yielded and bent upwards, as shown in Figure 6.9 (a). Most of them were torn off at the weld connection to

the stub, and some of the fractures were found to pass through the floor plates, as shown in Figure 6.9 (c) and (d). The anchor bolts in some cases pulled out for a few millimetres, but did not completely lose their pull-out resistance.

Unanchored baseplate

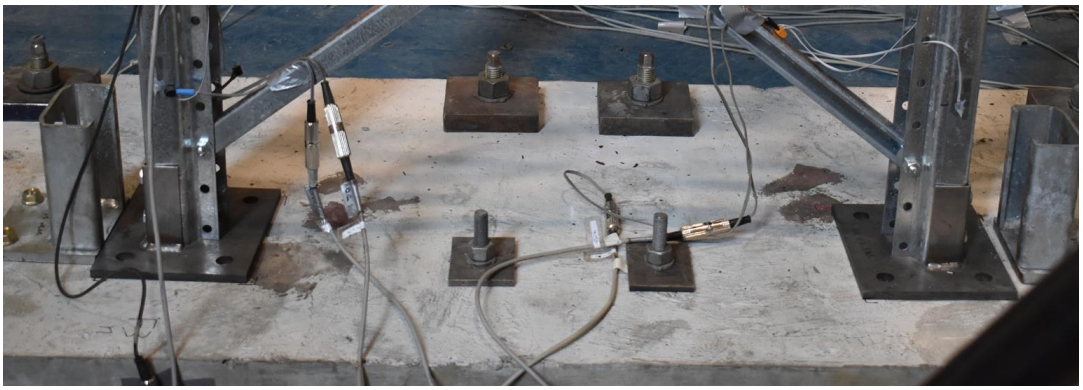

Figure 6.10: Unanchored baseplate setup: restraining cross-aisle movement while allowing frame uplift

The unanchored rack started its noticeable rocking behaviour from the 4th ground motion, which is the Kaikoura 2016 earthquake, 1.0 x design level ground motion, followed by the other two 1.0x of design level earthquake, taken from Northridge 1994 and Kobe 1995 earthquakes. Although these three ground motions have the same design intensity (all in 1.0x design level), the response of the unanchored rack frame varied significantly, as can be seen in Figure 6.11.

After surviving all four of the gradually increased intensity Kaikoura Earthquake ground motions and the first two Northridge and the first two Kobe Earthquakes, it overturned during the 3rd Northridge ground motion, which is 1.5x design level earthquake, as shown in Figure 6.12.

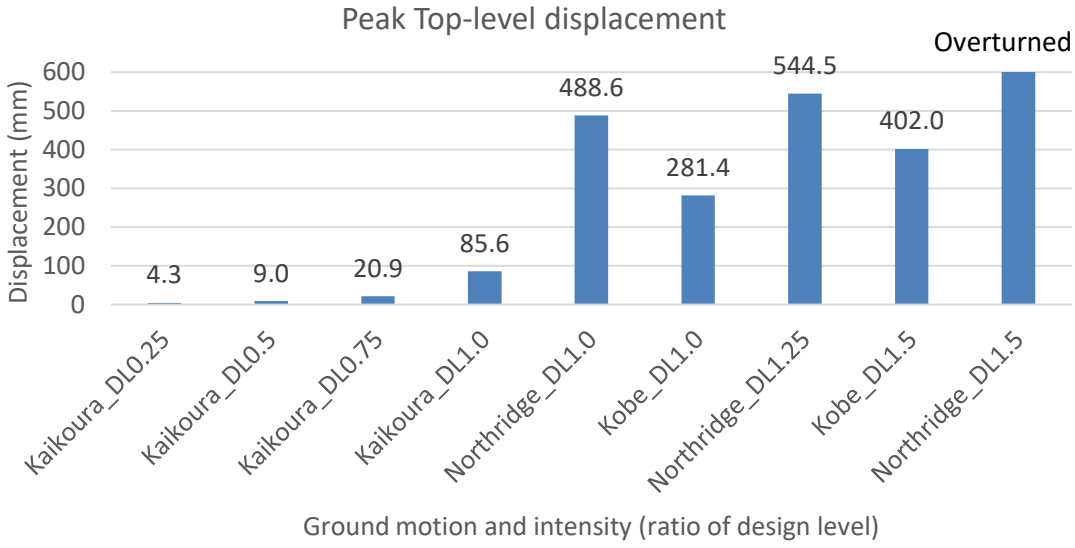

Figure 6.11: Peak top-level displacement of unanchored rack frame in different ground motions

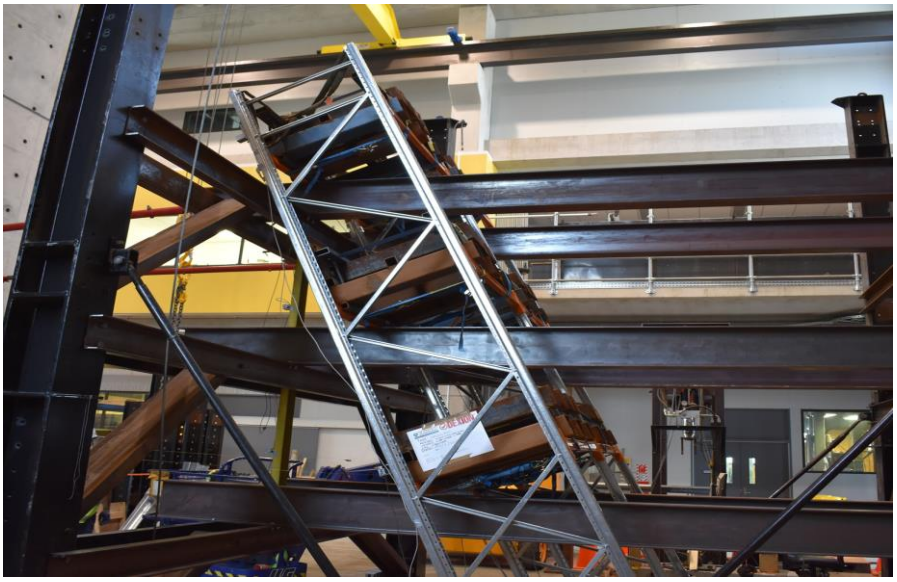

Figure 6.12: Unanchored baseplate frame overturned at design level 1.5x Northridge earthquake

The rack walked along the longitudinal direction slightly after each earthquake. It walked about 110 mm to one direction after all 4 Kaikoura earthquake ground motions, walked 20-50 mm after each of Northridge and Kobe Earthquakes. This indicates that the duration of the earthquake plays a key role in the walking distance, which was perpendicular to the direction of shaking.

Rigid baseplate

Rigid baseplates are wildly used throughout the world for pallet racking systems. Because of its thick floor plate, its deformation capacity and energy dissipation capacity is minimal, but it is much more robust than the ductile baseplate against impact damage to the column, which occurs regularly in-service . Therefore, during an earthquake event, the earthquake-induced energy will keep accumulated in the structure with a very limited dissipation pathway, just converting between kinetic energy and potential energy. With the increase of the total energy in the system, the internal force also increases, until one or more structural members suffer a failure. This was confirmed by this shaking table test.

The rack frame with a rigid baseplate survived the first 7 ground motions, up to 1.25x design level earthquake, with no noticeable damage. During the 8th ground motion, at 1.5x design level earthquake, Kobe Earthquake, the anchor bolts into the concrete were pulled out because of the very large pull-up force at the upright and baseplate connection. The concrete slab around the baseplate area was destroyed, as shown in Figure 6.13, down to the full depth of the anchor bolt (75 mm depth). The damaged slab was replaced by a new concrete foundation slab for the rest of the tests, which had been cast at the same time as the others so the age of the concrete in each foundation slab remained the same.

Figure 6.13: Rigid baseplate anchor bolt pulled out

However, this failure mode for the pallet racking system is not commonly seen in previous real earthquake events. The reason of this conflict is, in reality, during a severe earthquake event, pallets loaded on the rack frames are free to slide in between beams; in this experiment, the pallets are tightened to the beams with interlocking keys to fix their position, as shown in Figure 6.2. Pallet sliding isolates the mass on the rack frames, so the earthquake-induced forces in a regular rack can be significantly smaller than the pallet-tightened racks. On the other hand, the free sliding also causes falling of pallets if they slide too much. In current seismic design practice, the sliding of pallets is not well considered for commercial pallet racking systems and sliding will occur to a greater extent than what was allowed for in this project.

Friction slipper baseplate

The rack frames with friction slipper baseplates with 1 bolt tightened were first subjected to 12 ground motions and survived all with no visible damage. After that, an additional nine ground motions (omitting the first three less intense ground motions of the original 12) were applied to the rack frame with altered clamping bolt tightness and a two-bolt tightened case. Again, there was still no visible damage observed.

6.2.2 Discussion

The test results are summarised in Table 6.5:

Table 6.5: Test result summary for cross-aisle direction shakes

Baseplate Configuration	Peak Upright Axial Load (kN)*	Peak Top-Level Displacement (mm)	Peak Drift	Resilience	Failure Mode
Ductile Yielding Baseplate (DBP)	-88 kN	269	6.1%	2.3 X design level	Survive all shakes with baseplates fractured
Unanchored Baseplate (UBP)	-39 kN	Overturned	-	1.5 X design level	Overturned
Rigid Baseplate (RBP)	+81 kN	126	2.9%	1.25 X design level	Anchor bolts pulled-out, concrete floor damaged
Friction Baseplate with 1 bolt (FBP)	-28 kN	425	9.7%	2.3 X design level	Survive all shakes with no damage found
Friction Baseplate with 2 bolts (FBP2)	-35 kN	280	6.4%	2.3 X design level	Survive all shakes with no damage found

*** Positive value (+) as tension, negative value (-) as compression**

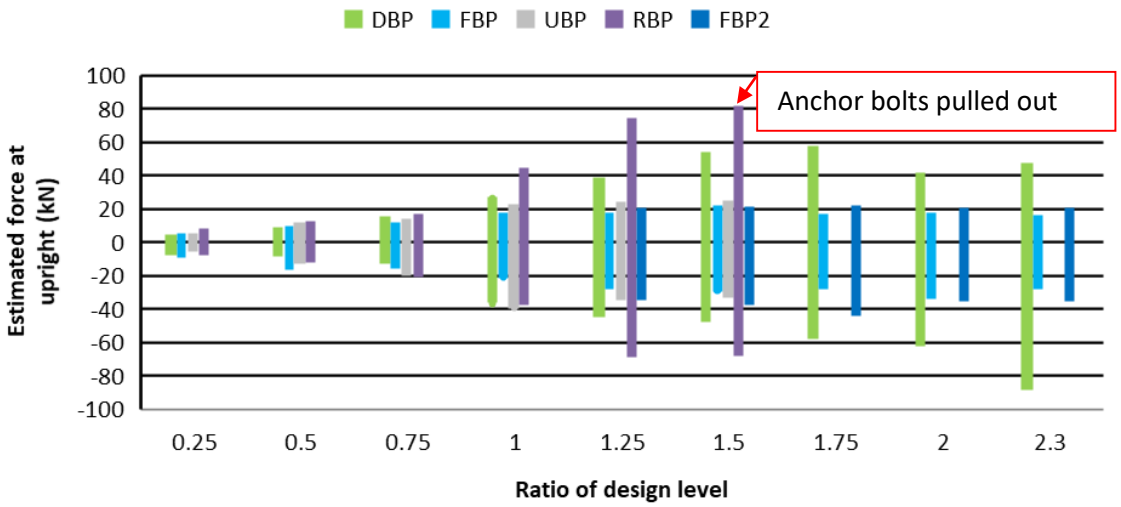

Figure 6.14: Estimated maximum force response at each design level of earthquakes at the middle frame upright, positive value for tension, negative value for compression.
DBP: Ductile yielding baseplate; FBP: Friction slipper baseplate with 1 bolt; FBP2: Friction slipper baseplate with 2 bolts; UBP: Unanchored baseplate; RBP: Rigid baseplate

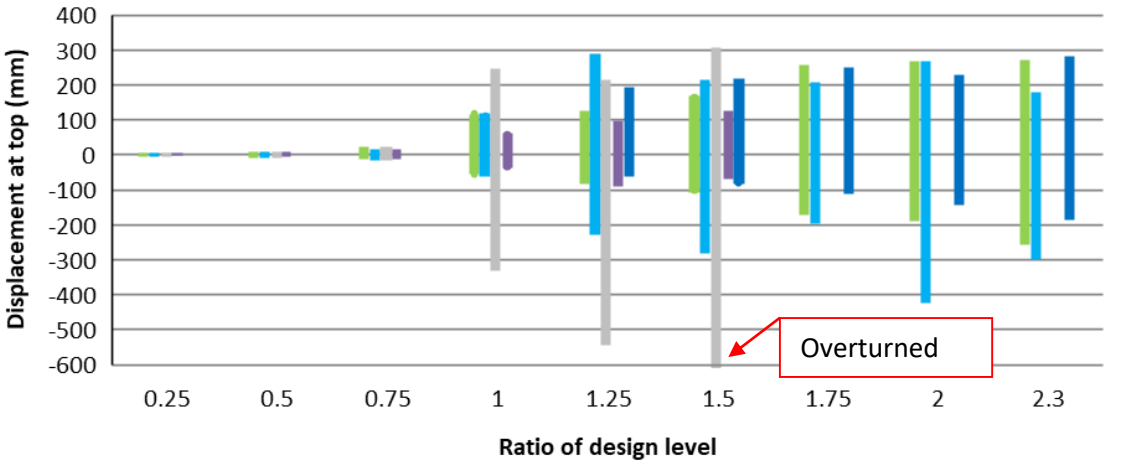

Figure 6.15: Top-level displacement at each design level of earthquakes of the middle frame

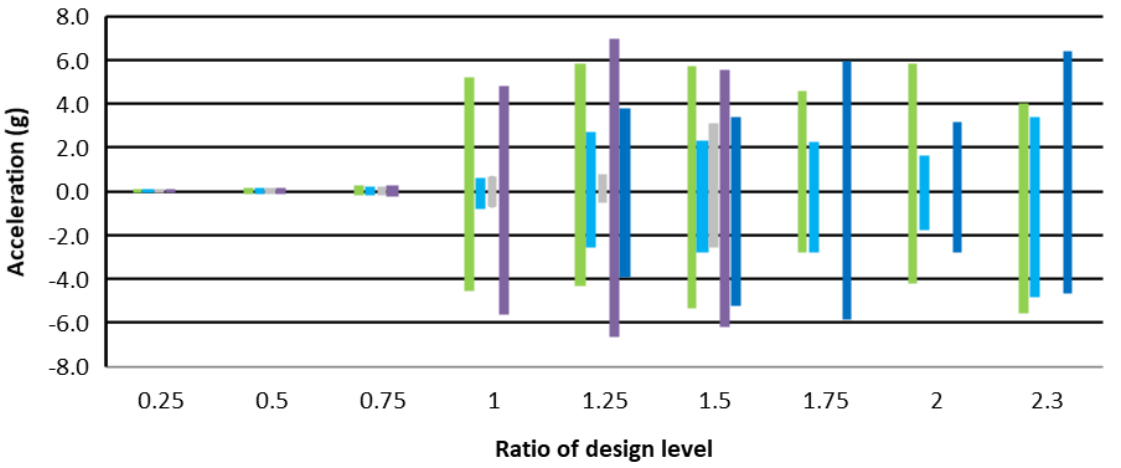

Figure 6.16: Peak acceleration recorded at the top level of the frame at each level of shaking

A set of strain-gauges was attached at the base of each upright, 200 mm above the floor, measuring the change of the strain. The upright axial load was derived from the strain reading to get an estimation of the change of the axial load. The estimated peak force response at each design level of earthquakes

of the middle frame upright is shown in Figure 6.14.

A set of wire displacement transducers were installed at each level of the rack frames to record the displacement of the rack. The top-level relative displacement at each design level of ground motions, for the middle frame, is shown in Figure 6.15.

A set of accelerometers was attached at each level of the rack frames to record the acceleration response of the rack during the shaking. The top-level acceleration for each design level ground motion of the middle frame is shown in Figure 6.16.

It is important to note that the peak load values shown in the tables and figures are not the actual loading carried by the uprights, they are the change of the axial load during the shaking. The actual upright loading must include the gravity force carried by each upright. This was approximately 12 kN for the middle uprights and 6 kN for the side uprights. In practice it varied slightly as the pallets moved around between tests.

As shown in Figure 6.14, the axial load response of the rack with rigid baseplates was always the largest compared to the other baseplate cases until, at 1.5X design level ground motion, it failed by anchor bolt pull-out due to the enormous tension force at the upright. The change of the axial load is approximately 81 kN and the actual peak tension force is approximately 69 kN. The static pull-out resistance of this two anchor bolt setup is approximately 40 kN, and since the tension of the upright during the shaking was a rapid impulse load and lasted for only a short period, the actual dynamic breaking load was roughly 70% higher than the static case. In actual design practice, the influence of loading speed is not considered, and it could be worthwhile to pay attention to this effect. Nevertheless, the damage of the concrete floor is an unacceptable consequence, not to mention the potential of rack collapse and injury to people.

Compared with the rigid baseplate, the ductile yielding baseplate shows the larger axial force response, especially in compression. During the last few records, the rack with the ductile baseplate behaved almost like a free rocking frame with a hook element. Uprights stomped on the floor heavily and rotated about the upright base until stopped at the other side of the upright by the baseplate anchored to the floor. At the end of the test, most of the baseplates were fractured, as shown in Figure 6.9. Because of the yielding and fracturing of the steel plate, a significant amount of seismic energy was dissipated by the baseplate, and the rack frame overturn and collapse was prevented up to the 2.3 X design level. Although this performance is better than for the rack with rigid baseplate, after a severe earthquake event, replacement of the baseplate can cost a significant amount of time and money, and result in discontinuity of the business. An even better performance was discovered with the friction slipper baseplate.

The rack frames with the friction slipper baseplate showed no damage after surviving all 12 + 9 ground motions up to 2.3 x design level. Compared with the other baseplate configurations, for the tests above 1.0 x design level, the rack frames with friction slipper baseplates always had the smallest axial load response, and the tension responses for each load case were very stable. This is because the bolts were tightened by a torque wrench to the selected torque after each shaking test to ensure a stable, controlled friction force. Also, since the seismic energy of the rack frames was significantly dissipated by the friction damper, the development of kinetic energy of the rack was controlled, which means the speed

of rack movement was limited. This was clearly noticed in comparing the video. The reduced speed led to a smaller stomping force when the upright impacted the floor, which is indicated by the axial compression force monitored and shown in Figure 6.14. The compression force at each load case for the friction slipper is much smaller than the ductile baseplate and rigid baseplate. The controlled axial load response limits the damage to the rack in the seismic event. No damage was observed in the rack frame with friction slipper baseplates. The business of the warehouse owner would not be interrupted after a severe earthquake event, and no replacement is required.

However, the benefits of the friction slipper baseplate are not free of charge. By allowing the rack frame to rock, the drift of the rack frame is much larger than the racks with rigid bases which don't allow the frame to rock. As shown in Figure 6.15, until the rigid baseplate fails, its drift is always the smallest compared to the other cases, which also results in a huge axial load at the uprights as shown in Figure 6.14. As can be seen from these two figures, the axial load and drift of the frame are mostly inversely proportioned to each other. This is because the total imported seismic energy is continuously increased for each load case, and the total energy equals the force multiplied by the displacement. Therefore, with the increment of the ground motion intensity, the response of the rack increases. The increasing response is indicated by the increasing axial load and displacement of the frames. For the ductile yielding baseplates, both the axial load and the displacement increase to represent an increasing response. For the friction slipper baseplate, the axial load remains very stable in all the load cases, and the 2-bolt frame has continuously larger values than the 1-bolt frame. Also, the change pattern of the frame displacement is very different. The 1-bolt frame shows a much larger response compared with the 2-bolt frame. The 1-bolt frame response does not continuously increase with increasing earthquake intensity as it does for the 2-bolt frame. Because of the smaller friction clamping force of the 1-bolt frame, less energy is dissipated by the friction damper, and more energy is dissipated through the rocking behaviour. A less-controlled rocking behaviour resonates more easily with the ground motion. Once rocking resonation occurs, the rack frame generates a much larger cycle of rocking, as shown at the 2x design level ground motion in Figure 6.15, which generates a much larger displacement than the 2.3x design level ground motion. Increasing the friction clamping force can limit the displacement response of the rack frame. As can be seen in Figure 6.15, the 2-bolt frame always has smaller displacement than the 1-bolt frame, with a slightly larger control friction force, as shown in Figure 6.14.

Although the pallets were tightened on the beams with two ratchet straps, they can still slide around on or between the beams when the frame acceleration is large enough for pallets to overcome the friction force between the pallets and the beams. Sliding pallets may cause strong impact to the uprights or beams when the interlocking key hits the beams under cross-aisle direction excitation or when the pallets hit the upright frame under down-aisle direction excitation. Those impacts were recorded by the accelerometers attached to the uprights and formed peak impulses, as shown in Figure 6.17. If the magnitude of the acceleration indicates the intensity of the impact for different baseplates in a real earthquake event, then the intensity of the impact indicates the likelihood of content spillage and pallets falling from the beams. As can be seen in the figure, compared with other rack frames, the rack with rigid baseplates has the most significant impact intensity at all design levels until it fails at

the 1.5x design level. After that, the frame with friction baseplates (2 bolts case) and the frame with ductile yielding baseplates get the largest position alternatively. The impact intensity of the rack frame with friction baseplates with 1 bolt tightened is always smallest comparing the three frames mentioned above.

The rack frame with unanchored baseplates had no friction sliding activated between the beams and pallets until it overturned at the Northridge Earthquake 1.5X design level. This is because, once the rack starts to rock, its acceleration stopped increasing and formed a plateau, as shown in Figure 6.18, below the acceleration threshold at which sliding of the pallets occurs. The very short duration impulse load shown in Figure 6.18 is evidence of the upright stomping on the concrete floor rather than the pallets impacting the uprights, which is much more intense. As can be seen in the figure, the stomping mostly happened when the rack frame displacement was close to 0, which indicates one of the uprights was contacting the floor, and the impulse of the acceleration was then formed by the stomping. The impact between upright and the floor is also a path of energy dissipation. A portion of seismic energy in the racking frame was dissipated by the high-frequency vibration of the system and converted to internal energy through material damping, friction and sound waves. A 20 Hz low-pass filter was applied to the acceleration time-history shown in Figure 6.18, the record before and after filtering is compared in Figure 6.19. Since the most of vibration formed by upright stomping is over 20 Hz, after the record was filtered, a flat and stable acceleration platform can be observed (green line) while the rack was rocking, which is the acceleration of the rack frame without the interference of the impact vibration. In comparison, the acceleration at top level of rigid baseplate frame under the same load case is shown in Figure 6.20. A series of severe impacts between the pallets and beams were observed during the shaking. As can be seen in the figure, the filtered reading shows that the rack frame acceleration response kept developing and formed a peak reaching almost 1 g, while the peak acceleration of the frame with unanchored baseplates was limited to roughly 0.2g (after the filtered low pass 20 Hz). The rack frames with friction baseplates show behaviour in between the above two cases. The acceleration response and internal force were limited by the controlled uplift: a massive amount of energy was dissipated by the friction damper, and a small portion was dissipated by the minor impact vibration, which together limited the internal force and acceleration.

Figure 6.21 plots the filtered acceleration time history of all the baseplates during Kobe Earthquake ground motion excitation, scale factor 1.475, 1.5x design level. As can be seen, the ductile yielding baseplate and the rigid baseplate has the largest peak acceleration impulse. The friction slipper baseplate in both 1-bolt and 2-bolt cases showed relatively smaller acceleration response. The unanchored baseplate showed the smallest acceleration response with a flat platform at each rocking period.

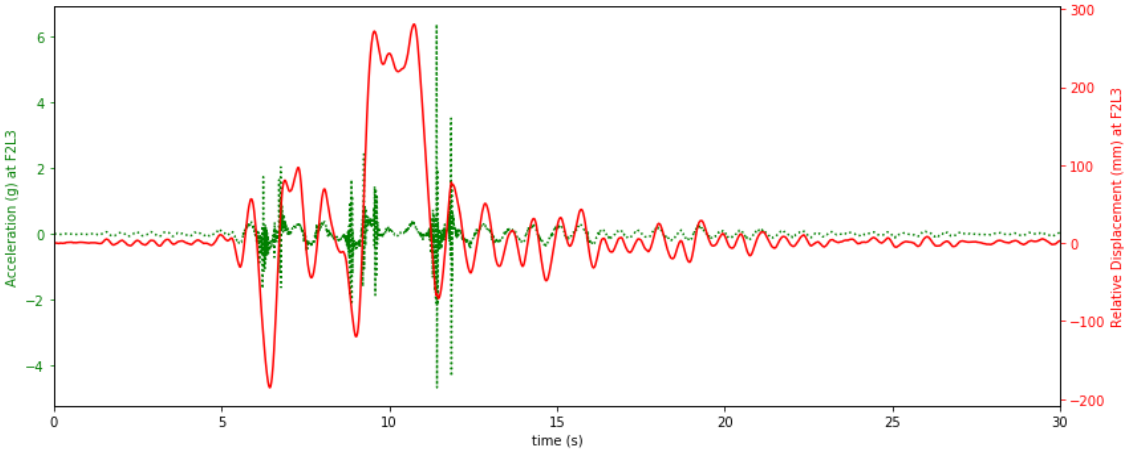

Figure 6.17: An example of displacement and acceleration time-history: Friction baseplate with 2 bolts, Kobe Earthquake 2.3X design level

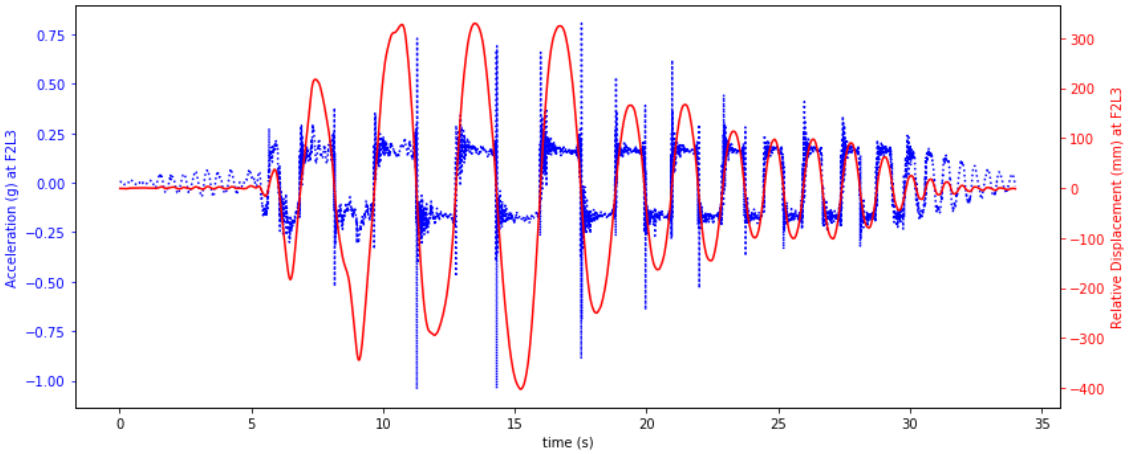

Figure 6.18: Displacement and acceleration time-history: Unanchored baseplate, Kobe Earthquake 1.5X design level

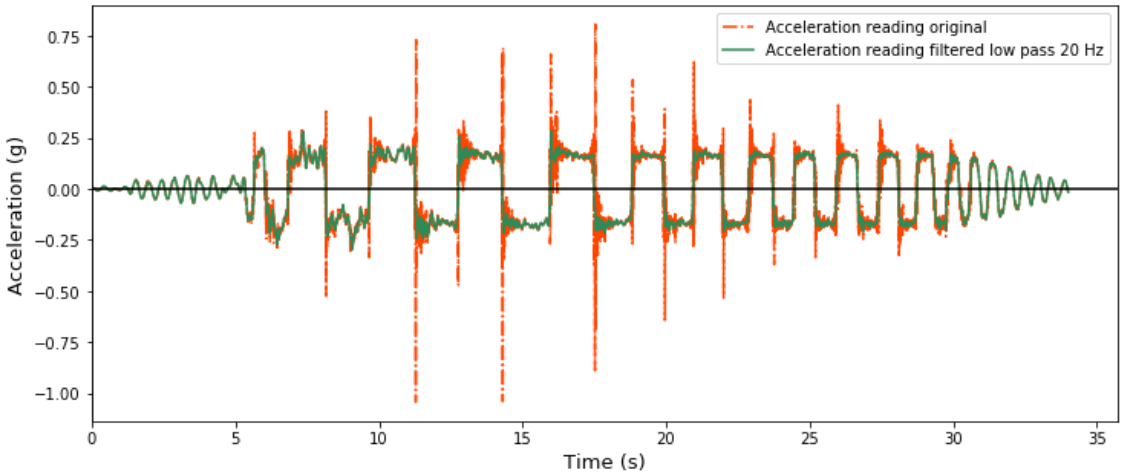

Figure 6.19: Acceleration time-history, comparing before and after filtered low-pass 20 Hz: Unanchored baseplate, Kobe Earthquake 1.5X design level

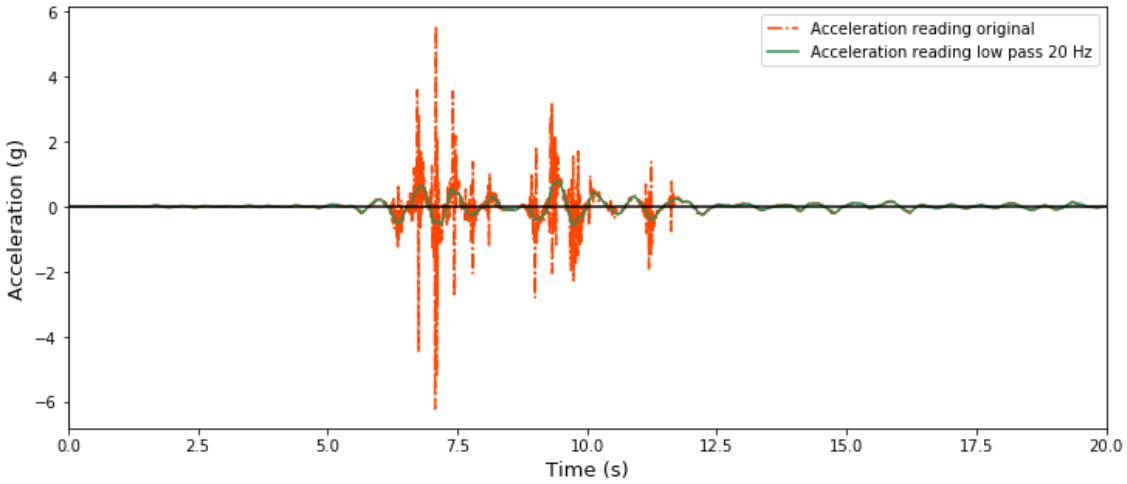

Figure 6.20: Acceleration time-history, comparing before and after filtered low-pass 20 Hz: Rigid baseplate, Kobe Earthquake 1.5X design level

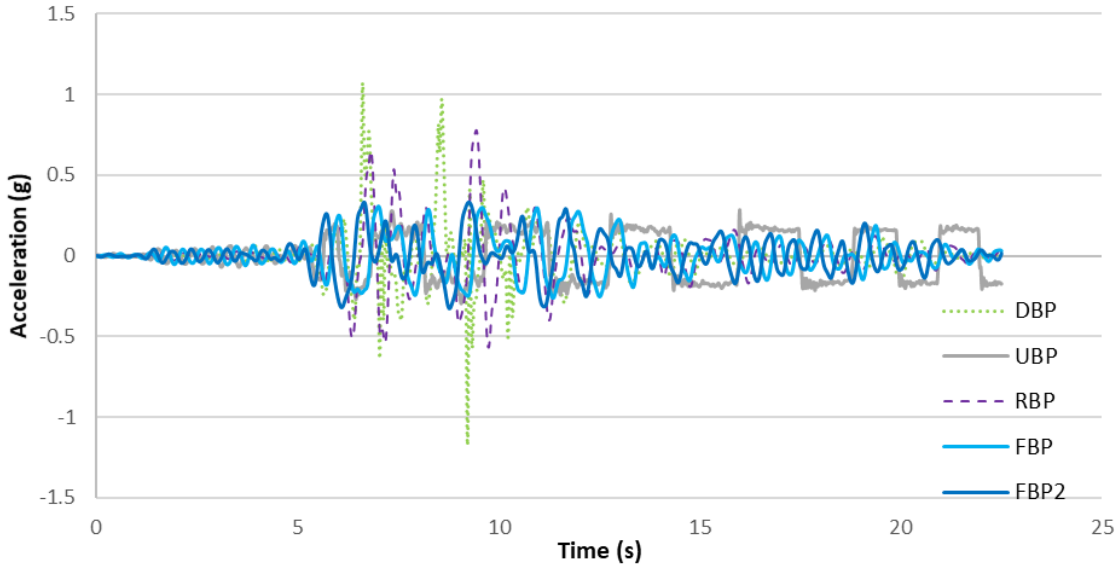

Figure 6.21: Acceleration recording, all baseplates, 20 Hz low-pass filtered: Kobe Earthquake 1.5x design level, SF = 1.475

6.2.3 Summary – Cross-aisle direction

Four rack frames, with different baseplate configurations, were tested on the shaking table to determine their seismic performance in the cross-aisle direction. Based on the experimental observations, the following conclusions can be drawn for the cross-aisle direction response of the rack frame with various types of base connections:

1. The friction slipper baseplate and the ductile yielding baseplate survived all the 12 ground motions up to 2.3x design level, however the friction slipper baseplate showed no damage but the ductile yielding baseplate showed extensive fracture and yielding.
2. The unanchored baseplate survived 8 ground motions up to 1.5x design level, and overturned at the 9th ground motion.
3. The rigid baseplate survived 7 ground motions up to 1.25x design level, and suffered anchor bolt pull out at the concrete floor at the 8th ground motion.

4. The rack frame with the friction slipper baseplates showed very stable and low-intensity axial tension and compression load.
5. The rack frame with the rigid baseplate showed the largest axial load response until it failed. The rack frame with the ductile yielding baseplates showed a larger axial load response than the friction slipper baseplates.
6. The rack frame with the friction slipper baseplate with one bolt tightened showed an unpredictable displacement response, caused by rocking resonance; while the rack frame with two bolts tightened showed a reasonable and smaller controlled displacement response.
7. The more rigid the base connection, the more likely it is that pallets can slide in between beams.
8. The friction slipper baseplate significantly reduce the acceleration response compared to the ductile yielding baseplate and the rigid baseplate.
9. The friction slipper baseplate dissipates a significant amount of seismic energy. The controlled and selectable friction force setting gives more design flexibility to engineers.
10. Overall, the friction slipper baseplate demonstrated the best cross-aisle direction seismic performance compared with the other three types of base connection, as shown by the controlled axial load, displacement, and relatively small acceleration response, along with the largest seismic resilience, and no damage from the tests.

6.3 Racking frame down-aisle direction shaking

After the cross-aisle direction shaking tests were conducted, the rack frames, with different base connections, were subject to a regime of shaking in the down-aisle direction. Key aspect of each rack were:

- Rack No. 5, with the ductile yielding baseplate, was relatively flexible in the down-aisle direction, with the ductile baseplate acting as a pin connection after around 0.03 rad of rotation.
- Rack No. 6, with the friction slipper baseplate, was relatively stiff in down-aisle direction rotation. Its moment bearing capacity is much larger than that of the ductile baseplate.
- Rack No. 7, with the Base Isolator, was very flexible in down-aisle direction rotation.

The component behaviour of the ductile yielding baseplate and the friction slipper baseplate in the down-aisle direction has been reported in Chapter 4 of this thesis.

The base isolator adopted in this test, shown in Figure 6.22, is a mature product on the current market. The seismic performance of this base isolated pallet racking system has been investigated for the cross-aisle direction [73][34][36]. These include full-scale shaking table tests, and the device improves the resilience of the rack in the cross-aisle direction. However, in the down-aisle direction, the improvement of this base isolation system is marginal. The arrangement of this base isolation system in the down-aisle direction is shown in Figure 20. The main isolation component is the laminated steel plate and rubber block bearing. The laminated bearing is a bonded system and allows the structure to move in the cross-aisle direction; it has a large energy dissipation capacity and a base isolation function. However, in the down-aisle direction, the system elements have significant clearance to allow the cross-aisle sliding to occur, meaning that they are very flexible in the down aisle direction. As discussed in Chapter 3 of this thesis, in the down-aisle direction seismic resisting system, the rack frame is considered as a moment frame and the distribution of the moment of a rack frame very much depends on the rotational stiffness of the beam-column connection and base-column connectors. If the base-column connection is too flexible, then the beam-column connection at the first beam level above the base will have to carry a much more significant moment, which may result in damage to the beam-column connector.

In this study, the down-aisle direction seismic performance of this base isolation system is tested by the shaking table test, and the test result and observations will be compared with the rack frame with the ductile yielding baseplates and the friction slipper baseplates.

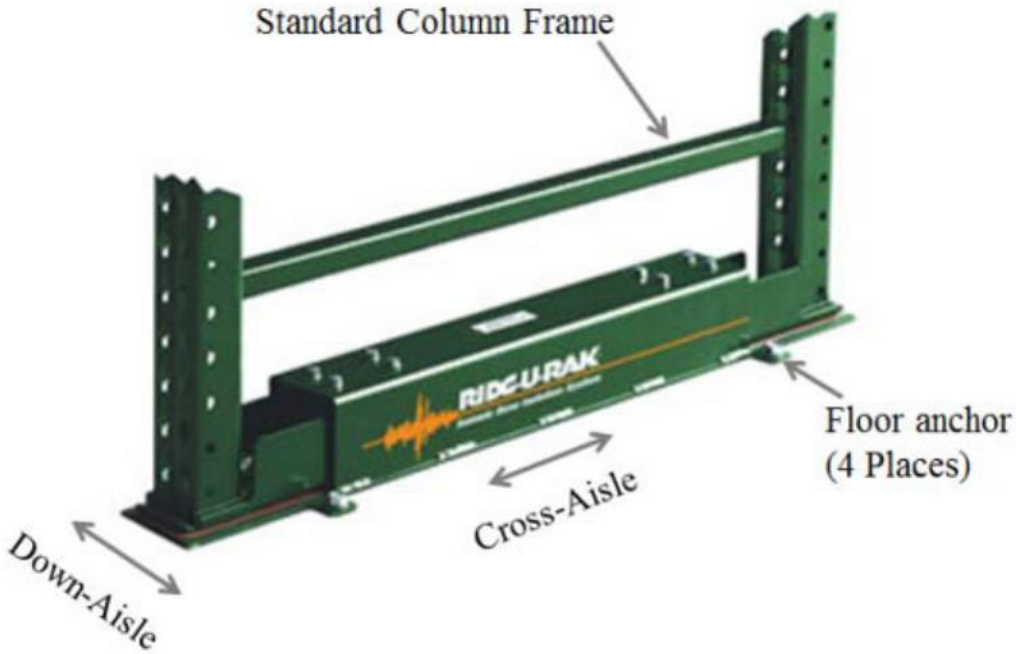

Figure 6.22: Ridg-U-Rak Base Isolation system for steel storage racks (from *Michael 20*13 [36]**)**

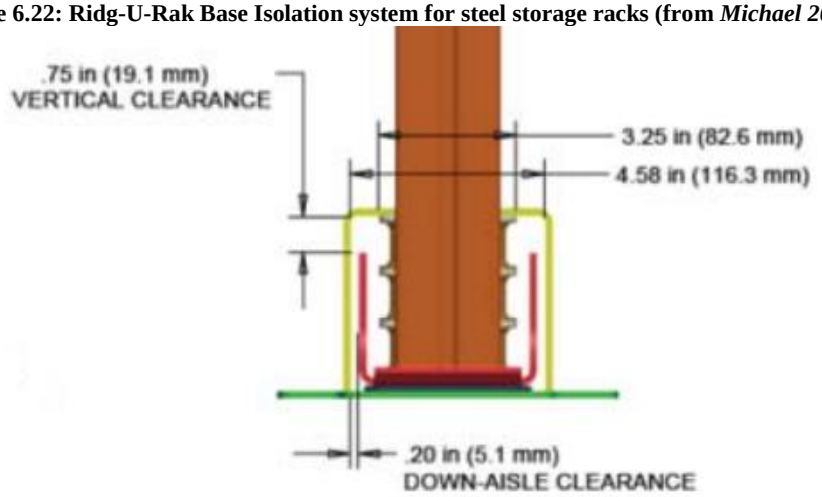

Figure 6.23: Down-aisle direction assembly and clearance of the base isolator (from R. J. Michael 2013 [36]**)**

The objectives of the down-aisle direction shaking table tests were to:

- Determine the rotation angle at the beam-column, base-column connections.
- Determine the resilience of the rack frames with different base connections to earthquakes above design level.
- Determine the failure mode of the rack frames with different base connections.

Figure 6.24: Down-aisle direction shaking table test setup, Base Isolator

The test setup is shown in Figure 6.24. The rack frame configuration for the down-aisle direction shaking table test was the same as for the cross-aisle direction, but with a change of shaking orientation. It is important to note again that in each round of 12 earthquake loadings, the rack frame damage keeps accumulating until final failure or the end of each test round. After each rack frame had gone through a test round, a new rack frame was constructed with the new base configuration. The base isolation system was tested first, followed by the ductile yielding baseplate, and then the friction slipper baseplate.

Portal gauges were used to measure the relative displacement between beam and uprights and base and uprights to derive the relative rotation angle of the beam-column and base-column connections. A set of wire displacement transducers were attached to each level of the rack frame to monitor the displacement of the frame at each level. A set of accelerometers were attached to each level on each upright to monitor the acceleration of the rack frame and record the pounding between the pallets and the upright frames.

6.3.1 Observations

After each shake, the rack frame was carefully inspected for damage. The down-aisle direction shaking caused no significant damage to the base connections. Both the friction slipper baseplates and the base isolator showed no damage after all the ground motions. A small residual deformation was observed at some ductile yielding baseplates. No fracture was found in any ductile yielding baseplate in the all down-aisle direction tests. The damage to the rack frames was concentrated at the beam-end connectors for all the rack frames.

The development of damage at the beam-end connector occurred in 4 stages, as shown in Figure 6.25: Stage 1: Rotation angle increased from 0 - 0.05 rad. Cracks observed on the paint surface at the corners of the box beams, and the cracks further developed along the beam with the increase in the rotation

angle.

Stage 2: Rotation angle reached around 0.07 rad. Cracks on the paint surface run through the whole depth of the box beam. Small cracks in the steel can be identified.

Stage 3: Rotation angle reached around 0.12 rad. Noticeable cracks were observed at the corner of the steel section. With further shaking, the crack width and length increased in both the vertical and horizontal directions.

Stage 4: The peak rotation angle of the beam-end connector reached 0.24 rad. Steel cracks at the top corner and the bottom corner further developed along the surface and eventually linked together and the crack ran through the whole depth of the beam. The outer surface of the box section lost its capacity completely; the beam carries the gravity load of the pallets with the steel remaining at the inner surface. Such severe damage was only observed at one beam-end connector at the last shake of the rack frame with the base isolator at the side rack frame.

Because of the configuration of the test racks, the moment distribution of the beam-end connectors in a rack decreases over the height of the rack. Therefore, the damage of the beam-end connector also decreases over the height. The bottom-level beam-end connector suffered the most damage, up to Stage 4; the middle beam level suffered some minor damage, limited at Stage 1; no damage was observed at the top beam level beam-end connectors. Additionally, the damage to the connectors connecting the side frames is more severe than to those connecting the middle frame. Also, due to the uneven capacity of each beam-end connector and uneven load distribution, in the same rack frame and the same location, some of the connectors suffered more damage than others. Inspection showed that, at the bottom-level, some connectors reached damage Stage 3, some of them were still at Stage 2.

Since the damage to the rack frame of each base configuration was accumulated through all the ground motions, a low-cycle fatigue effect to the beam-end connectors is significant. Also, the development of cracks in some damaged beam-end connectors can be very sudden and rapid during certain ground motions.

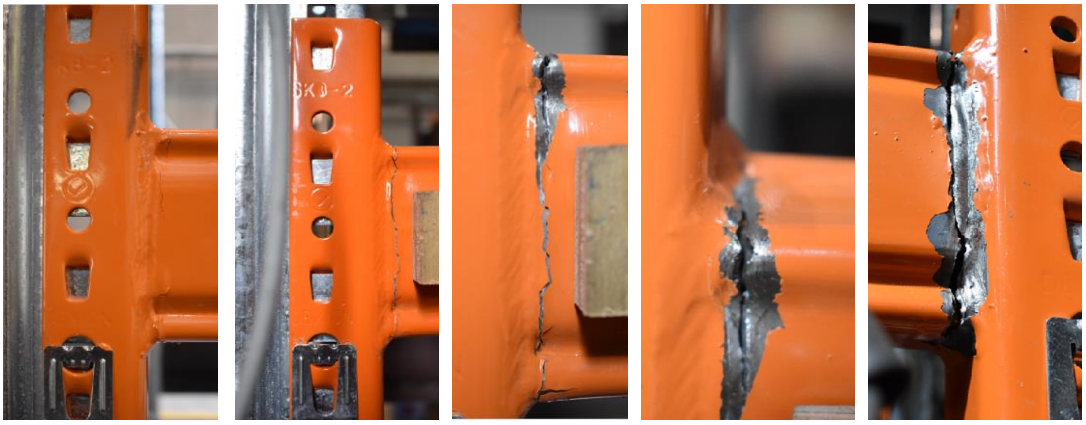

Stage 1 | **Stage 2** | **Stage 3** | **Stage 3 (crack at both directions)** | **Stage 4**

Figure 6.25: Crack development at the beam-end connection

6.3.2 Discussion

The rotation angles of the beam-end connectors at the bottom beam level and the baseplate-floor

connections were monitored by portal gauges. The averaged rotation angle of the base-floor connections of each rack frame is shown in Figure 26, the averaged rotation angle of the beam-end connectors at the bottom beam level is shown in Figure 6.27. These averaged values take the peak rotation angle of the rack response under each ground motion, with different design level intensities. It can be seen that the rack frame with friction slipper baseplates (Orange in the figures) has the smallest rotation angle in both the base-floor connections and the bottom-level beam-end connectors, for all the ground motion cases. The rack frame with the base isolators (Green) has the largest rotation angle in both measurements, except in the two lowest ground motion cases: 0.25x and 0.5x design level in the base-floor connections. Also, it can be seen that for both measurements, the rotation angles of the friction slipper baseplates do not show a rapid increment after each shaking, and stay relatively stable and constant. A rapid increase in the rotation angle can be seen for the rack frame with the ductile baseplate (Blue) at 2 x design level, which is the 10th ground motion, Kobe earthquake; and the rack frame with base isolators at 1.75x design level, which is the 11th ground motion, Northridge earthquake. The inspection after these two ground motions shows that in one of the beam-end connectors of both the frames, the damage has reached or is close to Stage 4, which means this connector would probably have fractured entirely in the next more intense ground motion. Therefore, to avoid the collapse of the rack frame or the falling of the pallets, the test was terminated. The rack frame with the ductile yielding baseplate survived 10 ground motions; the rack frame with the base isolator survived 11 ground motions; the rack frame with the friction slipper baseplate survived all 12 ground motions up to 2.3x design level earthquake. It is important to note that this is not the ultimate capacity of the frame with the friction slipper baseplates; the capacity of the shaking table had been reached, which prevented the generation of more substantial scaled ground motions.

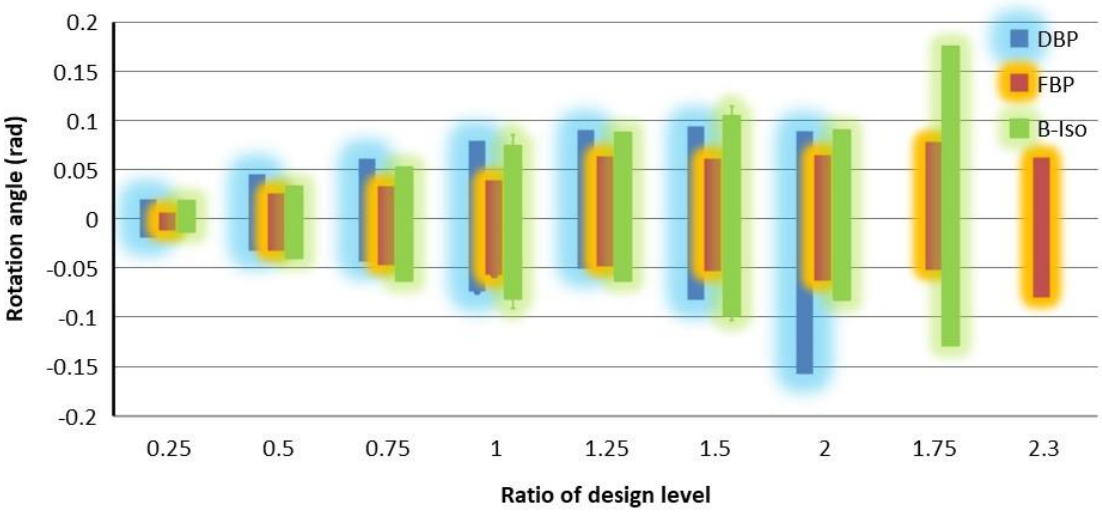

Figure 6.26: Average rotation angle of floor-upright connections

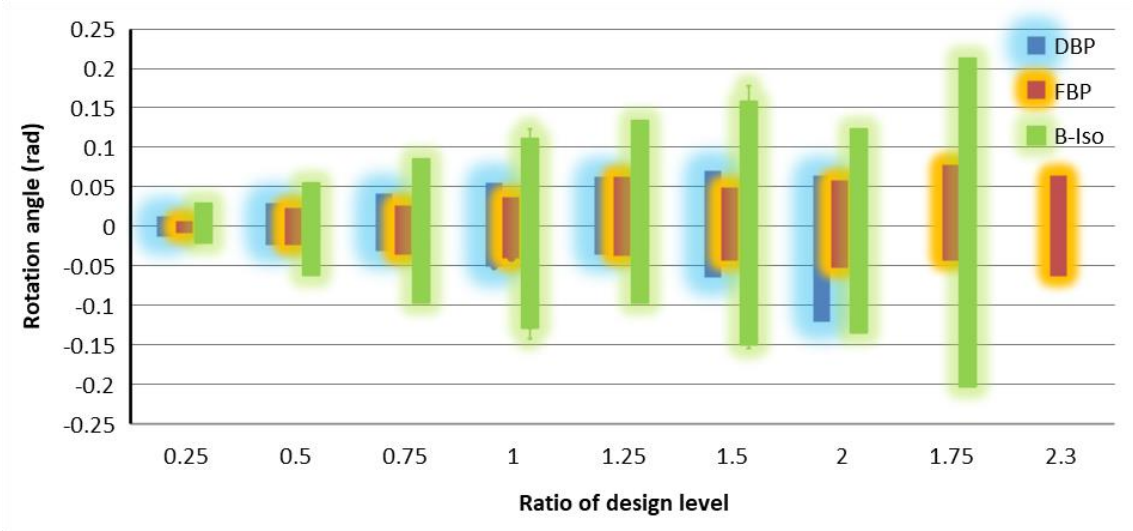

Figure 6.27: Average rotation angle of beam-end connectors at the bottom beam level

Table 6.6: Beam-end connector crack length and damage ratio: statistical analysis

		Friction Baseplate				Ductile Baseplate				Base Isolator			
Near side Beam 1		F1	F2	Damage %		F1	F2	Damage %		F1	F2	Damage %	
	CT	31	9	77.5%	22.5%	26	22	65.0%	55.0%	36	24	90.0%	60.0%
	CHT	33	7	67.1%	20.0%	26	34	38.8%	40.0%	43	19	58.8%	64.7%
	CHB	24	10			7	0			7	36		
	CB	20	5	50.0%	12.5%	13	0	32.5%	0.0%	14	30	35.0%	75.0%
Near side Beam 2		F2	F3	Damage %		F2	F3	Damage %		F2	F3	Damage %	
	CT	21	13	52.5%	32.5%	24	19	60.0%	47.5%	28	27	70.0%	67.5%
	CHT	22	8	31.8%	21.2%	49	11	57.6%	16.5%	42	36	100.0%	48.2%
	CHB	5	10			0	3			43	5		
	CB	5	5	12.5%	12.5%	9	10	22.5%	25.0%	40	13	100.0%	32.5%
Far side Beam 1		F1	F2	Damage %		F1	F2	Damage %		F1	F2	Damage %	
	CT	13	27	32.5%	67.5%	13	25	32.5%	62.5%	23	40	57.5%	100.0%
	CHT	8	32	21.2%	61.2%	9	51	14.1%	96.5%	23	51	67.1%	96.5%
	CHB	10	20			3	31			34	31		
	CB	10	14	25.0%	35.0%	5	17	12.5%	42.5%	30	26	75.0%	65.0%
Far side Beam 2		F2	F3	Damage %		F2	F3	Damage %		F2	F3	Damage %	
	CT	21	12	52.5%	30.0%	30	8	75.0%	20.0%	22	30	55.0%	75.0%
	CHT	18	10	60.0%	21.2%	43	10	87.1%	14.1%	21	36	77.6%	42.4%
	CHB	33	8			31	2			45	0		
	CB	31	3	77.5%	7.5%	13	3	32.5%	7.5%	39	0	97.5%	0.0%
	AVE	Length		Damage %		Length		Damage %		Length		Damage %	
		15.56		37.6%		17.09		39.9%		27.94		67.1%	

After all the shaking table tests were completed, a statistical analysis was conducted to measure the crack length in all the bottom-level beams for each of the three rack frames tested. The statistical result is shown in Table 6.6, the length of each crack and its damage ratio are listed in the table. In this table, F1, F2, F3 represent the beam-end connector connecting the Frame 1, 2 and 3 from left to right, Frame 2 is the middle frame, Frame 1 and 3 are the side frames. CT, CHT, CHB, CB represent the cracks at different surfaces of the box beam: CT represents the cracks at the top surface; CB represents the cracks at the bottom surface; CHT and CHB represent the cracks at the vertical surface of the box beam from the top and bottom edge respectively. The cross-section size of the box beam is

40x85 mm including the welding. The damage ratio is the length of the crack divided by the section length in its direction. In this table, the longer the crack is, the redder the cell colour is. It was evident that the damage to the base isolator frame is the most severe, followed by the ductile baseplate frame, the friction baseplate frame has the lowest level of damage at the beam-end connectors. The friction baseplate survived all the 12 ground motions, and its damage is still less severe than the ductile baseplate frame, which only survived 10 ground motions. The most severe damage in the rack frame was observed at a side frame beam-end connector with the base isolator. Its crack runs through the whole depth of the vertical surface and the whole width of the bottom surface of the box beam. This is the only connector that reached the Stage 4 damage level, as shown in Figure 6.25.

It is evident that in comparison with the other two types of base connections, the friction slipper baseplate shows the best seismic performance in the down-aisle direction, with the least damage and the largest resilience. The reason is the friction slipper has a larger rotational stiffness in the down-aisle direction with a large moment-bearing capacity. Therefore, it can carry a significantly large moment in the moment frame which reduces the burden on the beam-end connector. As compared in Chapter 4 of this thesis, under the same axial load and with the same amount of rotation, the friction slipper baseplate can take a bending moment up to a few times larger than the ductile yielding baseplate; and the base isolator has an even lower moment-bearing capacity. Additionally, the moment capacity of the friction slipper baseplate increases with rotation, and the ductile baseplate acts like a pin after 0.03 rad of rotation. Therefore, the large moment bearing capacity of the friction slipper baseplate allows the system to carry a large amount of seismic energy and dissipated it slowly instead of forming larger cracks and fracture the beam-end connectors.

6.3.3 Summary – Down-aisle direction

Three rack frames with different base connections were tested on the shaking table for their seismic performance in the down-aisle direction. Based on the experimental observations, the following conclusions can be drawn for the down-aisle direction response of the rack frame:

1. The rack frame with the friction slipper baseplates survived all 12 ground motions up to 2.3x design level earthquake. The rack frame with the base isolators survived 11 ground motions up to 2.0x design level earthquake. The rack frame with the ductile yielding baseplates survived 10 ground motions up to 2.0x design level earthquake.
2. The damage from the down-aisle direction excitation for all three rack frames is mainly concentrated on the beam-end connectors. The rack with the base isolators suffered the most severe beam-end connector damage after 11 ground motion excitations before failure; the rack with the ductile yielding baseplates suffered less damage than that of the base isolator, but only went through 10 ground motions before failure; the rack with the friction slipper baseplates suffered the least damage but went through all 12 ground motions without failure;
3. The rotation angle recorded for the rack frame with the friction slipper baseplates showed a very stable response through all the ground motions at both base-connections and beam-end connections, while the racks with the ductile baseplates and the base isolators have some response mutations in between each ground motion, indicating fracture at the beam-end

connector.

4. The down-aisle direction moment bearing capacity and rotational stiffness of the base isolator is very small, which causes the beam-end connector to carry an extensive amount of moment and to fail easily.
5. The friction slipper baseplate has the uprights and strong inner stubs well tightened, which gives strong moment bearing capacity to the base connection, which shares a heavy burden of the beam-end connectors;
6. The friction slipper baseplate rack shows the best seismic performance in the down-aisle direction shaking table test, compared with the other two base connections it has the least damage to the beam-end connectors and the largest seismic resilience.

6.4 Racking frame: 20 degree shaking

The rack frame with different base configurations was then tested on the shaking table in both the cross-aisle direction and the down-aisle direction; these are the principal directions to be considered for the seismic design of pallet racking systems. In conventional design practice, engineers consider these two directions independently and design the rack in the cross-aisle direction as a braced frame and the down-aisle direction as a moment frame. The interaction between these two directions is not considered. However, in reality, an earthquake shakes in both directions, and a rack frame response in one direction does have interaction with the other direction. The most common interaction is the influence of the rapidly changing upright axial load, caused by the cross-aisle direction action, on the down-aisle direction moment-rotation behaviour.

When a rack frame is undergoing an earthquake excitation, the cross-aisle direction component of the seismic force may lift uprights in one side creating a tension load, while at the same time increasing the compression load in the uprights of the other side. The down-aisle direction moment-rotation stiffness of a base connection very much depends on the axial compression load applied to the base connector; therefore, under a rapidly changing upright axial load, the connector moment-rotation stiffness is also changing rapidly, especially for the ductile baseplate. As described in Chapter 4 of this thesis, the moment bearing capacity of the ductile baseplate is determined by the upright axial load, losing almost all its rotational stiffness when there is low axial compression. The test results show that the ductile baseplate can only take a moment of roughly 500 Nm when there is almost no axial compression load and roughly 3000 Nm when there is 60 kN of axial load. The rapidly decreased moment carried by one side of the upright would have to be carried by the beam-end connectors which would increase the burden on them. This rapid increment of the moment could be significant for the survival of the rack frame. Not to mention the harm of the frame twisting caused by uneven rotation on both sides of the uprights.

For the friction slipper baseplate, its moment bearing capacity is 2800 Nm in the no axial load case and 5500 Nm in 60 kN axial load case, which is roughly 560% and 180% higher respectively, than that of the ductile yielding baseplate. Such a large moment bearing capacity allows the rack frame to carry a large amount of moment event when one side of the upright frame is lifting in the air.

In order to identify the influence of the interaction between these two excitation directions for the rack frame with the friction slipper baseplate and the ductile yielding baseplate, the rack frames were shaken at a 70 degree angle to the excitation direction of the shaking table, as shown in Figure 6.28. The primarily shaking direction is in the cross-aisle direction. Due to this orientation, the cross-aisle direction carries 94% (sin(70 °)) of the shaking and the down-aisle direction carries 34% (cos(70 °)).

The objectives of this test were to:

- Determine the behaviour of each rack frame under synchronous excitation in both directions
- Determine the baseplate-upright rotation angle of both frames when the upright can lift up during the excitation
- Determine the effect of twisting of the rack frame

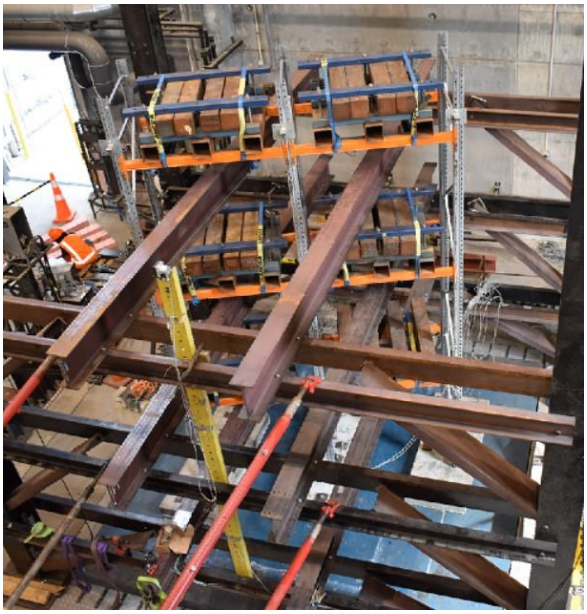

Figure 6.28: A photo of test setup in a 20-degree angle to the cross-aisle direction

6.4.1 Observations

Both rack frames survived all 12 ground motions up to 2.3 x design level earthquake. Significant frame twisting was observed during the shaking of the rack frame with the ductile yielding baseplates. The rack frames with the friction slipper baseplate showed no noticeable twisting.

No visible damage was found in the rack with friction slipper baseplates. The rack frame with the ductile baseplate shows severe damage at the baseplates and minor damage was found in the beam-end connectors (Stage 1 damage as shown in Figure 6.25). The damage of the ductile yielding baseplates is shown in Figure 6.29, from left to right, the three photos were taken before (a), during (b), and after (c) the ground motion excitations. It is evident that the upright has experienced significant twisting (b), which can be seen from the twisted upright corner and the thick mark left on the floor plate (c). Also, the baseplate was fractured at the weld, and the crack runs through the whole thickness of the floor plate (c). Noticeable residual deformation is observed. In addition, those baseplates at the side frames were damaged more severely than the those at the middle frame, this damage is also caused by the twisting effect.

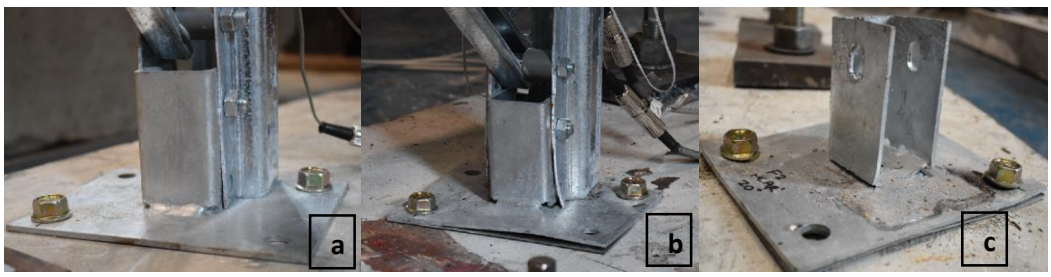

Figure 6.29: Ductile yielding baseplate before, during & after the test

The displacement time history of the rack frame with the friction slipper baseplates, in both cross-aisle and down-aisle directions, against the input ground motion are plotted in Figure 6.30. The monitored point is at the top-level middle frame. Because the excitation direction is at about 20 degrees to the cross-aisle direction, the peak down-aisle direction displacement is roughly 1/3 of the

cross-aisle direction displacement. As can be seen in the figure, while the rack frame is still uplifting at one side in the cross-aisle direction, the down-aisle has gone through a full cycle of vibration: 8s – 12s.

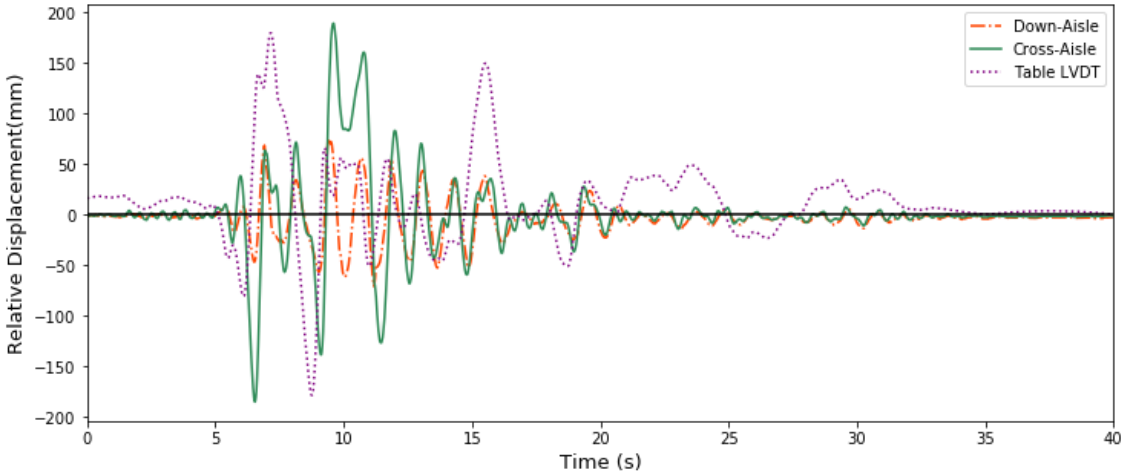

Figure 6.30: Displacement time history of the frame in both directions with the input ground motion. Friction slipper baseplate, Kobe earthquake SF = 2.258, 2.3x design level

At each side of the rack frame, namely the far side and the near side, the rotation angles of these beam-end connectors at the bottom beam level were monitored by portal gauges. Figure 6.31 and Figure 6.32 plot the averaged rotation angles recorded at both sides of the rack frame during Kobe Earthquake motion, scale factor of 2.258, which is 2.3x design level. The averaged rotation angle at each side shows the amount of rotation and deformation. As can be seen in Figure 6.31, for the rack frame with the friction slipper baseplate, the rotation angles at both sides are very close to each other, which means the rack frame undergoes almost no twisting. However, the rack frame with the ductile yielding baseplate shows very different rotation angles at each side of the rack frame, which is consistent with observations of significant twisting of the racking system during the shaking motion excitations. A small residual rotation is observed for both frames, again, the rack with the ductile baseplates shows more substantial residual rotation and a noticeable uneven rotation angle at both sides. The significant difference between the twisting response of these two structures is the result of the different baseplate connection geometry. The strong inner stub of the friction baseplate effectively limits the twisting of the upright.

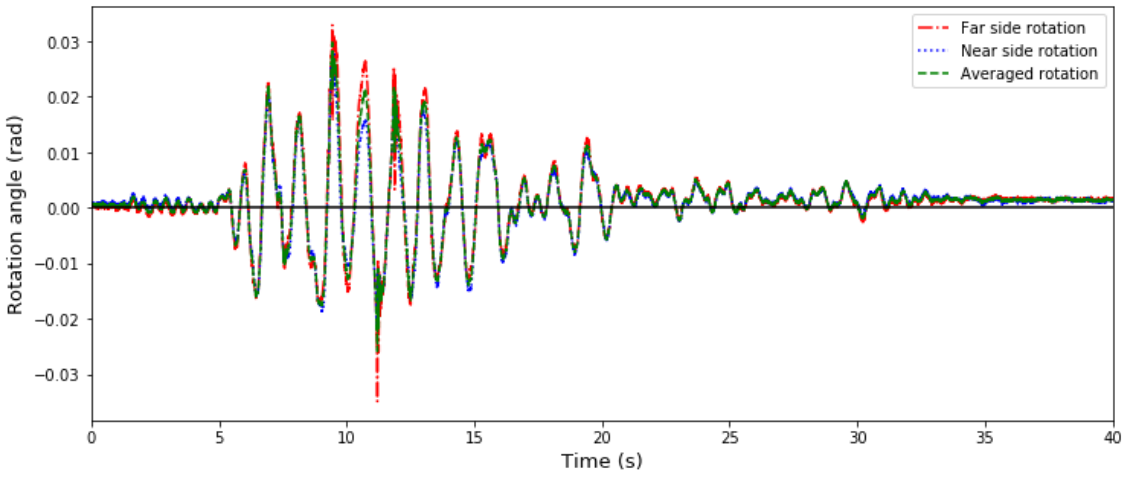

Figure 6.31: Rotation angle of both sides of the rack frame, Friction Slipper Baseplate, Kobe Earthquake SF = 2.258, 2.3x design level

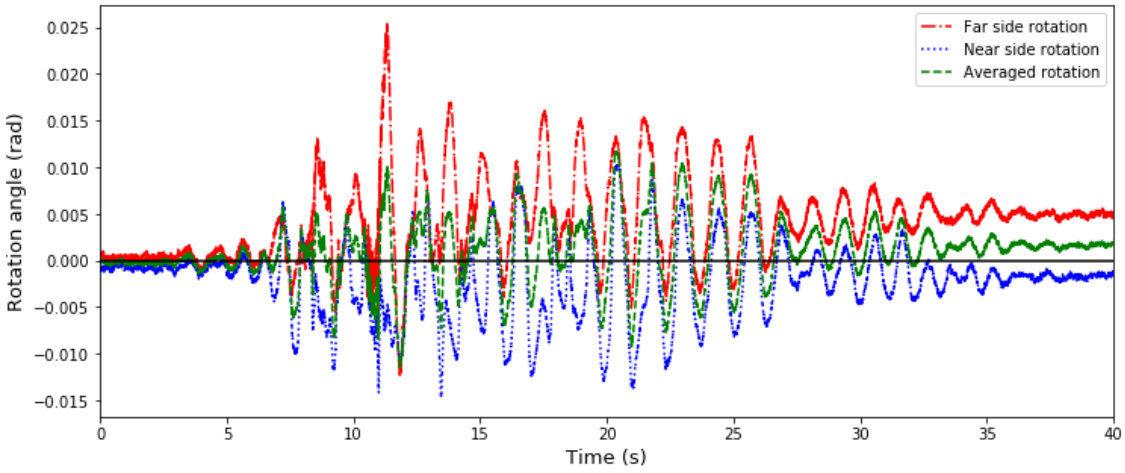

Figure 6.32: Rotation angle of both side of the rack frame, Ductile Yielding Baseplate, Kobe Earthquake SF = 2.258, 2.3x design level

6.4.2 Discussion

The peak displacement recorded during each ground motion in the cross-aisle direction for the rack with friction slipper baseplate and the ductile yielding baseplate is shown in Figure 6.33; the peak displacement recorded in the down-aisle direction is shown in Figure 6.34. Since the excitation direction is about 20 degrees to the cross-aisle direction, the peak down-aisle displacement is approximately 1/3 ($\tan 20^{o} \approx 0.36$) of the cross-aisle displacement for both racks at most of the ground motions over 1.0 x design level, the average value is 0.379. It is interesting to observe that in all the Northridge Earthquake ground motions, the rack frame with the friction slipper baseplates has larger displacement response than the rack with the ductile yielding baseplates except at the 1.0 x design level; and has a smaller displacement response in all the Kobe Earthquake ground motions, especially at the last two high-intensity ground motions. This may be because the dominant periods of those two earthquakes have a noticeable influence on the response of each rack frame, which has a corresponding resonant period. This is especially the case for the Northridge Earthquake, which has a high energy component of shaking over a period range of 0.4-0.7s, which would generate rocking resonance of the frame with the friction slipper baseplates. Another possible effect is that the twisting of the rack frame may dissipate a significant amount of seismic energy due to the friction between the pallets and the beams. Since the twisting at the rack with ductile baseplates is much more significant than the rack with the friction slipper baseplates, this energy dissipation path is much more pronounced for the ductile baseplates, which may noticeably reduce the response of the rack.

The rack deformation response shows the twisting of the rack frame with the ductile yielding baseplate is significant; this would activate additional energy dissipation paths, i.e., the friction force between the pallets and the beams, and the yielding and steel fracture of the baseplates and uprights. Since a significant amount of seismic energy was dissipated, the rack frame with the ductile baseplate shows less deformation response. The rack frame with the friction slipper baseplate shows no twisting. Therefore, the deformation at both sides is simultaneous, which causes more pronounced deformation.

The twisting of the rack frame with the ductile baseplate also consumed a large amount of seismic energy from the cross-aisle and down-aisle directions, which also reduces the response at these two directions.

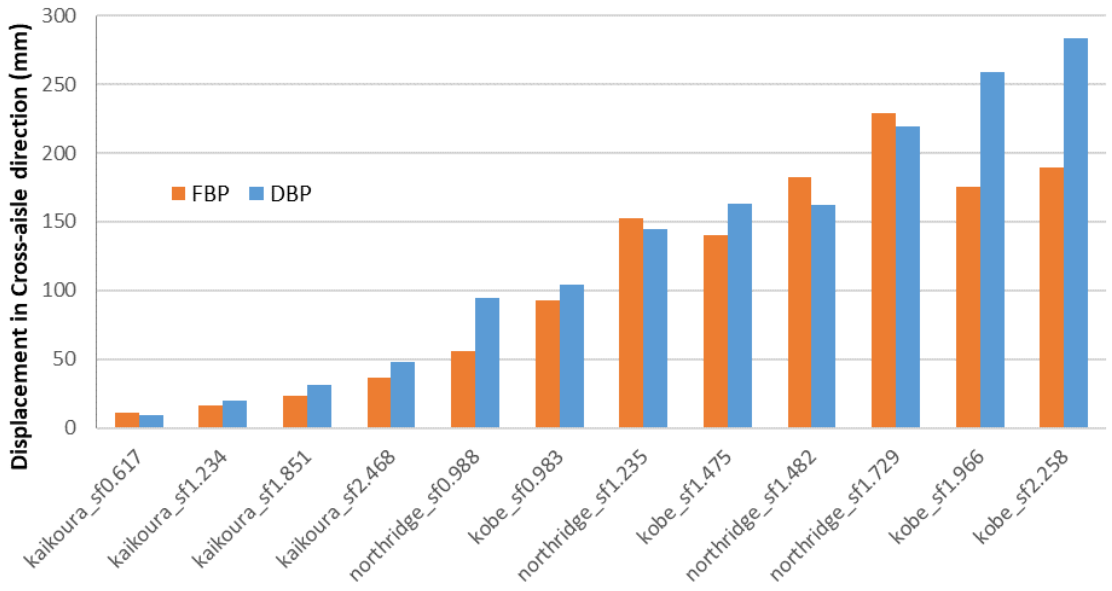

Figure 6.33: Peak displacement of each ground motion in the cross-aisle direction. FBP: friction slipper baseplate, DBP: ductile yielding baseplate

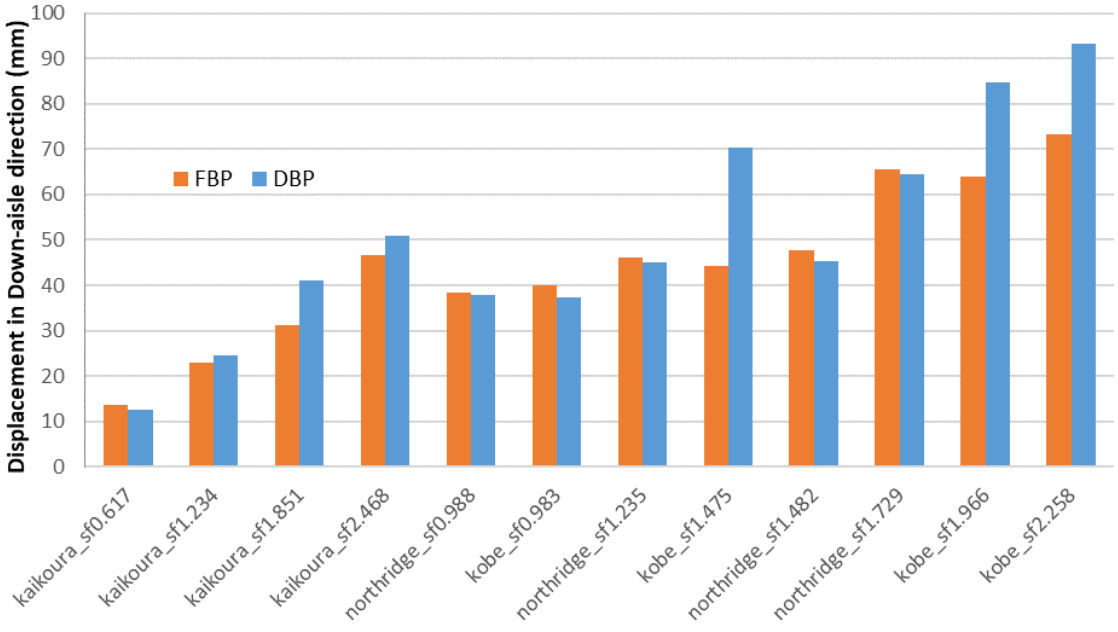

Figure 6.34: Peak displacement of each ground motion in the down-aisle direction. FBP: friction slipper baseplate, DBP: ductile yielding baseplate

6.4.3 Summary - Bi-axial excitation

To identify the influence of bi-axial excitation, two rack frames: the first with friction slipper baseplates and the second with ductile yielding baseplates; were tested on the shaking table at a 70 degree angle to the excitation direction. Both racks survived all 12 ground motions. Based on the

experimental observations, the following conclusions can be drawn for the bi-axial excitation of the rack frame with the tested base connections:

1. Significant twisting was observed for the rack with the ductile yielding baseplates during the bi-axial excitation, while the rack with the friction baseplates showed no noticeable twisting.
2. The ratio of the displacement recorded at each direction is close to $\tan 20^{o}$, which is the angle to the direction of the excitation.
3. Severe damage was observed in the ductile yielding baseplates, and no damage was found in the friction slipper baseplates.
4. The Northridge Earthquake ground motions have relatively more influence on the displacement response of the rack with the friction slipper baseplate; in the bi-aisle excitations, the Kobe Earthquake ground motions have a relatively significant influence on the rack with the ductile yielding baseplates.

6.5 Conclusions

A series of shaking table tests have been conducted to determine the seismic performance of the rack frames with different base-connections in 3 different directions, as follows:

In the cross-aisle direction, the friction slipper baseplate, the ductile yielding baseplate, the unanchored baseplate and the rigid baseplate;

In the down-aisle direction, the friction slipper baseplate, the ductile yielding baseplate, and the base-isolator;

In the 20 degrees to the perpendicular to the excitation direction, the friction slipper baseplate and the ductile yielding baseplate.

The experimental observations show that the friction slipper baseplate exhibits the best seismic performance in both the cross-aisle and the down-aisle directions compared with all the other base-connections tested. It protects the rack frame and concrete floor from damage, reduces the risk of overturning in the cross-aisle direction, and minimises the damage at beam-end connectors in the down-aisle direction, without sustaining damage to the connection itself. Moreover, this high level of seismic performance can be delivered by a simple and cost-effective baseplate with almost no additional cost. The significantly reduced internal force and frame acceleration response enable a more cost-effective and safer design of pallet racking system.

Chapter 7 Design Parameters for Selective Pallet Racking Frames with Friction Slipper Baseplates

7.1 Introduction

The studies documented in chapters 3 to 6 have shown that selective pallet rack frames with friction slipper baseplates can behave in a dependably ductile manner, with a significant energy dissipation capacity. The objective of this section is to use the experimental results to develop the design parameters for the design of a rack frame with friction slipper baseplates, in both the cross-aisle direction and the down-aisle direction. This can be used as a reference by engineers to maximise the benefit of the friction slipper baseplate in design practice.

7.1.1 Scope

This section provides recommendations for the seismic design of selective storage racking systems using the Friction Slipper (FS) baseplate according to the Earthquake Loadings Standard *NZ 1170.5*[74] and the design guideline from BRANZ [65].

The recommendations do not apply to mobile storage systems, drive-in, drive-through, shuttle and cantilever racks or to static steel shelving systems. However, the FS baseplate has potential to deliver the same level of benefit for types of racking systems that it has been shown to deliver for selective racking systems.

These recommendations come from a comprehensive experimental testing programme into the component performance of the FS baseplate and the system performance of pallet racking systems up to 6-levels (i.e. 6 levels of suspended pallet load; 10-m-high). Therefore, the information provided here is for racking systems below 10-meter-high, although this is approximate, not a fixed limit. The dynamic performance of pallet racking systems does change with an increase in the number of loading levels and overall height; becoming less first mode dominated as these increase. This can cause behavioral changes, which influence the demand on the system and members, especially in the cross-aisle direction where higher mode effects can lead to a significant increase in the demand on braces and connections. A friction splice system is being developed to address this for taller racking systems, but that is outside the scope of this study.

Some of the recommended design parameters given herein are dependent on the number of load levels and height as noted in the relevant section.

The applicable standards may be sub-divided into loading standards and resistance (material) standards.

In consideration of loading on racking systems, the primary reference standards for New Zealand are:

- AS/NZS 1170.0 Structural design actions – general principles
- AS/NZS 1170.1 Structural design actions – permanent, imposed and other actions
- AS/NZS 1170.5 Structural design actions – earthquake actions.
- The relevant material standards are:

- AS/NZS 4600:2018 Cold-formed steel structures
- NZS 3404:2009 Steel structures standard
- AS 4084:2012 Steel storage racking.

Generally, the cold-formed steel structures standard, AS/NZS 4600, will apply for the rack member design because the metal thickness on most members is less than 3 mm.

In this study, the main focus is on the seismic design. The earthquake action standard NZS 1170.5 is applied.

7.1.2 Standards and design guidelines

Although storage pallet racking system may not be considered as a general building, the design consideration is in accordance with NZ 1170.5 Structural Design Actions: Earthquake actions.

The BRANZ manual for seismic design of high-level storage racking systems with public access is the only current New Zealand design guide that includes design examples, seismic calculations, and details of verification testing. This design guide was initially published in 2006 [75][61]. As a result of the large number of pallet racking collapses experienced during the earthquakes in September 2010 and February 2011, BRANZ re-evaluated the design criteria to increase the resilience of pallet racking systems against collapse in earthquakes. A draft version of the revised BRANZ racking design guide (2012) is available but has not been published yet. However, the performance concepts required and framework for design are adequately presented in this draft version.

The Christchurch earthquake series demonstrated the importance of having resilience against collapse in earthquakes that are more intense than those considered in the previous racking system design. The performance requirement applied is that the racking system behaviour should remain essentially the same, with significant damage or collapse not occurring for an earthquake intensity of at least 1.5X the ultimate limit state (ULS) design intensity. This is typically applied through NZS 1170.5 with a requirement for the structural system to withstand 1.5X the deformation expected from the ULS design level event without a significant change in behaviour or loss of deformation capacity.

7.2 Elastic site hazard spectra

See Section 4 of the BRANZ 2012 guide [65] for more details.

To determine the seismic loading to a rack frame in a particular condition, we must generate the site hazard spectra. Determine the elastic site hazard spectrum, $C(T_1)$, using the following equation from NZS 1170.5:

$$C(T_1) = C_h(T_1).Z.R.N.(T_1, D) \qquad \textbf{Equation 7.1}$$

The spectral shape factor, $C_h(T_1)$, is determined for the site subsoil class and rack first mode natural period, T_1. (Details are given in Section 4.1 of the BRANZ guide).

For the ultimate limit state, the horizontal design response spectra is:

$$C_d(T) = \frac{C(T)S_p}{k_\mu}$$

Equation 7.2

The structure performance factor S_p should be determined in accordance with NZS1170.5 Clause 4.4; for the friction sliding system the value will be 0.7 as the structural ductility factor for both cross-aisle and down-aisle directions of loading is greater than 2. Note that for Time History Analysis (not used in routine racking design) the scaling factor on the earthquake records does not use S_p directly but uses $(1 + S_p)/2$ in accordance with Clause 5.5.2.

BRANZ 2006 allows a minimum value of S_p of 0.7, but the BRANZ 2012 draft version defines it to be 1.0. For further explanation, please consult Section 4.4 of BRANZ 2012 draft guide and Clause 3.3.3 of the 2006 version. The argument for using a value of 1.0 was that racks are skeletal structures without factors such as high redundancy, mass and size, soil structure interaction effects, and non structural elements which are in typical buildings and which contribute to these building systems having a higher strength and stiffness than the models: the principal reason behind the S_p factor. This is correct, and it means that the S_p factor for racks is expected to be less than that for buildings. However, the impact on the buildings in Christchurch of the 2010/2011 Canterbury earthquake series has enabled the actual S_p to be determined for a number of steel framed buildings that performed in accordance with expectations and for which the effective S_p could be obtained. This is between 0.3 and 0.5, rather than the 0.7 minimum value currently used. On that basis, use of S_p = 0.7 for pallet racks with design and detailing to develop $\mu \geq 2$ is justified. That value has also been used in the design of the racks for the experimental testing (snap-back and shaking table) undertaken in this research programme and from which these design procedures have been developed. Therefore S_p = 0.7 should be used for selective pallet racking systems with FS baseplates for both directions of loading. This is also consistent with European recommendations, which use a system overstrength of 1.5 ($\approx 1/0.7 = 1.43$) and with USA recommendations.

The hazard factor, *Z*, shall be taken from Table 3.3 in Clause 3.1.4 of AS/NZS 1170.5, and varies from 0.13 to 0.6 depending on the location of the rack.

The importance level is typically 2. It can be

The return period factor, R_u, depends on both the limit state condition being considered and the design life of the racking system. The normal design working life for a building is 50 years. However, the normal working life of a pallet rack is under 25 years and this value is used in design. This is consistent with racking practice in which a pallet racking system will typically be installed into a building for a much shorter period of time than the design life of the building itself. (It is important to ecognize the regulatory requirements associated with the choice of design life. A choice of a 25-year design life means that once the 25 years have elapsed, the Territorial Authority can require that the rack is altered to continue to comply with the applicable provisions of the Building Code to at least the same extent as before the alteration.)

The importance level is typically **2**.

BRANZ draft design guide 2012 requires that a 50-year design working life MUST be used in public access situations. The derived return period factors are presented in the following table.

Table 7.1: Design life consideration of racking systems

Design working life (years)	Importance level	Annual probability of exceedance for ULS	R_u (ULS)	Annual probability of exceedance for SLS	R_s (SLS)
50	2	1/500	1.00	1/25	0.25
25	2	1/250	0.75	1/25	0.25

For detailed information, please check Table 3.3 of AS/NZS 1170.0 and Table 3.5 of AS/NZS 1170.5.

The near-fault factor, *N(T1,D)* is explained in Clause 3.1.6 of AS/NZS 1170.5. BRANZ 2012 has a more detailed explanation and requirement regarding this factor; it requires that storage racking system design for regions susceptible to near-fault effects and of high importance need to include inelastic time history analysis to determine the ductility demand, (Section 4.1 of BRANZ 2012 draft design guide).

7.3 Particular design parameter considerations in cross-aisle direction

The design is using the Equivalent Static Method (ESM) in accordance with NZS 1170.5 [74], with the following values of key parameters used:

7.3.1 Rack first mode natural period T_1:

For the cross-aisle direction period, in BRANZ design guide 2006, the period calculation is allowed to be simplified and taken as equal to or less than the ratio of the short period spectral shape factor divided by spectral shape factor at a period of 1.0 s. The effective seismic weight, W_t (determined in Section 3.2) is used in the period calculation. However, the draft version 2012 points out that using the full seismic weight in the period calculation overestimates the period. A value of 80% of the total seismic weight should be used. Alternatively, a pushover test on a full-scale model of the cross-aisle frame is recommended. (See Clause 3.3.1.1of BRANZ 2006; Clause 4.2.1 of BRANZ 2012 draft design guide and Clause 3.1.3 of AS/NZS 1170.5).

$C_h(T)$ is based on the period from the analysis including P-Δ effect and with the column bases pinned. That is more realistic than fixed although for the cross-aisle braced frame it does not make much difference. Note that this is conservative because it does not allow for rocking behaviour, which will increase T_1 and therefore reduce the magnitude of the design seismic load, typically.

7.3.2 Structural ductility factor μ

As elaborated in the Chapter 5, based on the test results, a ductility factor of 5 would be proper for

design purpose for racks up to 5 levels and a height limit of 8 meters. For higher racks, higher mode effects can become significant, and further development of the friction racking system is underway to address that.

7.3.3 Uplift force / Friction sliding force & Overstrength factor

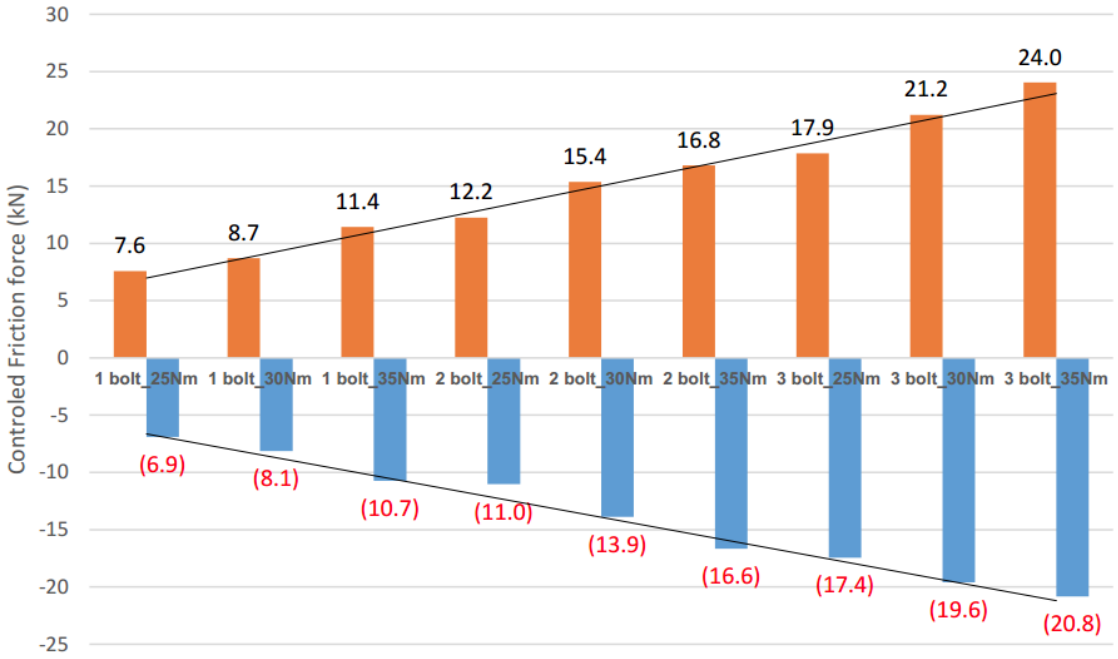

Figure 7.1: Bolt configuration VS Friction clamping force

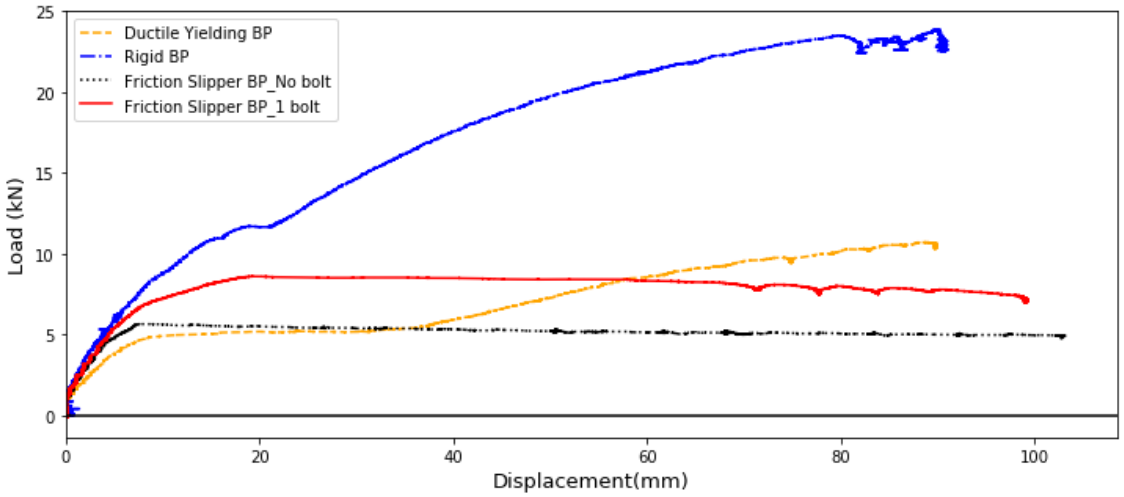

Figure 7.2: Pull-over load-displacement curves for rack frames with 4 baseplate assemblies

Once the analysis is undertaken, this will determine the design tension force in the uplifting column which will determine the amount of friction sliding force required to be developed. There will be a balancing act between the tension force and the uplift capacity of the anchor bolts can achieve.

The uplift force should be determined as the following procedures:

1. Start with the minimum uplift force F_{upmin}, which is in the bolt configuration of 1 bolt with an associated torque of 25 Nm. As shown in Figure 7.1 (details available in Chapter 3).

2. Take the ductility factor μ_{des}= 5 and undertake the cross-aisle design.

3. If there is no design tension uplift, decrease the ductility factor μ and repeat the design by reducing the value of μ until the uplift tension force = F_{upmin}. This should take only 1 iteration. It gives the value of μ_{des} to use for the rest of the design. It is important to note that second-order effects should be considered for this but probably won't require an increase in the design actions due to the cross-aisle direction being relatively stiff.

4. Obtain the elastic displacement with the ductility factor μ_{des} generated from Step 3 at the top of the rack to give the design inelastic displacement and check this is within the 5% drift limit.

5. Use the inelastic displacement from Step 4 to determine the design uplift displacement for the Friction Slipper baseplate and put the uplifting factor of 1.5 on that for the design of the baseplate, especially the stub height.

6. Design the bracing system members for the actions from Step 3. Take an overstrength factor of 1.1 for the cross-aisle direction upright-baseplate connection uplift force and floor anchor bolt pull-out force design.

7. Check the upright force can meet the 1.5x1.1Q case, and if that governs the size, then the designers should go for a higher friction force F_{up}. Also, the friction force can't be larger than 1.5 times of the gravity load which may prevent self-centering of the rack frame.

A more substantial overstrength factor is usually adopted for seismic resisting steel system design to generate the designed mechanism. For example, with an Eccentrically Braced Frame (EBF) system, the desired mechanism is a strong brace frame weak active link mechanism, and this requires an overstrength factor of at least 1.5 to be applied to the active link nominal shear capacity for the sizing of the rest of the frame members. However, for the friction sliding baseplate system, the experimental tests show that, once the friction uplift starts, the demand does not increase and that any increased resistance to sliding at high drift levels is compensated for by a drop in capacity due to P-Δ effects, so that the slope of the base shear force / top lateral deflection relationship is zero or slightly negative, as shown in Figure 7.2 (Available from Chapter 5). This means that the peak load on which to design the members of the system (especially the braces and their connections) from the Step 6 above (which references back to Step 3) will be the load at which sliding commences, and that is the reason why the capacity design overstrength factor can be reliably taken as 1.0. The protection afforded by the strength reducing factor on the member capacity determination side of the equation is sufficient to cover any small increase in system effects. This zero increase in required strength for the capacity design process is another very big advantage of the Friction Sliding system over any other system. A factor of 1.1 is adopted here in Step 6 to count the effect of small variation of the friction force.

Note that this applies for racking systems up the height limits specified; for taller systems, higher mode effects may increase the forces on the braced system to the point where localised failure could occur. This is being addressed by the development of a friction column splice which is the next step in this programme of ongoing increased resilience for pallet racking systems.

7.4 Particular design parameter considerations in down-aisle direction

7.4.1 Rack first mode natural period T_1:

For the down-aisle direction period, the BRANZ design guide provides an alternative way of determining initial elastic connection rotational stiffness experimentally for the period calculation (see Clause 4.2.2 and Clause 9.1.1 of BRANZ 2012).

$C_h(T)$ based on the period from the analysis including *P-Δ* effect and with rotational springs with rotational stiffness k_m at the column base and also at the ends of the beams at their connections to the columns. It is essential to include the rotational spring value from experimental testing for the connection. This spring should be positioned at the outer face of the column with a rigid member from the column centreline to the column face.

7.4.2 Structural ductility factor μ

As elaborated in Chapter 4 and Chapter 6, in the down-aisle direction the use of friction slipper baseplate does not limit the ductility of the structure. The overall ductility is limited by the beam-end connector applied. A suggestion on determine the overall system ductility is to determine the beam-end connector ductility experimentally and divide it by 1.25 to get the system ductility for using the Equivalent Static Method of design. This is lower than the recommended factor of 1.5 from NZS 1170.5 [76], because the friction slipper baseplate was un-damaged in the testing and there is nothing to indicate the behaviour would have changed if it have been deformed further.

7.4.3 Rotational stiffness of semi-rigid rotational spring at upright-base connection

The rotational stiffness of the upright-base connection varies widely depending on the vertical axial load of each upright. Therefore, when numerical modelling is carried out, each semi-rigid spring should have a rotational stiffness based on its upright loading condition, as can be found in Table 4.2, of Chapter 4.

Chapter 8 Conclusions and Future Development

A novel component, the friction slipper baseplate, has been designed and developed to very significantly improve the seismic performance of a selective pallet racking system in both the cross-aisle and the down-aisle directions.

This thesis documents the whole progress of the development of the friction slipper baseplate from the design concept development to experimental verification. The test results on the component joint tests, full-scale pull-over and snap-back tests and full-scale shaking table tests of a steel storage racking system are presented.

This section presents the conclusions from this work and recommendations for ongoing development of the friction based system for enhanced pallet racking seismic performance.

8.1 Cross-aisle direction performance

The friction slipper baseplate allows the rack frame to uplift at the upright base during a severe earthquake event. The earthquake-induced rocking behaviour limits the seismic loading demands on the rack frame and increases the period of vibration of the frame so as to slow down the rate of seismic energy input into the critical components of a structure. At the same time, the friction damper embedded at the baseplate-upright connection dissipates a significant amount of seismic energy to limit the seismic response and force demands. The seismic mechanism doesn't require permanent damage to fulfill these functions nor generate residual deformations, thereby avoiding the need to repair or replace either the frame or the baseplate.

The quasi-static component uplift behaviour of the friction slipper baseplate has been investigated through the axial cyclic test of the baseplate-upright joint. The test results have shown that the friction slipper baseplate can generate a wide range of stable, controlled friction force by adjusting the bolt group configuration. It can dissipate a significant amount of energy while there is no residual deformation formed with only negligible scratch found. The influence of loading rates and loss of bolt tightness during sliding have both been found to be negligible.

The full-scale frame quasi-static pull-over and snap-back tests were then conducted to evaluate the ductile and dynamic free-vibration behaviour of the rack frame with the friction slipper baseplate. It was found that the rack frame can reach a lateral drift limit of over 7%, corresponding to a dependable design drift limit of 5% in the cross-aisle direction with stable, bi-linear behaviour and no damage to the baseplate or the racking system. The damping ratio is introduced to quantify the energy dissipation capacity of the friction slipper baseplate. Comparing to 3-6% of damping ratio for other types of the system tested, a rack frame with friction slipper baseplates can reach a damping ratio of 20%. Moreover, the unique friction sliding connection limits the development of tension uplift force to a predictable and stable level, meaning that the anchor bolts on both the tension and the compression side of the uprights are protected from overload damage.

Finally, a comprehensive set of full-scale shaking table tests have been conducted to compare the seismic performance of the rack frames with various types of baseplate configurations. The test results

show that the rack frame with the friction slipper baseplate survived all the 12 ground motions up to 2.3x design level earthquake without any noticeable damage. Comparing to the performance of other types of baseplate configurations, it does not overturn like the unanchored baseplate; it does not pull the anchor bolt out of concrete slab like the rigid baseplate; it does not fracture the baseplate like the ductile yielding baseplate. The axial load monitored at upright bases remains stable during rocking, unlike that in the ductile baseplate or rigid baseplate systems. The peak acceleration at the loaded levels of the rack is also reduced by the friction slipper baseplate. Although the drift was slightly higher than the ductile baseplate on some occasions, it can be controlled by a larger friction force applied to the baseplate-upright connection. Additionally, the selectable friction force setting allows engineers to design the rack frame to differing needs, for example limiting the tensile uplift force for a frame installed onto a low strength concrete slab.

Overall, the friction slipper baseplate has demonstrated the best cross-aisle direction seismic performance compared with the other three types of base connections, as shown by the controlled axial load, displacement, and relatively small acceleration response, along with the largest seismic resilience, and no damage from the tests.

8.2 Down-aisle direction performance

In the down-aisle direction, the robust but flexible design of the friction slipper baseplate enables a strong and stiff floor-upright connection up to column base rotational angles corresponding to over 7% lateral drift, without forming plastic deformation in the columns or failure in the baseplate. This floor-upright connection can share a large portion of moment demand of the moment frame and reduces the rotational demand on the beam-upright connector at the first suspended level, thereby reducing the damage to the rack frame during a severe earthquake. Besides this, the friction slipper baseplate allows the rack frame to perform in a very ductile behaviour, which also reduces the seismic demand of a rack frame.

The floor-upright moment-rotation tests were conducted to determine the moment-rotation behaviour of the friction slipper baseplate. The test results clearly show that the friction slipper baseplate produces a much larger moment resistance and rotational stiffness over the ductile yielding baseplate. It can remain a considerable large amount of moment resistance while the ductile baseplate loses most of its moment resistance in a large rotation. Moreover, such a favourable behaviour is achieved without any permanent deformation while the ductile baseplate forms considerable plastic deformation.

A series of full-scale shaking table tests were conducted to compare the down-aisle direction seismic behaviour of the rack frames with the friction slipper baseplate, the ductile yielding baseplate and the base-isolator. The test results show that the rack frame with the friction slipper baseplate demonstrated a very stable response and survived all the 12 ground motions with lesser damage compared to the other systems tested which also failed at lower levels of seismic excitation. The observed damage was concentrated at beam-upright connection in the down-aisle direction excitations. No damage were observed at the friction slipper baseplate and the base-isolator, while a small residual deformation was observed at some ductile yielding baseplates.

Overall, the friction slipper baseplate shows the best seismic performance in the down-aisle direction shake table test compared with the other two base connections, in that it underwent the least damage while withstanding the highest intensity of shaking of the three systems tested.

8.3 Bi-direction excitation response

The current engineering design practice considers the rack frame in its cross-aisle direction and down-aisle direction separately, however, the rack frame is very likely to be shaken in both direction in a real earthquake event. During a bi-direction excitation, the rapid changing of axial load at both sides of the upright frames can result in a rapid reduction of rotational stiffness and moment resistance at the baseplate connection. The robust design of the friction slipper baseplate enables it to remain a reasonably large resistance when the column is subject to zero compression load or tensile uplift from the rocking response in the cross-aisle direction.

A series of shaking table tests were conducted to identify the influence of the interaction between the two excitation directions of rack frames with the friction slipper baseplate and the ductile yielding baseplate. Both tested frame survived all the 12 ground motions. However, the rack frame with the friction slipper baseplates survived with no noticeable damage, while the rack frame with the ductile yielding baseplates survived with severe damage at the baseplates and the base of uprights. Significant twisting was observed for the rack with the ductile yielding baseplates during the bi-axial excitation, while the rack with the friction baseplates showed no noticeable twisting. It was also noticed that different response was activated by different ground motions for the two rack frames tested.

8.4 Summary of findings

The extensive experimental observations show that the friction slipper baseplate exhibits the best seismic performance in both the cross-aisle and the down-aisle directions compared with all the other base-connections tested. It protects the rack frame and concrete floor from damage, reduces the risk of overturning in the cross-aisle direction, and minimises the damage at beam-end connectors in the down-aisle direction, without sustaining damage to the connection itself. Moreover, this high level of seismic performance can be delivered by a simple and cost-effective baseplate with almost no additional cost. The significantly reduced internal force and frame acceleration response enable the more cost-effective and safer design of the pallet racking system with minmal extra cost for the baseplate.

8.5 Future developments

The development of the friction slipper baseplate enables cost-effective design of a selective pallet racking system with high seismic resilience and greater resistance to operational damage. However, the friction slipper baseplate in itself is not a complete solution for all selective pallet racking systems. This section presents the concepts for future developments to extend the friction based solutions to a wider range of selective pallet racking systems.

8.5.1 Friction splice

The benefits of the friction slipper baseplate mostly come with the rocking behaviour of a rack frame. However, for racks taller than 10 meters, the rack may not rock, and the uplift at the upright base will not occur. Because of higher mode effects, the critical point at a tall rack frame may be at somewhere above the base with extensive shear and bending moment demand.

Wiebe and Christopoulos 2014 [77] numerically investigated the influence of higher mode effects to a controlled rocking heavy steel braced frame and found that higher mode effects could dominate the seismic response of a tall steel frame. However, they showed that allowing the frame to rock at multiple joints can effectively reduce the peak frame forces, as well as the overturning moment. The rocking steel frame designed with multiple mechanisms could save 26% steel compared to the steel frame designed with rocking at the base only. Conceptually this is turning a rigid rocking cross based spine into an articulated rocking cross braced spine.

Inspired by this study, the design concept of a friction splice is proposed. Rack splices are widely used to join two pieces of relatively short uprights together to form a longer upright. Conventional rack splice is considered to join two uprights rigidly and doesn't allow relative movement between the joined uprights. The two joined uprights are considered to be one long continuous upright in engineering design. For most of the tall racks those higher more them 10 meters, the uprights are commonly joined by rack splices. Since the rack frames are so tall, higher mode effects would dominate the seismic response of the rack frames. If a splice could allow the joined uprights to move relative to each other with a friction damper to dissipate seismic energy taking advantage of this relative movement, the seismic response and force demand of the rack frame would be significantly reduced.

The concept drawing of the friction splice is shown in Figure 8.1. The bolt group (blue) with different torque combination can generate a wide range of friction force for engineers to design the friction damper behaviour according to their needs. The interlocking bolt set (green) can lock the joined uprights in a selected range of uplift so as to control the inter-storey and overall drift of the rack frame. In this case, the bolt set in the bottom column is connected into the column wall through nominally sized holes while the bolt set into the top column are connected by slotted holes. However, it is possible that the bolt set into the top column could be eliminated

The robust inner stub provides extensive shear resistance for the uplifting column. Preliminary research has been conducted to determine its shear bearing capacity and found it is robust and reliable [78]. There are two variations of the friction splice, with and without a middle plate. The existing of the middle plate would not only increase the stability of the joint between two uprights but also allows different upright sections to be used in each side of the plate. The top half portion of the upright frame takes much smaller loads than the bottom half, but most of the time they are joined by the same upright sections. The friction splice with a middle plate would enable the use of different upright sections to be used to minimize the cost of the rack beside the benefit of significant reduction on force demand of the rack frame.

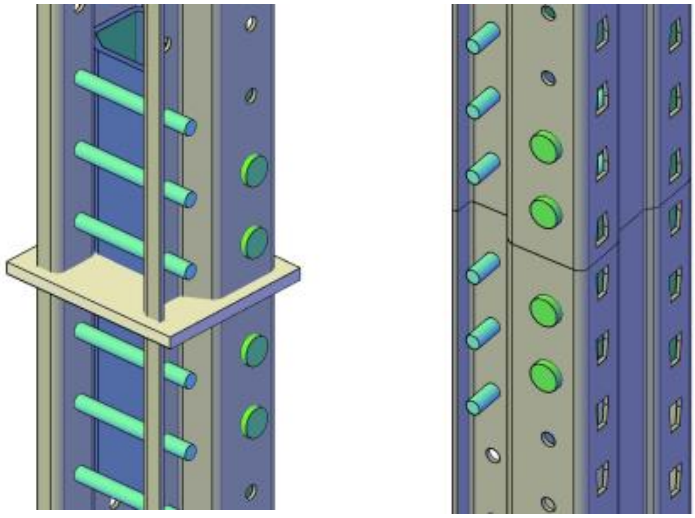

(a) With a middle plate **(b) Without a middle plate**

Figure 8.1: Concept drawing of the friction splice, with and without a middle plate

8.5.2 Friction spacer

Selective racks are mostly with back-to-back frames joined by spaces to create a flue space between the rack rows and help keep rack rows straight and uniform. However, conventional spacers are not considered as structure members; engineers design the rack frame row by row independently. Depending on the manufactures, various spacers are used on the market with different fixity and capacity, as shown in Figure 8.2. To the best knowledge of the author, there is no spacer designed for dissipating seismic energy.

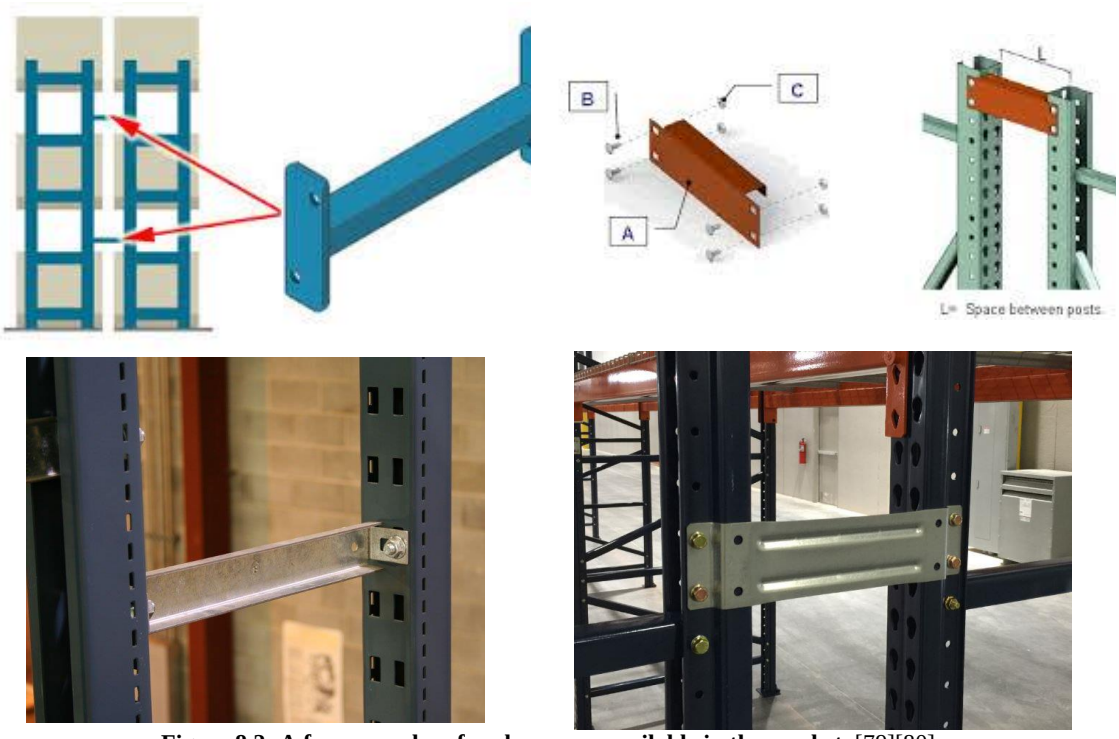

Figure 8.2: A few examples of rack spacers available in the market [79][80]

Eatherton *et al.* 2008 [81] proposed a controlled rocking steel braced frame with self-centring post-tensioning strands and energy-dissipation fuses, as shown in Figure 8.4 and Figure 8.5. By employing

both PT strands and energy dissipating fuses, the system was found to be able to sustain large earthquake ground motions with minimal damage and without residual drift. The controlled rocking braced frame concept has been introduced to pallet racking systems; the energy-dissipating fuses concept can also be introduced to a rack frame as a spacer, which can be an energy-dissipating component. The steel yielding damper used in Eatherton *et al.*'s study would not be affordable for a commercial racking system. Additionally, the dissipating fuses may request replacement after a severe earthquake event, which would interfere with business continuity. A cost-effective and damage-free seismic spacer is demanded.

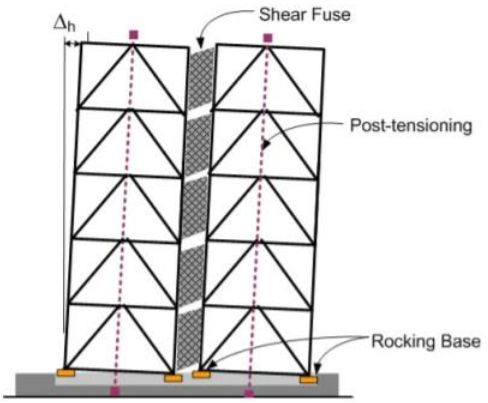

Figure 8.3: Controlled rocking frame with self-centring PT strands and energy-dissipating fuses [81]

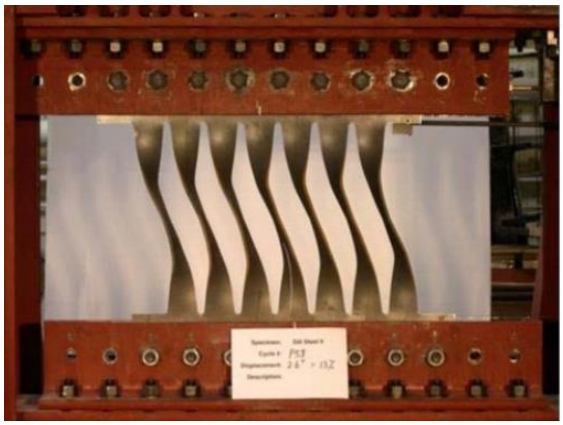

Figure 8.4: Steel energy-dissipating fuses

Figure 8.5 shows a proposed design concept of an energy-dissipating spacer with friction damper. The bolt group setting can control the friction force. It is designed to make the rack frames to behave fully rigid during everyday operation and allow relative movement between two upright frames during a severe earthquake. The relative displacement during an earthquake can dissipate seismic energy by the controlled friction force. With such a spacer, the seismic demand on drift and impact between frames and walls can be significantly limited.

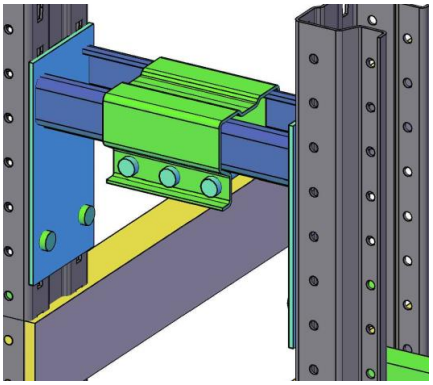

Figure 8.5: Proposed design concept of the friction spacer

8.5.3 Frictional rotating beam-column connection

In the down-aisle direction, the rack is considered as a moment-frame. The beam-upright connection is always a critical design issue to the seismic performance of a rack frame. Most of the current beam-upright connections are either tab-to-slot connections (Figure 8.6) or bolted connections (Figure 8.7). The tab-to-slot connection is relatively more ductile, flexible and dissipates energy by steel yielding

and fracturing. The bolted connections rigidly fix the beams to the uprights, which makes it stiffer, stronger and also more expensive and with less energy dissipation capacity and ductility.

G. C. Clifton 2005 [10] developed a friction sliding hinge joint to replace the conventional beam-column connection for steel moment resisting frames, and this has been widely used in New Zealand. As shown in Figure 8.8, instead of forming irrecoverable plastic deformation at the beam-column joints, it is designed to be rigid up to ultimate limit state and sliding under severe seismic events: dissipation of energy through the friction damper mechanism results in minimal damage. The tightness of the bolt groups connecting the bean and the column can be adjusted to achieve optimal seismic performance. This concept is a relatively easy and cost-effective way to achieve significant seismic resistance and can potentially be used in a racking system.

A proposed friction moment connection is shown in Figure 8.9. A trapezoid-shape steel plate with a few slots can be connected to the upright with a bolt group. The pre-open slots allow the beam to rotate about the connection. At the end of the beam, a thin layer of high hardness rubber (shown in red in Figure 8.9) is attached to provide a buffering and distribute the stress evenly. The design concept requests the connection to behave rigidly to the ultimate limit state and rotate in a ductile manner during a severe earthquake. The energy dissipation can be from both the bolted friction damper and the deformation of rubber. Such a damage-free and cost-effective moment-frame connection can significantly improve the seismic performance of the racking system.

Figure 8.6 : A tab-to-slot connection

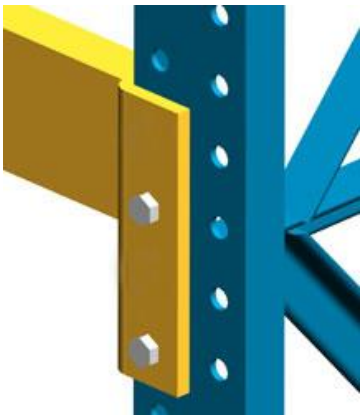

Figure 8.7 : A bolted moment connection

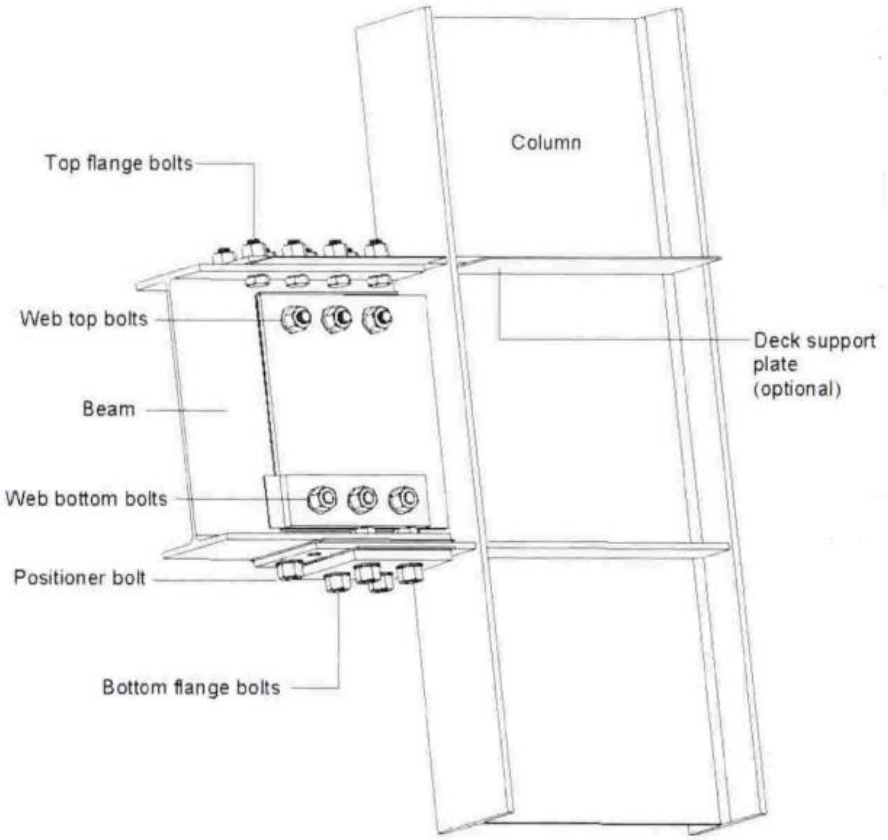

Figure 8.8: Friction sliding hinge joint for a moment frame beam-column connection (from [10])

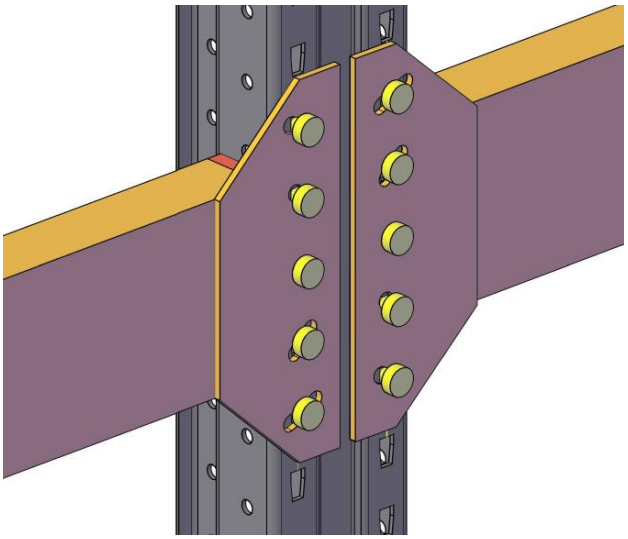

Figure 8.9. Proposed friction moment connection for rack frames.

8.6 The application of the design concept in general buildings

The design concept of combining rocking behaviour with a friction damper has been shown to significantly improve the seismic performance of selective pallet racking system as a cost-effective and damage-free solution. This design concept can also potentially be introduced to general buildings. Recently, a new multi-storey student accommodation building was designed with a "Damage

Avoidance Design" philosophy [82]. The cost-effective new system used was developed with the research outcomes provided by HERA and the University of Auckland, in which prestressed Ringfeeder Springs and Sliding Hinge Joints were applied. This is a good example to apply a similar seismic design to a general building.

It is important to note that there are a few significant differences between general buildings and selective pallet racking systems. A pallet selective racking system doesn't have seismic serviceability limit state (SLS) requirements on drift, which require a rocking system not to start rocking until a defined level of seismic load is reached. They also don't have other structural and non-structural drift sensitive components, which are a significant part of the reason that NZS 1170.5 limits the maximum inter-storey drift to 2.5% of the storey height. For pallet racking systems, as long as the pallets or container on the racks are stable, the lateral deflection limit is that associated with overall rack stability, divided by 1.5 in accordance with the MCE reserve of deformation embodied in NZS 1170.5. Testing, as described earlier in this thesis and by others, has shown that the rack stability drift limit is over 10% , meaning that the current recommended drift limit of 5% easily incorporates the 1.5 MCE factor from NZS 1170.5

These differences are significant and need careful consideration when applying the rocking friction concept to actual buildings.

References

[1] C. K. Chen, R. E. Scholl, and J. A. Blume, “Earthquake simulation tests of industrial steel storage racks,” in *Proc., 7th World Conf on Earthquake Engineering*, 1980, pp. 379–386.

[2] C. Bernuzzi and M. Simoncelli, “An advanced design procedure for the safe use of steel storage pallet racks in seismic zones,” *Thin-Walled Struct.*, vol. 109, pp. 73–87, 2016.

[3] Australian Standard, “AS 4084-2012_Steel storage racking Australian Standard ®,” in *Steel Storage Racking*, 2012.

[4] J. Crosier, M. Hannah, and D. Mukai, “Damage to steel storage racks in industrial buildings in the darfield earthquake,” *Bull. New Zeal. Soc. Earthq. Eng.*, vol. 43, no. 4, pp. 425–428, 2010.

[5] ABS Group, “Seattle, Washington Earthquake of February 28,2001 （M6.8）,” 2001.

[6] M. Bruneau, C. Clifton, G. A. MacRae, R. Leon, and A. Fussell, “Steel Building Damage from the Christchurch Earthquake of February 22, 2011,” *Bull. New Zeal. Soc. Earthq. Eng.*, vol. Draft, no. 4, pp. 297–318, Dec. 2011.

[7] R. Park, “Evaluation of ductility of structures and structural assembages from laboratory testing,” *Bull. New Zeal. Natl. Soc. EarthquakeEngineering*, vol. 22, no. 3, pp. 1–34, 1989.

[8] S. R. Uma and G. Beattie, “Observed performance of industrial pallet rack storage systems in the canterbury earthquakes,” *Bull. New Zeal. Soc. Earthq. Eng.*, vol. 44, no. 4, pp. 388–393, 2011.

[9] I. Connor, “Performance of steel storage racks in the Darfield Earthquake,” *Bull. New Zeal. Soc. Earthq. Eng.*, vol. 45, no. 2, pp. 61–70, 2012.

[10] G. C. Clifton, “Semi-rigid joints for moment-resisting steel framed seismic-resisting systems,” University of Auckland, 2005.

[11] W. Y. Loo, P. Quenneville, and N. Chouw, “A low damage and ductile rocking timber wall with passive energy dissipation devices,” *Earthq. Struct.*, vol. Vol.9, no. 1, pp. 127–143, 2015.

[12] M. Ormeño, M. Geddes, T. Larkin, and N. Chouw, “Experimental study of slip-friction connectors for controlling the maximum seismic demand on a liquid storage tank,” *Eng. Struct.*, vol. 103, no. April 2016, pp. 134–146, 2015.

[13] G. A. MacRae, G. C. Clifton, H. Mackinven, N. Mago, J. Butterworth, and S. Pampanin, “The sliding hinge joint moment connection,” *Bull. New Zeal. Soc. Earthq. Eng.*, vol. 43, no. 3, pp. 202–212, 2010.

[14] D. M. Hoogeveen, “Failure of pallet racking systems in earthquakes,” Auckland, 2012.

[15] G. Macrae, G. C. Clifton, M. Bruneau, A. Kanvinde, and S. Gardiner, “Lessons from steel structures in Christchurch earthquakes,” *8 th Int. Conf. Behav. Steel Struct. Seism. Areas, July 1-3*, no. February 2011, pp. 1474–1481, 2015.

[16] C. Clifton, M. Bruneau, G. MacRae, R. Leon, and A. Fussell, “Steel structures damage from the Christchurch earthquake series of 2010 and 2011,” *Bull. New Zeal. Soc. Earthq. Eng.*, vol. 44, no. 4, pp. 297–318, 2011.

[17] S. R. Uma and G. Beattie, “Observed performance of industrial pallet rack storage systems in the canterbury earthquakes,” *Bull. New Zeal. Soc. Earthq. Eng.*, vol. 44, no. 4, pp. 388–393, Dec.

2011.

[18] C. . Chen and S. A. Freeman, “Dynamic response of steel industrial storage racks,” in *3rd Specialty Conference*, 1975, no. 6, pp. 837–864.

[19] C. K. Chen, R. E. Scholl, and J. A. Blume, “Seismic study of industrial steel storage racks,” *Rep. to Natl. Sci. Found. Rack Manuf. Inst.*, no. June, 1980.

[20] C. K. Chen, “Seismic analysis of building frames with semirigid connections,” *Rep. to Natl. Sci. Found. Rack Manuf. Inst.*, 1983.

[21] C. Chen and R. Scholl, “Earthquake resistance of industrial steel storage racks,” *Seventh Int. Spec. Conf. Cold-Formed Steel Struct.*, no. I, pp. 327–344, 1984.

[22] C. Castiglioni, P. Carydis, and P. Negro, *Seismic behaviour of steel storage racking systems*. Milan, Italy: Springer, 2009.

[23] C. Bernuzzi and C. A. Castiglioni, “Experimental analysis on the cyclic behaviour of beam-to-column joints in steel storage pallet racks,” *Thin-Walled Struct.*, vol. 39, no. 10, pp. 841–859, 2001.

[24] L. Ślęczka and A. Kozłowski, “Experimental and theoretical investigations of pallet racks connections,” *Adv. Steel Constr.*, vol. 3, no. 2, pp. 608–628, 2007.

[25] F. Gusella, M. Orlando, A. Vignoli, and K. Thiele, “Flexural Capacity of Steel Rack Connections Via The Component Method,” *Open Constr. Build. Technol. J.*, vol. 12, no. Suppl-1, M3, pp. 90–100, 2018.

[26] G. Ballio, C. Bernuzzi, and C. Castiglioni, “An approach for the seismic design of steel storage pallet racks,” *Stahlbau*, vol. 68, no. 11, pp. 919–928, Nov. 1999.

[27] A. Filiatrault, R. E. Bachman, and M. G. Mahoney, “Performance-based seismic design of pallet-type steel storage racks,” *Earthq. Spectra*, vol. 22, no. 1, pp. 47–64, 2006.

[28] P. Sideris, A. Filiatrault, M. Leclerc, and R. Tremblay, “Experimental investigation on the seismic behavior of palletized merchandise in steel storage racks,” *Earthq. Spectra*, vol. 26, no. 1, pp. 209–233, 2010.

[29] X. Zhao, T. Wang, Y. Chen, and K. S. Sivakumaran, “Flexural behavior of steel storage rack beam-to-upright connections,” *J. Constr. Steel Res.*, vol. 99, pp. 161–175, 2014.

[30] B. P. Gilbert and K. J. R. R. Rasmussen, “Bolted moment connections in drive-in and drive-through steel storage racks,” *J. Constr. Steel Res.*, vol. 66, no. 6, pp. 755–766, 2010.

[31] X. Feng, M. H. R. Godley, and R. G. Beale, “Rotational stiffnesses of semi-rigid baseplates,” in *14th International Specialty Conference on Cold-Formed Steel Structures*, 1998, pp. 323–334.

[32] N. Baldassino, C. Bernuzzi, and R. Zandonini, “Performance of base-plate connections joints of steel storage pallet racks,” 2011.

[33] B. P. Gilbert and K. J. R. Rasmussen, “Determination of the base plate stiffness and strength of steel storage racks,” *J. Constr. Steel Res.*, vol. 67, no. 6, pp. 1031–1041, 2011.

[34] A. Filiatrault, P. S. Higgins, A. Wanitkorkul, J. A. Courtwright, and R. Michael, “Experimental seismic response of base isolated pallet-type steel storage racks,” *Earthq. Spectra*, vol. 24, no. 3, pp. 617–639, 2008.

[35] V. Kilar, S. Petrovčič, D. Koren, and S. Šilih, “Cost viability of a base isolation system for the

seismic protection of a steel high-rack structure," *Int. J. Steel Struct.*, vol. 13, no. 2, pp. 253–263, 2013.

[36] R. J. Michael, "Design and development of a seismic isolation system for commercial storage racks," CASE WESTERN RESERVE UNIVERSITY, 2013.

[37] LokiBase, "LokiBase isolation system," 2019. [Online]. Available: http://www.lokibase.com/.

[38] V. Kilar, S. Petrovcic, S. Silih, and D. Koren, "Financial aspects of a seismic base isolation system for a steel high-rack structure," *Inf. la Construcción*, vol. 65, no. 532, pp. 533–543, 2013.

[39] W. Housner, George, "The behavior of inverted pendulum structures during earthquakes," *Bull. Seismol. Soc. Am.*, vol. 53, no. 2, pp. 403–417, 1963.

[40] R. W. Clough and A. A. Huckelbridge, "Preliminary experimental study of seismic uplift of a steel frame," *Rep. to Natl. Sci. Found. Am. Iron Steel Inst.*, vol. August, no. Report No UCB/EERC-77/22, 1977.

[41] A. A. Huckelbridge, "Earthquake simulation tests of a nine story steel frame with columns allowed to uplift," *Rep. to Natl. Sci. Found. Am. Iron Steel Inst.*, vol. August, no. Report No. UCB/EERC-77/23, 1977.

[42] M. J. N. Priestley, R. J. Evison, and A. J. Carr, "Seismic repsonce of structures free to rock on their foundations," *Bull. New Zeal. Natl. Soc. EarthquakeEngineering*, pp. 141–150, 1978.

[43] X. Wang and P. L. Gould, "Dynamics of sturctures with uplift and sliding," *Earthq. Eng. Struct. Dyn.*, vol. 22, no. September 1992, pp. 1085–1095, 1993.

[44] L. Wiebe, C. Christopoulos, R. Tremblay, and M. Leclerc, "Mechanisms to limit higher mode effects in a controlled rocking steel frame . 1 : Concept , modelling , and low-amplitude shake table testing," *Earthq. Eng. Struct. Dyn.*, vol. 42, no. September 2012, pp. 1053–1068, 2013.

[45] L. Wiebe, C. Christopoulos, R. Tremblay, and M. Leclerc, "Mechanisms to limit higher mode effects in a controlled rocking steel frame . 2 : Large-amplitude shake table testing," *Earthq. Eng. Struct. Dyn.*, vol. 42, no. August 2012, pp. 1069–1086, 2013.

[46] D. Roke, R. Sause, J. M. Ricles, and N. Gonner, "Design Concepts for Damage-Free Seismic-Resistant Self-Centering Steel Concentrically Braced Frames," in *Structures Congress 2009*, 2009, pp. 1421–1430.

[47] B. P. Gilbert and K. J. R. Rasmussen, "Experimental test on steel storage rack components," *Civ. Eng.*, no. October, pp. 1–61, Oct. 2009.

[48] B. P. Gilbert and K. J. R. Rasmussen, "Stiffness tests, failure tests and load transfer in steel drive-in storage racks," *Res. Rep. - Univ. Sydney, Dep. Civ. Eng.*, no. 900, pp. 1–103, Oct. 2009.

[49] B. P. Gilbert and K. J. R. Rasmussen, "Experimental test on steel storage rack components," *Civ. Eng.*, no. October, pp. 1–61, 2009.

[50] L. Mendes-Victor, C. S. Oliveira, J. Azevedo, and A. Ribeiro, *The 1755 Lisbon Earthquake: Revisited*. Springer Science & Business Media, 2008.

[51] T. Azuhata, M. Midorikawa, T. Ishihara, and A. Wada, "Simplified prediction method for seismic response of rocking structural systems with yielding base plates," *13th World Conf. Earthq. Eng.*, no. 371, 2004.

[52] T. Azuhata, M. Midorikawa, T. Ishihara, and A. Wada, "Shaking table tests on rocking structural

systems with base plate yielding," in *SEWC2002*, 2002, pp. T2-7-a-2.

[53] W. Y. Loo, C. Kun, P. Quenneville, and N. Chouw, "Experimental testing of a rocking timber shear wall with slip-friction connectors," *Earthq. Eng. Struct. Dyn.*, vol. 1, 2014.

[54] X. Ma, "Seismic Design and Behavior of Self-Centering Braced Frame with Controlled Rocking and Energy-Dissipating Fuses," *Dep. Civ. Environ. Eng. Stanford Univ.*, no. Report No.174, p. 414, 2011.

[55] M. Eatherton, J. Hajjar, X. Ma, H. Krawinkler, and G. Deierlein, "Seismic design and behavior of steel frames with controlled rocking: part I-concepts and quasi-static subassembly testing," *Struct. Congr. 2010*, pp. 1534–1543, 2010.

[56] S. Gledhill, "A practioners guide to design and delivery of controlled rocking steel braced," in *Steel Innovations Conference 2015*, 2015, no. September.

[57] H. Roh and A. M. Reinhorn, "Modeling and seismic response of structures with concrete rocking columns and viscous dampers," *Eng. Struct.*, vol. 32, no. 8, pp. 2096–2107, Aug. 2010.

[58] L. Wiebe and C. Christopoulos, "Performance-Based Seismic Design of Controlled Rocking Steel Braced Frames . I : Methodological Framework and Design of Base Rocking Joint," *Struct. Eng.*, no. November, p. 8214001, 2015.

[59] J. Hajjar *et al.*, "Controlled rocking of steel frames as a sustainable new technology for seismic resistance in buildings," *Int. Assoc. Bridg. Struct. Eng. Symp. Congr. Rep.*, 2008.

[60] T. Azuhata, M. Midorikawa, and T. Ishihara, "Seismic response reduction of buildings by rocking structural systems with adaptive dampers," *Smart Struct. Mater.*, vol. 6169, no. 2006, pp. 61691B_1-61691B_9, 2006.

[61] G. J. Beattie and S. R. Uma, "A revised guide for the design, construction and operation of high level storage racking systems following the Darfield earthquake," *9th Pacific Conf. Earthq. Eng.*, no. 178, 2011.

[62] N. Baldassino and R. Zandonini, "Industrial steel racks: tests, design and codes," *Adv. Struct.*, pp. 229–235, 2003.

[63] A. Firouzianhaji, A. Saleh, and B. Samali, "Non-linear finite element analysis of base-plate connections used in industrial pallet rack structures," 2014.

[64] European Standard, "BS EN 15512:2009 Steel static storage systems — Adjustable pallet racking systems — Principles for seismic design," in *British Standard*, 2013.

[65] G. Beattie and B. Deam, *Seismic Design of High Level Storage Racking Systems with Public Access*. Auckland, 2012.

[66] New Zealand Standard, *NZS 1170.5:2004 Structural Design Actions*, 2004th ed. 2013.

[67] C. K. Chen, R. E. Scholl, and J. A. Blume, "Seismic response of industrial steel storage racks," in *5th Specialty Conference*, 1980, no. I, pp. 429–450.

[68] T. Azuhata, M. Midorikawa, and T. Ishihara, "Earthquake damage reduction of buildings by self-centering systems using rocking mechanism," *14th World Conf. Earthq. Eng.*, 2008.

[69] D. H. Johnson, R. J. Michael, M. C. Pollino, J. D. Redovan, E. E. Moser, and B. A. Macdonald, "Development of a Seismic Isolation System for Commercial Storage Racks," in *Volume 4: Dynamics, Control and Uncertainty, Parts A and B*, 2012, vol. 4, no. PARTS A AND B, p. 609.

[70] R. Michael, J. A. Courtwright, E. Ferro, A. Filiatrault, P. S. Higgins, and A. Wanitkorkul, "Development of a new base isolation system for seismic isolation of steel pallet storage racks," *9th US Natl. 10th Can. Conf. Earthq. Eng. 2010, Incl. Pap. from 4th Int. Tsunami Symp.*, vol. 2, pp. 1040–1049, 2010.

[71] H. Krawinkler, N. G. Cofie, M. A. Astiz, and C. A. Kircher, "Experimental study on the seismic behavior of industrial storage racks," *Dep. Civ. Environ. Eng. Stanford Univ.*, vol. November, no. Report No. 41, 1979.

[72] J. R. Maguire, L. H. Teh, C. L. Lee, G. C. Clifton, and J. B. P. Lim, "Three-dimensional simulation of the dynamic rocking response of a cold-formed steel pallet rack," in *2018 NZSEE Conference*, 2018, no. 2018.

[73] A. Filiatrault, P. S. Higgins, A. Wanitkorkul, and J. Courtwright, "Experimental Stiffness of Pallet-Type Steel Storage Rack Teardrop Connectors," *Pract. Period. Struct. Des. Constr.*, vol. 12, no. 4, p. 210, 2007.

[74] New Zealand Standard, *NZS 1170.5 Structural Design Actions*. .

[75] G. Beattie and B. Deam, "Seismic Design of High Level Storage Racking Systems with Public Access," *Published by BRANZ Ltd, Porirua, New Zealand*. Auckland, 2007.

[76] New Zealand Standard, *NZS 1170 . 5 : 2004*. 2013.

[77] L. Wiebe and C. Christopoulos, "Performance-Based Seismic Design of Controlled Rocking Steel Braced Frames. II: Design of Capacity-Protected Elements," *J. Struct. Eng.*, vol. 141, no. 9, p. 04014227, 2015.

[78] P. FRANCOIS, Z. Tang, and G. C. Clifton, "Testing and analyses of the Friction splice to improve the resilience of pallet racking systems against earthquakes," *Lab Report, Univ. Auckl.*, 2018.

[79] Cisco-Eagle, "Structural Pallet Rack Row Spacers," 2019. [Online]. Available: http://www.cisco-eagle.com/catalog/category/1293/structural-pallet-rack-row-spacers. [Accessed: 30-May-2019].

[80] RackandShelf.com, "Row Spacers for Pallet Rack," 2019. [Online]. Available: https://rackandshelf.com/product/storage-products/warehouse-racks/pallet-rack-accessories/row-spacers-pallet-rack/. [Accessed: 30-May-2019].

[81] M. R. Eatherton, J. F. Hajjar, G. G. Deierlein, H. Krawinkler, S. Billington, and X. Ma, "Controlled Rocking Of Steel-Framed Buildings With Replaceable Energy-Dissipating Fuses," *14th World Conf. Earthq. Eng.*, 2008.

[82] S. M. Gledhill, G. K. Sidwell, and D. K. Bell, "The damage avoidance design of tall steel frame buildings - Fairlie Terrace Student Accommodation project, Victoria University of Wellington," *NZSEE Conf.*, no. 63, p. Paper Number 63, 2008.

Appendix

Example calculation for designing a rack frame with friction slipper baseplate

A design example calculation based on Equivalent Static Method (ESM) is conducted here to provide designers with a worked example for designing a rack frame with Friction Slipper Baseplate (FBP).

A1. Frame Considered:

Consider a selective rack frame built on a site with Soil Class C conditions in Wellington (Z = 0.4). The frame configuration is shown in Figure A1. The rack frame is a 4.8-m-tall, 3-level, 2-bay structure loaded with 6 pallets, 800 kg on each. The dimension of the frame is shown in Figure A2. The rack frame can be considered as a Moment Resistance Frame (MRF) in its down-aisle direction and as a Braced Frame (BF) in its cross-aisle direction, respectively.

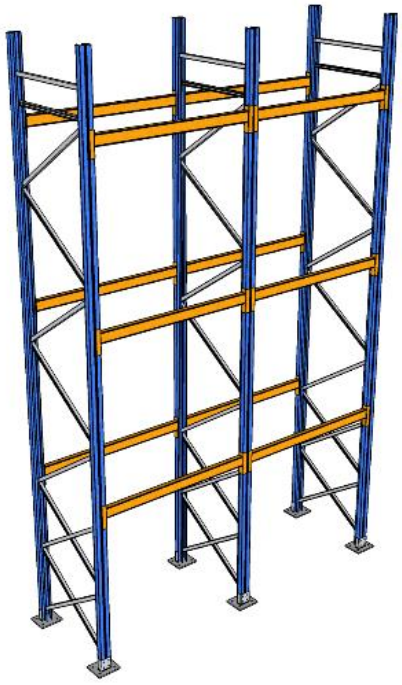

Figure A1: Frame configuration

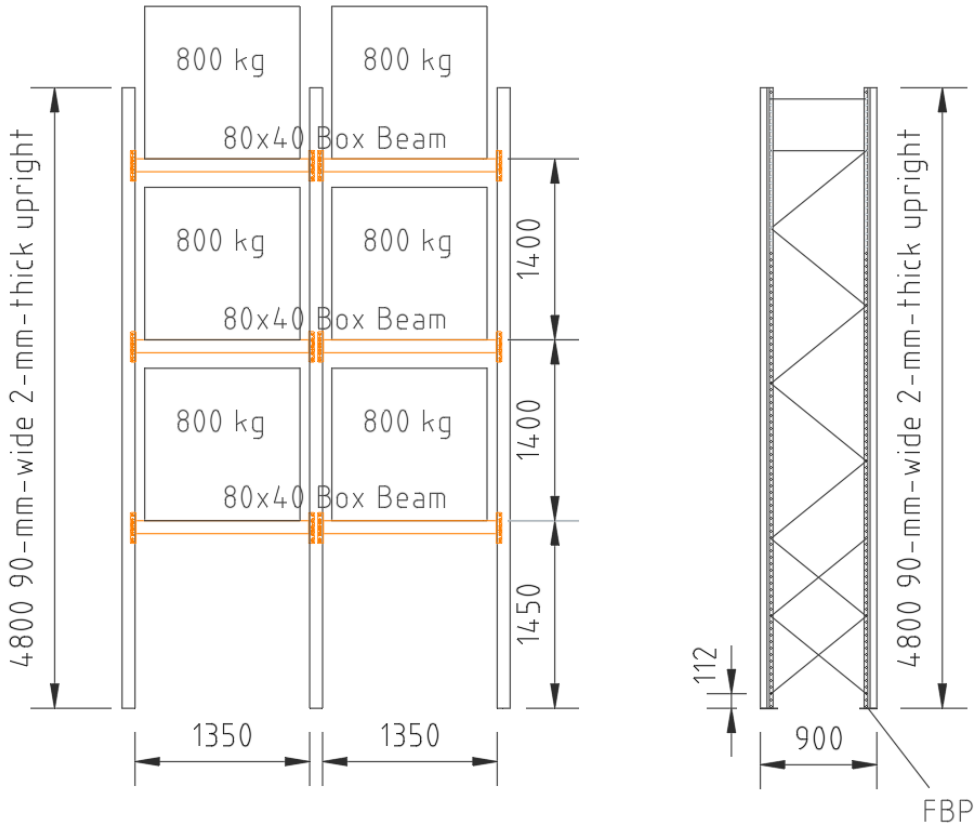

Figure A2: Rack frame elevation in down-aisle (moment frame) and cross-aisle (braced frame) direction

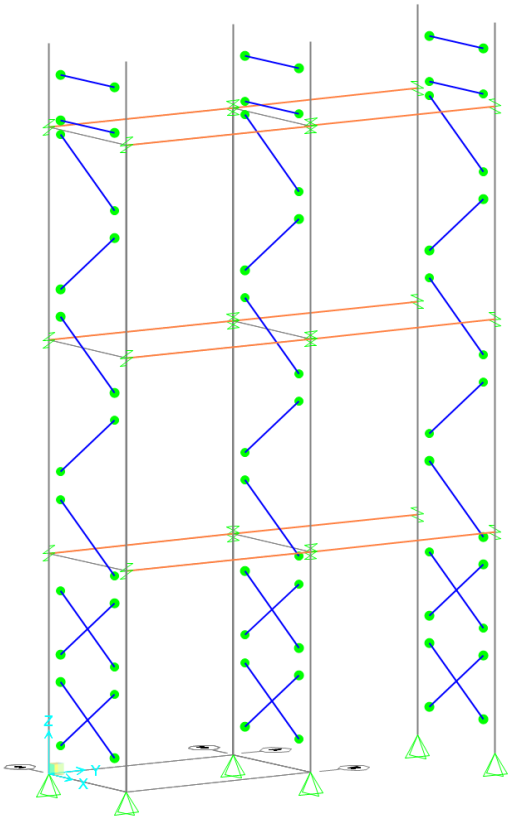

Figure A3: 3D structural model in SAP2000

A2. Create the structural model

The preliminary section selections are: 90-mm-wide 2-mm-thick uprights; 80-mm-deep, 40-mm-wide box beams, 2 X-bracings at the bottom and then followed by standard bracing. This is determined from the general non-seismic design requirements based on factored vertical loading and standard industry practice.

Create a 3D structural model in SAP2000, as shown in Figure A3. It is essential to carry out the following points:

1. Set the upright base joint as pin base.
2. Release the inplane moment fixity of both ends of the bracing connections in the plane of the frame.
3. Connect the beam to uprights with beam end connector rotational springs, which have assigned semi-rigid moment-rotation characteristics that have been determined experimentally. As shown in Figure A4, the moment-rotation curve of the 80x40 box beam is plotted. The beam end connector assigned in the model is a multi-linear link matching the experimental result.

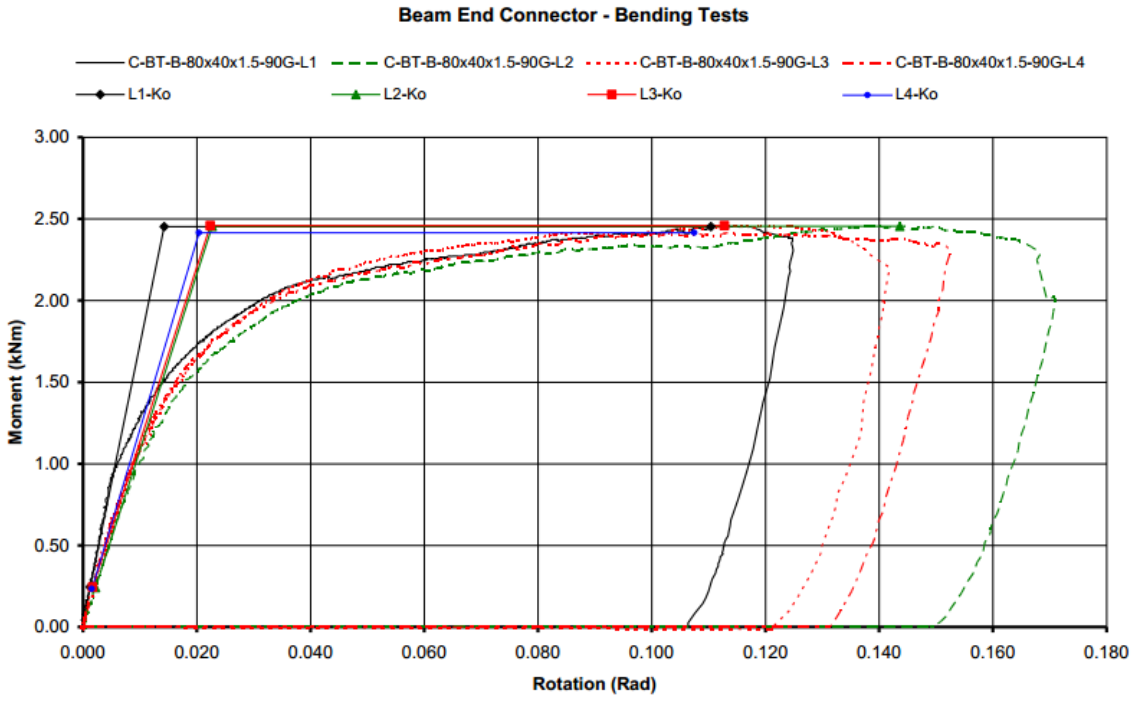

Figure A4: Beam-end connector moment-rotation test result

4. Assign the pallet load to the beams uniformly and determine the upright compression load at the base.

5. Assign the base-link connection according to the experimental result described in Chapter 4.
6. *P-Δ* effect should be considered in the modelling, using the large displacement option in the push-over analysis.

Obtain the numerical natural period of the frame in both directions from the model: T_{cross} = 0.39s, T_{down} = 1.10s. As a comparison, the natural periods from the experimental observation are T_{cross} = 0.40s, T_{down} = 1.01s.

A3. Determine the lateral seismic coefficient:

The hazard factor, $Z = 0.4$ for wellington

Soil Class C

The return period factor, $R_u = 0.75$, for 25 years Design life, Importance Level of 2

The near-fault factor, $N(T_1,D)$ = 1

The structure performance factor S_p should be determined in accordance with NZS1170.5 Clause 4.4; for the friction sliding system the value will be 0.7, as the structural ductility factor for both cross-aisle and down-aisle directions of loading is greater than 2.

The spectral shape factor, $C_h(T_1)$, in the cross-aisle direction $C_h(T_{cross}) = 2.36$, in the down-aisle direction $C_h(T_{down})$ = 1.13.

The elastic site hazard spectrum, $C(T_1)$, is determined by the following equation:

$$C(T_1) = C_h(T_1).Z.R.N.(T_1, D)$$

In the cross-aisle direction $C(T_{cross}) = 0.708$, in the down-aisle direction $C(T_{down})$ = 0.338.

A4. For cross-aisle direction design of racks with friction slipper baseplate

The uplift force should be determined as the following procedures:

1. Start with the minimum uplift force F_{upmin} = 7.6 kN
2. Take the ductility factor μ_{des}= 5 and undertake the cross-aisle design.

3. Determine the upright base uplift force with the lateral seismic load coefficient determined above according to Equivalent Static Method (ESM). If there is no design tension uplift, when μ_{des}= 5, decrease the ductility factor μ and repeat the design by reducing the value of μ until the uplift tension force = F_{upmin}.= 7.6 kN; in this example that reduces the ductility to μ_{des} = 4.13.
4. Assign the seismic load to the structural model to obtain the elastic displacement, $\Delta_{elastic}$ = 13.4 mm. Scale $\Delta_{elastic}$ by μ_{des} to obtain the inelastic displacment $\Delta_{inelastic}$ = 13.4 x 4.13 = 55.3 mm, Top drift = $\Delta_{inelastic}$ / H = 55.3/4800 = 1.15% < 5%. H is the height of the frame.
5. Determine the Uplift Displacement $\delta_{uplift} = \Delta_{inelastic}$ / *(H/W) = 55.3/ (4800/900) = 10.4 mm.* The Design Uplift Displacement δ_{uplift} = δ_{uplift} X 1.5 = 15.6 mm
6. Design the bracing system members for the actions from Step 3. Check the floor anchor bolt pull-out force with an overstrength factor of 1.1.
7. Check the friction force < 1.5x upright gravity load: F_{up} =7.6 <1.5x6.1 to ensure the gravity load will overcome the friction resistance to being the column back down onto the baseplate.

A5. For down-aisle direction design of racks with friction slipper baseplate

Based on the experimental result of the beam end connector test and baseplate-upright connection test, the ductility of the frame can be obtained. For the beam end connector, the yielding rotation is around 0.02 rad, and the ultimate rotation is around 0.1 rad. The μ_{BEC} = 0.1/0.02 /1.25 = 4. The ductility factor of baseplate is even larger as explained in Chapter 4. Take ductility factor value of 3 for system ductility in down-aisle design. Sp = 0.7.

Determine the down-aisle direction lateral seismic load with the seismic coefficients determined above.

Assign the seismic load to the structural model in the rack frame to obtain the deformation of the rack, the moment distribution of the beams and the uprights.

The elastic deformation of the rack is $\Delta_{elastic}$ *= 33.7 mm.* Scale it by the ductility factor of 3 to obtain the inelastic deformation $\Delta_{inelastic}$ *= 33.7* x *3 = 101.1 mm.*

The moment distribution of beams and the uprights is shown in Figure A5.

Check the section capacity and the beam end connector capacity is satisfactory in accordance with AS/NZS 4600.

The seismic design is now complete.

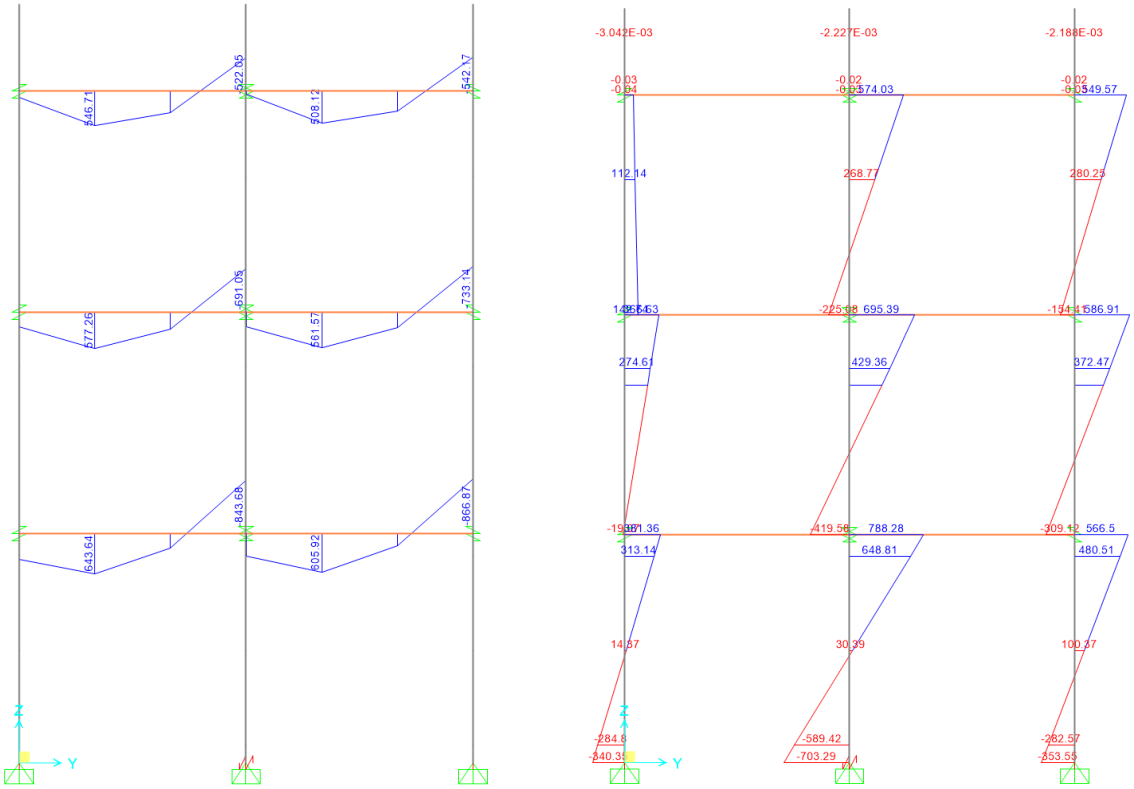

Figure A5: The moment distribution of beams and the uprights